

Faculty of Engineering and Science

**Geochemistry and Mineralogy of Clastic Sediments of Tukau Formation:
Implications on Provenance and Tectonic Setting**

Vivian Anak Dayong

**This thesis is presented for the Degree of
Master of Philosophy (Geology)
of
Curtin University**

May 2018

Declaration

To the best of my knowledge and belief this thesis contains no material previously published by any other person except where due acknowledgment has been made.

This thesis contains no material which has been accepted for the award of any other degree or diploma in any university.

Signature: 

Date: 30TH APRIL 2018

Acknowledgement

Praise the Lord that this never easy journey finally comes to an end! First of all, I would like to thank my thesis committee; to my supervisors Associate Professor **Dr.Chua Han Bing** and especially to Associate Professor **Dr.R.Nagarajan** for his great support and guidances throughout the years. With this also, I would like to thank my current Chairperson, Associate Professor **Dr.Dominique Dodge-Wan** and my former chairperson, Associate Professor **Dr.Michael Danquah**. I am truly grateful to **Dr.Franz Kessler** who helped in field trip, sampling, and discussion on the regional tectonic settings and during publication; **Dr.John Jong**, JX Nippon Oil & Gas Exploration (Deepwater Sabah) Limited for the financial support for various mineralogical analysis and allowed to use the data for the present study and **Dr.P.D.Roy** for helping in XRF analysis and interpretation of the data and **Dr.M.P.Jonathan** for helping interpretation and publication. My special thanks to Dr.Nagarajan, for the financial support for trace and rare earth elements analysis and geochronology study through his Curtin Malaysia Research Incentive fund and SRI Fund of which helped to generate. Thank you to Curtin Malaysia for providing me the research facilities. Many thanks to our lab staff members, **Ms.Marilyn and Ms.Rassti** for their supports in making sure the storage and facilities are well maintained throughout my research. Also I would like to thank former Applied Geology undergraduate students for helping during thin sections preparations.

Completing this theses brought a never-ending hardships and frustrations especially for the past couple of months. Often I felt like falling into the state of depressions, but, I am lucky enough to have few people whom I can share my hardships with. Therefore, I would like to thank my friends (**Cynthia Paul, Florence Singa, Jameson Malang, Bradly Endes and Lucian**) for being there when it was really unbearable and too stressing. A Special Thanks to all Applied Geology staff members for their kind word of encouragements throughout the years. Not to forget, former Dean of Graduate School **Professor Marcus Lee**, for his advices and always being encouraging. Also extend my sincere thanks to **Professor Clement Kuek**, the Dean R&D and **Ir. Professor Lau Hieng Ho** for their supports throughout my study. Last but not least, to my family members especially my Dad (**Dayong Sabot**) for continuous support in term of financial and encouragements. No words can describe how much I appreciate each and every single things that all of you had done throughout these times. Thank you from the bottom of my heart. “ In everything give thanks; for this is the will of God in Christ Jesus for you.”- *1 Thessalonians 5:18*

Abbreviations

CIA	– Chemical Index of Alteration
GPS	– Global Positioning System
HFSE	– High Field Strength Elements
ICP	– Inductively coupled plasma
LILE	– Large Ion Lithophile Elements
Ma	- Mega Annum/Million Years
NW	– Northwest
PAAS	– Post Archean Australian Average Shale
PPL	– Plane Polarized Light
ppm	– Part per million
QEMSCAN	- Quantitative Evaluation of Minerals by Scanning Electron Microscopy
REE	– Rare Earth Elements
SE	– Southeast
SEM	– Scanning Electron Microscope
TTE	– Transition Trace Elements
UCC	– Upper Continental Crust!
Wt%	- weight percentage
XPL	– Cross Polarized Light
XRD	– X-ray Diffractometer
XRF	– X-ray Fluorescence

Abstract

Provenance studies are intended to reconstruct and to interpret the history of sediments from their original source area until their final deposition process. A provenance study is proposed on the clastic sedimentary rocks of the Tukai Formation in the North-West Borneo after a comprehensive literature survey. The sedimentary rocks of the Tukai Formation are well exposed along the Bakam and Brick Valley of Sg.Rait region. The main aim of the research is to provide combined methods (i.e. mineralogy (bulk and clay), heavy mineral morphology, petrography, bulk rock geochemistry, heavy mineral chemistry and U-Pb dating of zircons) from the clastic rocks of the Tukai Formation to infer the provenance, tectonic setting and paleoweathering. Petrographically, Tukai sandstones are classified into quartz arenites and sublitharenites, litharenites whereas based on bulk geochemistry the clastic rocks are classified into quartz arenite, sublitharenite, litharenite, wacke and shale. Mineralogically, Tukai sedimentary rocks mainly consist of quartz, followed by clay minerals illite, illite-smectite and kaolinite. Feldspars are recorded minor or rare. Minor amount of heavy minerals recorded are rutile, tourmaline, zircon chromites and garnet. Texturally, the clastic rocks of the Tukai Formation can be classified into kaolinitic sandstone, laminated siltstone and sandy siltstones. The maturity and weathering intensity of the sedimentary rocks are considered as highly matured and moderate to intensive weathering. Based on the integrated study, the sedimentary rocks of the Tukai Formation is derived from the sedimentary to meta-sedimentary rocks dominated source (recycled sediments) with minor contribution from granitoids and ultramafic rocks (altered serpentinites). The Rajang Group of rocks mainly consist of sedimentary to meta-sedimentary rocks with minor amount of granites and ultramafic rocks which have been recycled during Neogene. The U-Pb geochronology of the zircon indicates that the zircons are derived from various sources, but randomly shows some clusters in their age as Cretaceous, Triassic, and Proterozoic which are comparable to Schwaner Mountain granitoids, Peninsular Malaysia tin bearing granitoids and older zircons from Indo-Australian plates (??) and are comparable to the other studies carried out in the Borneo Island. Tectonically, the Tukai Formation sedimentary rocks were deposited in a passive margin with minor extent towards active margin boundary. However, climate has played a major role on the chemistry of the sedimentary rocks of the Tukai Formation.

Keywords: provenance, mineralogy, petrography, mineral chemistry, U-Pb geochronology, Tukai Formation, NW Borneo

Contents

Declaration.....	I	
Acknowledgements.....	II	
Abbreviations.....	III	
Abstract.....	IV	
List of Tables.....	VIII	
List of Figures.....	IX	
1	CHAPTER 1	
1.1	Background.....	1
1.2	Problem Statement and Research Gap.....	3
1.3	Objectives.....	5
1.4	Significance.....	5
1.5	Regional Geology.....	6
1.6	General Section of Study Area.....	7
1.7	Outline of Thesis.....	9
2	CHAPTER 2	
2.1	Introduction.....	10
2.2	Provenance.....	10
2.3	Tectonic Settings.....	11
2.4	Paleoweathering.....	15
2.5	Clastic sedimentary Rocks.....	16
2.5.1	Sandstone.....	17
2.5.2	Mudrock.....	18
2.6	Petrography and Geochemistry Methods.....	19
2.6.1	Petrography.....	19
2.6.1.1	Quartz.....	20
2.6.1.2	Feldspar.....	20
2.6.1.3	Rock fragments/Lithic fragments.....	21
2.6.2	Quantitative Mineralogy.....	22
2.6.3	Whole Rock Bulk Geochemistry.....	23
2.6.3.1	Major elements.....	24
2.6.3.2	Trace Elements.....	25
2.6.3.3	Rare Earth Elements (REE).....	26
2.6.3.4	Heavy Minerals.....	26

	2.6.3.5	Zircon Dating.....	27
2.7		Status of Research in Northern Borneo.....	28
3		CHAPTER 3	
3.1		Introduction.....	31
3.2		Research Methodology.....	31
3.3		Sample Types and Sampling.....	31
3.4		Petrography.....	33
	3.4.1	Thin Section Preparation.....	33
	3.4.2	Petrography laboratory analysis.....	34
3.5		Sedimentary Textures.....	34
	3.5.1	Measuring grain size.....	34
	3.5.2	Grain shape.....	35
3.6		Mineralogy and Mineral Chemistry.....	36
	3.6.1	QEMSCAN® Analytical Parameter.....	37
	3.6.1.1	QEMSCAN® Data Processing.....	37
	3.6.2	X-Ray Diffraction (XRD).....	37
	3.6.2.1	Whole Rock Geochemistry.....	39
	3.6.2.2	Clay Speciation.....	39
	3.6.3	Heavy Mineral Separation and Analysis.....	39
	3.6.3.1	SEM Imaging Parameters.....	40
	3.6.3.2	QEMSCAN® Parameters.....	40
3.7		Geochemical Analysis.....	41
	3.7.1	U-Pb Geochronology of Zircons.....	43
4		CHAPTER 4	
4.1		Introduction.....	47
4.2		Results.....	47
	4.2.1	Petrography.....	47
	4.2.1.1	Quartz Arenites.....	48
	4.2.1.2	Sublitharenites.....	48
	4.2.2	Bulk Mineralogy.....	53
	4.2.3	X-Ray Diffraction (XRD).....	55
	4.2.4	Heavy Minerals.....	57
	4.2.4.1	Heavy Mineral Grain Morphology.....	59

4.3	Mineral Chemistry.....	61
4.3.1	Detrital Tourmaline.....	61
4.3.2	Detrital Chromium Spinel.....	61
4.3.3	Detrital Garnet and Ilmenite.....	64
4.4	Geochemistry Results.....	65
4.4.1	Geochemical Classification of Sandstone.....	65
4.4.2	Major Oxides.....	69
4.4.3	Trace Elements.....	70
4.4.3.1	Transitional Trace Elements (TTE: Sc, V, Cr, Mn, Co, Ni, Cu, Zn).....	70
4.4.3.2	Large ion lithophile element (LILE; Rb, Cs, Ba, Sr, Be).	70
4.4.3.3	High field strength elements (HFSE; Zr, Hf, Nb, Ta, Y, Th, U, and W).....	70
4.4.3.4	Rare Earth Elements.....	72
4.4.4	Geochemistry of zircon grains.....	74
4.5	Discussion.....	77
4.5.1	Paleoweathering.....	77
4.5.2	Maturity.....	82
4.5.3	Provenance.....	83
4.5.4	The Possible Provenance Area.....	93
4.5.5	Tectonic Setting.....	94
5	CHAPTER 5	
5.1	Introduction.....	99
5.2	Conclusions.....	99
5.3	Future Recommendations.....	100
6	References.....	103
7	Appendices.....	135
8	Published Paper Related to the Study.....	142

List of Tables

Table 3.1	Description of the mineral categories reported in this study with QEMSCAN and combination with BSE and X-ray signals.....	38
Table 3.2	List of elements analyzed, detection limit and instruments details.....	42
Table 4.1	Modal Composition of the rocks of the study area based on QFL.....	50
Table 4.2	XRD results for Tukai Clastic sediments (WR=whole rock; -2 μ m = clay speciation).....	57
Table 4.3	Representative composition of detrital Tourmalines from sediments of the Tukai Formation.....	63
Table 4.4	Representative Composition of detrital Chromian spinels from sediments of the Tukai Formation.....	64
Table 4.5	Representative composition of detrital ilmenite and garnets from sediment of the Tukai Formation.....	65
Table 4.6	Statistical summary of the geochemical data of the sediments of the Tukai Formation.....	66

List of Figures

Figure 1.1	Location and Geology Map of the study area (after Liechti et al., 1960). Adapted from (Nagarajan et al., 2015).....	8
Figure 2.1	Discriminant diagram as suggested by Roser and Korsch (1986) utilizing the chemical compositions of the clastic sedimentary rock.....	13
Figure 2.2	Discriminant diagram as suggested by Bhatia (1983). Similarly, Bhatia (1983) also utilizing major elements to discriminate the tectonic settings.....	13
Figure 2.3	Discriminant diagram as suggested by Herron (1988). The discrimination diagram was built based on the ratios of oxides (Fe_2O_3/K_2O) and (SiO_2/Al_2O_3). It is used for separating fine-grained sediments rich in Aluminium from immature coarse-grained sediments.....	14
Figure 2.4a	New major element (M) based multidimensional discriminant function diagram for the discrimination of active (A) and passive (P) margin settings (Verma and Armstrong-Altrin, 2016).....	14
Figure 2.4b	New combined major and trace element (MT) based multidimensional discriminant function diagram for the discrimination of active (A) and passive (M) margin settings (Verma and Armstrong- Altrin, 2016).....	14
Figure 2.5	A-CN-K Ternary diagram suggested by Nesbitt and Young (1984). CIA value ranging from 70-100 is consider as moderate to high degree of chemical weathering. Meanwhile 50-70 CIA value represents low degree of chemical weathering.....	16
Figure 3.1	Stratigraphic log and sample position from the Tukai Formation exposed near the Brick Valley of Sg.Rait region (the outcrops exposed near Sg.Rait region is shown in the photos) Credit: Dr. Franz Kessler.....	32
Figure 3.2	Example of grain size scale for rough grain size estimation.....	35
Figure 3.3	Example of grain size visual sorting estimating chart.....	35
Figure 3.4	Example of grain images for estimating the roundness of sedimentary particles. After Powers (1953).....	36
Figure 3.5	Cathodoluminescence images of selected zircon grains of Sample 1.....	45

Figure 3.6	Cathodoluminescence images of selected zircon grains of sample 2.....	45
Figure 3.7	Cathodoluminescence images of selected zircon grains of Sample 3.....	46
Figure 4.1	Plotted QFL Diagram after Folk (1974) for sandstone classification. Majority sample fall into quartz arenite.....	49
Figure 4.2 (a-f)	Microphotographs of the quartz arenites and sublitharenites from the Tukai Formation, NW Borneo (a,c,d,k) Abundance grain types made of quartz and lithic fragments. (b) Large lithic fragment from metamorphic origins (schist) with small mica. (f) Lithic fragments exist as larger grains in sample 54b with minor quartz veins.....	51
Figure 4.2 (g,h)	Mono and polycrystalline quartz grains, (i) a larger lithic fragment in sample 54b. (k) Abundance grain types made of quartz and lithic fragments. (j) Quartz grains show an alignment (l) iron oxide cement with some clay minerals (Fe-coated) (PPL view).....	52
Figure 4.3	QEMSCAN Modal mineralogical distributions of the Tukai Clastic Sediments.....	54
Figure 4.4	Mineralogical image of a selected area of the surface of the sample showing the distribution of the inorganic phases. The organic phases are not estimated which are blank in the image (white colour).....	55
Figure 4.5	X-ray diffractogram with the main mineral peaks identified together with the Rietveld difference plot. (Sample S9).....	56
Figure 4.6	QEMSCAN image grid illustrating range of grain types present within each sample.....	58
Figure 4.7	Distribution of Heavy minerals in the sediments of Tukai Formation.....	59
Figure 4.8 (a-i)	Morphological features of heavy minerals separated from the sediments of the Tukai Formation (Zr= Zircon; Rut = Rutile; Tour = Tourmaline; Mon = Monazite; Cr = Chromian spinel; Ilm = Ilmenite).....	62
Figure 4.9	Geochemical classification of clastic sediments of the Tukai Formation (after Herron, 1988) (Refer this plot for the symbol description).....	69
Figure 4.10	UCC normalized major oxides and trace elements recorded in Tukai sediments.....	71

Figure 4.11	Chondrite normalized REE pattern for Clastic Sediments of Tukau Formation.....	73
Figure 4.12	Chondrite normalized REE pattern for the average Sandstone and shales of Tukau Formation.....	74
Figure 4.13	U-Pb Concordia plots for all age populations and younger age populations for the zircons extracted from the sandstones of the Tukau Formation.....	75
Figure 4.14	Relative frequency zircon age plots for the zircons extracted from sandstones of the Tukau Formation.....	76
Figure 4.15	Al ₂ O ₃ - (CaO* +Na ₂ O) - K ₂ O (A-CN-K, in molecular proportion; Nesbitt and Young, 1982) ternary diagram shows the intensity of weathering for the Sediments of Tukau Formation.....	81
Figure 4.16	Al ₂ O ₃ -Zr-TiO ₂ plot showing the sorting trend for the clastic sediments of the Tukau Formations (after Garcia et al., 1991).....	83
Figure 4.17	Major oxide based provenance discrimination plot shows the possible provenance for the Tukau sediments (after Roser and Korsch, 1988).....	86
Figure 4.18	Hf Vs. La/Th bi-plot shows the provenance fields for the Tukau sediments (after Floyd and Leveridge, 1987).....	87
Figure 4.19	Detrital Tourmalines, plotted on the provenance discriminant Ca-Fe _{total} -Mg ternary diagram of Hendry and Guidotti (1985) adopted from Mange et al. (2007); b. Detrital Tourmalines, plotted on the provenance discriminant Al-Fe _{total} -Mg ternary diagram of Hendry and Guidotti (1985).....	89
Figure 4.20	Al-Fe-Mg diagram (in molecular proportions) for detrital tourmaline from Tukau Formation. Zone A-Li-rich granitoids, pegmatites and aplites, zone B-Li-poor granitoids, pegmatites and aplites, Zone C-hydrothermally altered granitic rocks, Zone D-Aluminous metapelites and metapsammites, Zone E-Al-poor metapelites and metapsammites, Zone F-Fe ³⁺ -rich quartz-tourmaline rocks, calc-silicates and metapelites, Zone G-Low Ca ultramafics, Zone H-metacarbonates and metapyroxenites (after Hendry and Guidotti, 1985).....	90
Figure 4.21	Chemical composition of chromites to discriminate their protoliths. a) Trivalent major cation plot (Fe ³⁺ -Al ³⁺ -Cr ³⁺), discriminating between different types of ultramafic complexes (after Cookenboo et al. 1997) b. Al ₂ O ₃ versus Cr ₂ O ₃ plot for the accessory fresh chrome spinels (after Bonavia et al., 1993). c. Variation of Mg/(Mg+Fe ²⁺) against Cr/(Cr+Al) of detrital chrome spinels from the sediments of Tukau Formation (Fields of spinels from harzburgites and lherzolites	

	after Pober and Faupl, (1988) and field of Greek ophiolites after Gartzos et al. (1990).....	92
Figure 4.22	QFL Diagram after Dickinson (1970) for determination of tectonic settings. Majority sample fall into recycled orogenic. 8 samples fall into craton interior provenance type.....	96
Figure 4.23	K ₂ O/Na ₂ O vs. SiO ₂ tectonic discrimination diagram (Roser and Korsch 1986) for clastic sediments of the Tuaku Formation (some quartz arenites are not included due to absence of Na ₂ O content).....	96
Figure 4.24	Discriminant-function multi-dimensional diagram (after Verma and Armstrong-Altrin, 2013) showing the tectonic setting for the high-silica clastic sediments from the Tukau Formations. The subscript m1 in DF1 and DF2 represents the high silica diagram based on log-ratios of major elements. The discrimination function equation are DF1(Arc-Rift-Col)m1 = (-0.263 × In(TiO ₂ /SiO ₂)adj) + (0.604 × In (Al ₂ O ₃ / SiO ₂)adj) + (-1.725 × In (Fe ₂ O ₃ t/ SiO ₂)adj) + (0.660 × In (MnO/ SiO ₂)adj) + (2.191 × (MgO/ SiO ₂)adj) + (0.144 × In(CaO/ SiO ₂)adj) + (-1.304 × In (Na ₂ O/ SiO ₂)adj) + (0.054 × In (K ₂ O/ SiO ₂)adj) + (-0.330 × In (P ₂ O ₅ / SiO ₂)adj) + 1.588. DF2(Arc-Rift-Col)m1 = (-1.196 × In(TiO ₂ /SiO ₂)adj) + (1.604 × In (Al ₂ O ₃ / SiO ₂)adj) + (-0.303× In (Fe ₂ O ₃ t/ SiO ₂)adj) + (0.436 × In (MnO/ SiO ₂)adj) + (0.838 × (MgO/ SiO ₂)adj) + (-0.407 × In(CaO/ SiO ₂)adj) + (1.021 × In (Na ₂ O/ SiO ₂)adj) + (-1.706 × In (K ₂ O/ SiO ₂)adj) + (-0.126 × In (P ₂ O ₅ / SiO ₂)adj) - 1.068.....	97
Figure 4.25	a. Discrimination diagrams based on major elements (oxides) and b. based on major and trace elements (after Verma and Armstrong-Altrin (2016).....	98

CHAPTER 1

INTRODUCTION

1.1 Background

A provenance study concentrates on how a particular sedimentary rock has been derived from its source rocks from the source area (Prothero and Schwab, 2013). In other words, provenance analysis is an attempt to reconstruct the parent-rock assemblages of sediments as well as the climatic-physiographic conditions under which the sediments formed (Weltje and von Eynatten, 2004; Garzanti et al. 2007). Information on the provenance and their tectonic settings during deposition lies in the mineralogy and chemical compositions of the sedimentary rocks (ie. Dickinson and Suczek, 1979; McLennan, 1989; McLennan et al., 1990; Zhiming et al., 2003). In addition, petroleum exploration, other natural resources and paleogeography reconstruction relied on the understanding on the tectonic settings of the ancient basin (ie: Armstrong-Altrin and Verma, 2005; Verma and Armstrong-Altrin, 2013; Oni et al., 2014).

It was realized due to the complexity of the sedimentary processes, relying on one single method to decipher the provenance would not be sufficient and unsatisfactory (Kutterolf et al., 2008; Reimann et al., 2015). There are two methods most often employed by researchers to conduct provenance studies and determine tectonic settings of sedimentary formations; petrography and geochemistry. These two methods may be used independently or combined. Petrography is a method that examines rocks' thin sections to determine their mineralogical composition using a polarizing microscope. However, the petrographic method is limited to sandstones, which in argillite-mudrock sequences are rarely use for determining provenance and tectonic settings (Blatt, 1985).

Meanwhile, some geochemical methods may examine the chemical composition contained in rocks and minerals through various analyses such as Inductively Coupled Plasma Mass Spectrometry (ICP-MS/ICP-OES) and Energy Dispersive X-Ray Spectroscopy (SEM-EDS). Despite not providing mineralogical information (Basu, 2017), the geochemistry method allows argillite-mudrock sequences to be analyzed and can generate bulk chemical data. The geochemical

data such as major, trace and rare earth elements reflect the source rocks' original characteristics (Dickinson, 1985; Fedo et al., 1996). This allows the bulk chemical data to act as supplement to support the petrographic approach (Siever, 1979). Therefore, researchers are opting to combine both methods to receive satisfying data and for validity purposes (eg: Von Eynatten, 2003; Nagarajan et al. 2007; Armstrong-Altrin et al. 2013; 2014; 2015; Bjørlykke, 2014; Nagarajan et al. 2014, 2015, 2017a; Malaza et al., 2016; Pacle et al., 2017). Both methods have become complementary techniques to each other and have allowed for a clearer understanding of sedimentological processes, source rocks, provenance and tectonic evolution (Bjørlykke, 2014; Malaza et al., 2016).

Recommendations by several researchers (e.g. Heller and Frost, 1988; Dallmeyer and Neubauer, 1991; Ibbeken and Schleyer, 1991; Morton, 1991; Handler et al., 1997; Dunkle et al., 1998; Morton and Hallsworth, 1999; Von Eynatten, 2003; Nagarajan et al. 2007; Armstrong-Altrin et al. 2013; 2014; 2015; Nagarajan et al. 2014; 2015; Basu et al., 2016) have also stated the petrographic method should be further complemented with additional analytical discrimination methods such as mineral chemistry, bulk-rock chemistry, and thermochronology and geochronology on detrital minerals (Ramkumar et al., 2018). PePiper et al. (2016) in their research concluded that interpreting provenance solely on detrital geochemistry is insufficient; it must be supported by heavy minerals analysis and REE geochemistry.

Moreover, heavy minerals such as tourmaline and chromite spinel are among the important heavy minerals that can be used to decipher the provenance (Hendry and Guidotti, 1985; Morton, 1991; Asiedu et al., 2000; Weltje and von Eynatten, 2004; Mange and Morton, 2007; White et al., 2016). Morton and Hallsworth (1999) emphasize how analyzing heavy minerals will reduce the effects of easily diluted minerals (eg: quartz, feldspars, carbonates and clay minerals) which creates a broad generalization for provenance studies. Mechanically and chemically stable tourmaline is a common accessory mineral in many rock types and terrains (all grades of metamorphic rocks, granitoid intrusive rocks and associated aplites, pegmatite veins and hydrothermal aureoles, metamafic rocks, meta-ultramafic rocks) and also occurs in many clastic sedimentary rocks as detrital or authigenic mineral developed during late stages of diagenesis (Henry and Guidotti, 1985; Bortnikov et al., 2008). Furthermore, tourmaline geochemistry may

help in revealing the composition of the local environment (ie: Henry and Guidotti, 1985; Henry and Dutrow, 1992; Shi et al., 2016) and also the geochemical discrimination of provenance (Mange and Morton, 2007). Chromite spinel is a good petrogenetic indicator of basic and ultramafic sources since they contain many cations and those atomic ratios vary based on the physico-chemical conditions of the parent magma (cooling rate, crystallization temperature, composition and oxygen fugacity (Arey, 1992). Chromite spinels have been widely used in the studies of the origin and tectonic setting of mantle-derived peridotites (e.g: Arai, 1992; Asiedu et al., 2000; Kamenetsky et al., 2001; Zimmermann and Sapalietti, 2009; Mange and Morton, 2007; Meinhold, 2009; Ishwar-Kumar et al., 2016; Unlu et al., 2017). The geochemical evaluation improves with the usage of trace and rare earth elements for interpreting provenance (e.g. Bhatia and Crook, 1986; McLennan, 1989; Floyd et al., 1991; McLennan et al., 1993; Armstrong-Altrin et al., 2015). As an example, adapting rare earth elements in deciphering provenance and source rocks has been discussed in Taylor and McLennan (1985). Source rocks also have been identified through geochemical ratios such as Ti/Al (McLennan, et al., 1979); Al_2O_3/TiO_2 (Hayashi et al., 1997); La/Sc, Th/Sc, Th/Cr, La/Co, Th/Co (Cullers, 1994, 2000; Cullers and Podkovyrov, 2000; Cullers et al., 1988); Cr/V (McLennan et al., 1993) and La/Th vs. Hf diagrams (Floyd and Leveridge, 1987).

The integrated method is particularly important especially in a region like North Borneo where mixed sediment sources might have occurred (Van Hattum et al., 2006; 2013; Nagarajan et al., 2014, 2015; 2017a). Combining all these analytical methods has produced an integrated data set which has also allowed us to assess the relative incidence of the diverse factors controlling sediment composition, including source-rock lithology, weathering, and recycling. This data in turn, will guide us into deeper understanding of the geologic evolution not only for the Tukai Formation but also for the entire Neogene rocks of NW Borneo. Indirectly, through these study's results, it can contribute to developing a proper database for the Neogene lithological formations and units.

1.2 Problem Statement and Research Gap

Due to the fact that, the oil and gas are mainly extracted from the offshore basins less exploration studies have been carried out on the onshore formations. In addition, due to the tropical climate,

exploration of fresh outcrops is really challenging. However, recent studies have emphasized more on the onshore sedimentary formations as an analog for the offshore formations. The existing literature examining the Sarawak region has showed less attention being given to the geochemistry, provenance and paleoweathering on onshore clastic sediments except few older and recent studies published after we started this research in the NW Borneo (i.e. Van Hattum et al., 2006, 2013; Nagarajan et al., 2014, 2015, 2017a,c). Tectonic interpretations and reconstructions have been made with computer-based, tectonic modelling and seismic data with few in the field studies (i.e Mat-Zin and Swarbrick, 1997; Singh et al., 2009; Cullen, 2010; Morley et al., 2008; Vijayan et al., 2013). Among the reviewed published literature, the main focus has been given to stratigraphy (eg: Morrison and Lee, 2003; Kosa, 2015), structural geology (eg: van der Zee and Urai, 2005; Morley et al., 2008), depositional tectonic settings (eg: Lim and Mohd Shafea, 1994; Abd Rahman et al., 2014; Collins et al., 2017), marine geophysical survey (eg: Zampetti et al., 2004), faunal assemblages and petroleum geology (eg: Keij and Harcourt, 1965; Wan Hasiah, 1999; Ingram et al., 2004; Ali and Padmanabhan, 2014; Togunwa et al., 2015; Collins et al., 2017) and a few studies have concentrated on the provenance of the Neogene sediments (eg: Nagarajan et al., 2014, 2015 and 2017a, c). Also, a complete mineralogical and geochemical characteristics of sedimentary formations of NW Borneo have not been addressed yet in detail. Based on the detailed literature review (summarized under chapter 2 section 2.7) from NW Borneo, it is clear that limited published papers particularly in discussing the provenance and tectonic setting found despite being grouped into Neogene rocks.

A first regional study on the sedimentary to metasedimentary rocks of Cenozoic age was conducted by van Hattum et al (2006) and stated that the sediments of Broneo are not from Borneo based on the zircon chronology. Then in 2013, the same authors (van Hattum et al., 2013) come up with an update that the sediments of Borneo was majorly derived from the Sothern part of Borneo and possible external input form sediments from outside Borneo during the deposition of Rajang-Croker Group of sediments. Due to lack of information on the Neogene sedimentary formations, Nagarajan et al. (2014) initiated a preliminary geochemical study for Tukai sediments by using a limited data set (concentrated on lower part of Tukai Formation). Their results has shown that the clastic sediments of the Tukai Formation are mainly derived from felsic source region with some additional contribution from the mafic to ultramafic group of rocks and they

were deposited in a complex tectonic setting. In order to understand a complete source area characteristics, weathering intensity and tectonic setting a combined approach was planned and executed in the present study to address the major research questions.

- What type of source rocks was exposed to deliver the sediments of Tukai Formation during Miocene?
- Under what kind of tectonic settings does the source rock being formed?
- What is the mineralogy of the sandstone and geochemical characteristics of sandstones and shales of the Tukai Formation?

This research study also indirectly looking into consideration whether the results show any similarities with Southwest Sarawak as published by Ferdous and Farazi (2017) or whether there is a connection to the studies by Galin et al. (2017) from the Rajang Group. The Rajang Group was formed around 30-40Ma. Their findings showed that; (1) the sources for Rajang Group sediments were consisted of acid igneous rocks with presents of metamorphic and reworked sedimentary rocks (2) tectonic settings was a non-active subduction margins.

1.3 Objectives

The aim of the research is to fulfill the reseearch qestions stated above by studying mineralogical, petrographical and geochemical characteristics of the clastic sedimentary rocks of the Tukai formation through the following rearch objectives.

1. To study the mineralogical and petrographic characteristics of the sandstones
2. To study the chemical composition of sandstones and mudstones
3. To infer the paleo-weathering, provenance and tectonic setting of clastic sediments of the Tukai Formation through combined/integrated approach.

1.4 Significance

The focus of this study was to find out their source rock characteristics and tectonic settings. The advantage of the study is combination of various methods to solve our research question which have been achieved in this research by using various methods such as mineralogy (bulk mineralogy

and clay mineralogy), heavy mineral separation, morphology of heavy minerals, mineral chemistry, bulk geochemistry and petrography (only for sandstone). The detailed classification of the clastic sediments of the Tukai Formation through petrographical and geochemical method are discussed which will help us to explain the characteristics of potential reservoir rocks of the Baram River basin. This study also have addressed on the climatic controlling factors in the source region which were controlling the chemical weathering during Upper Miocene to Lower Pliocene. In particular, the chemistry and geochronology of heavy minerals pin-pointing their source clearly through the Tukai sedimentary rocks were recycled from sedimentary-meta-sedimentary dominated source area. Overall this study have solved the complex problems related to the Provenance and Tectonic Setting of the Tukai Formation from North-West Borneo.

1.5 Regional Geology

The island of Borneo is politically governed by three different countries; Malaysia (Sabah and Sarawak), Indonesia (Kalimantan) and Brunei. Borneo is the world's third largest island having a complex geological history resulting from the Mesozoic accretion of ophiolitic, island arc materials and microcontinental fragments onto the continental core of the Paleozoic Schwaner Mountains in the South-West of the island (Hutchison, 1989; Metcalfe, 1996). This geological composition could also be due to the fact Borneo is surrounded by plate boundaries, marginal ocean basins and arc systems (Fuller et al., 1999; Wilson and Moss, 1999; Nagarajan et al., 2014).

The Cenozoic Era (Paleogene to Neogene) of Borneo experienced intense tectonic events such as upliftment and subsidence caused by extensions and rotations which have multiple interpretations by various authors (Hall, 2013). Generally, the Cenozoic Era (Middle to Late Miocene) was subject to some important geological events such as mountain building, volcanism, erosion and changes in sedimentation patterns, which later shaped the current landmass of Borneo (Hall and Nichols, 2002; Hall, 2013).

The Cenozoic Era started (~ 66 Ma) with the main events taking place between the Paleogene until the Neogene; a) The Paleogene, which represents the transgression, happened due to a rise in sea level or subsidence of the land by tectonic events and the Neogene, the major regression occurred due to the lowering sea level or a tectonic uplift. The sea level began to fall at the beginning of the Middle Miocene time (~ 23 Ma) creating a major Neogene regression causing

a change in the depositional patterns. During this time, Sundaland in central Kalimantan was uplifted by the tectonic event, which initiated the construction of the delta complex through eastward-westward flowing rivers (Beddoes, 1981). A fluvial-deltaic depositional pattern began to prograde westward into Sabah, Brunei and northern Sarawak through Western Kalimantan. The regression was halted by a minor transgression during the Late Miocene, which encouraged deposition of the marine shale onto the Miocene delta areas. The orogeny occurred in the Late Miocene-Pliocene then was discontinued by the marine transgression. During this time, areas in central and eastern Kalimantan were uplifted and igneous rocks were intruded into Western Kalimantan. The uplifted region supplied sediments during the Plio-Pleistocene regression to all the surrounding basins. In Sabah/Sarawak, the sediments have been redeposited as turbidite in the deeper basins (Wilson and Moss, 1999).

Over the years, several studies have been conducted on the Cenozoic sediments around Borneo (eg: van Hattum et al., 2006; 2013; Hall and Nichols, 2002; Witts et al., 2012; Cullen et al., 2012; Marshall et al., 2015; Parham et al., 2016; Wang et al., 2016; Breitfeld et al., 2014; 2017; Galin et al., 2017). Studies involving the possible source for Cenozoic sediments have been published by several researchers; some have suggested the sediments were derived from South East Asia/Indochina (ie: Hall, 1996; Hutchison, 1996; Metivier et al., 1999; van Hattum et al., 2006; Breitfeld et al., 2014; 2017; Galin et al., 2017) while other researchers have suggested the Cenozoic sediments could have been derived from around Borneo itself (Hall and Nichols, 2002; van Hattum et al., 2013). The study of Cenozoic sediments has also attracted researchers as the sediments have contributed to the development of the major hydrocarbon grounds around Borneo such as in the Kutei Basin (eg: Satyana et al., 1999; Curiale et al., 2005) and Sarawak Basin (eg: Jia and Abd Rahman, 2009; Ben-Awuah and Padmanabhan, 2015).

1.6 General Section of the Study Area

The Northern Sarawak mainly covered by sedimentary rocks of Neogene age and the younger rocks extends towards North and NNE. These sedimentary rocks are belong to Nyalau Formation, Setap shale Formation, Tangap Formation, Sibuti Formation, Belait Formation, Lambir Formation, Miri Formation and Tukai Formation. The study area (Tukai Formation) is exposed along Miri-Bakam area, located approximately 40 km from Miri towards South West (**Figure 1.1**) and is well exposed nearer to the Bakam and Sugai Rait region (Lat: 4.248586° and Long: 113.959417°;

Figure. 1a,b). The Tukai Formation, have been deposited as a result of transgression, regression and through the tectonic events that occurred in Borneo during Neogene period (~10Ma – 2.58 Ma) and Tukai Formation is the youngest among the Neogene Formations with alternate layers of siltstone and mudstone with occasional massive siltstone, sandstone and mudstones. Also thin micro-conglomerate at the channel base and coal lenses is also observed. Pyrite concretions and amber balls are often observed along with iron rich layers.

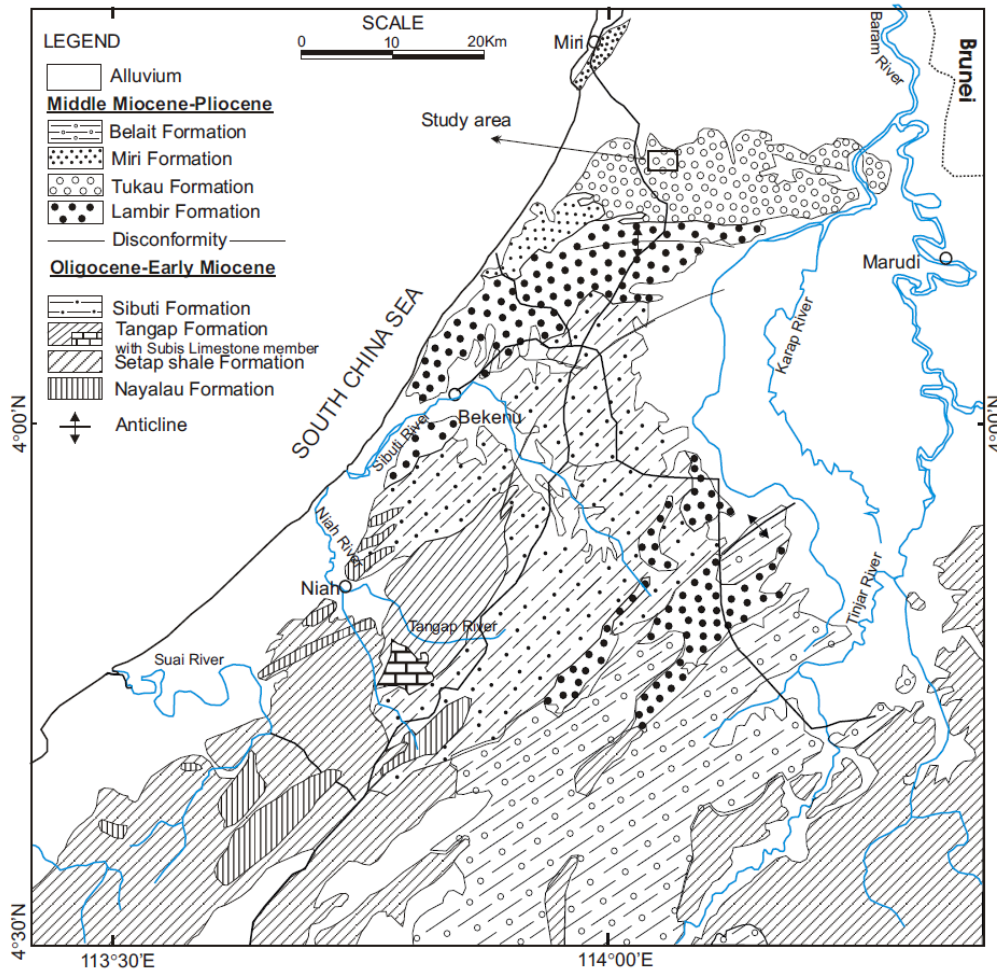


Figure 1.1 Location and Geology map of the study area (after Liechti et al., 1960). Adapted from (Nagarajan et al., 2015)

The Tukai Formation is a structurally complex feature formed as a domal anticlinal uplift, located along the Tukai I Bakam / Baram trend. It is dissected at the shallow level by normal synthetic and antithetic faults. These fault system divide the field into seven fault blocks. The

major hydrocarbon accumulations are between 700 to 2000 meters and the main prospective sequence consists of fine to very fine grained sands of the upper cycle V of Late Miocene age and deposited in a deltaic, fluviomarine, coastal to near shore environment.

Based on the relative absence of planktic foraminifers, the Tukai Formation is considered to be formed in shallow marine to deltaic environments. The absence of foraminifers (except some brackish water forms), the presence of lignite layers and amber balls have led Hutchison (2005) to conclude that the Tukai Formation was deposited on a coastal plain. Hutchison (2004) stated that the uplift of the Borneo landmass in the Mid-Miocene causing all newly formed formations to be deposited along the coastal plain and growing thicker seawards. The basal part of the Tukai Formation conformably overlies the Lambir Formation near Sungai Liku in the eastern Lambir Hill, where it is conformably overlain by the Liang Formation near Miri. Kessler (2010) described that the formation to be deposited in a shoreface environment; consisting of medium to coarse-grained sandstone with micro-conglomerates at the channel base. The presence of lignite layers and amber balls supports for the coastal plain depositional setting (Hutchison, 2005). Nagarajan et al. (2014) have been described the geochemical characteristics of the basal part of the Tukai Formation and inferred that some ultramafic input were expected.

1.7 Outline of the Thesis

Chapter 1 presents the outline, geological settings and objectives of the present study. Literature review on the geological background of the study area and research problems are summarised in Chapter 2. Chapter 3 is discussing a detailed methodology of the various techniques adopted in this study. Various results such as mineralogy (bulk and clay mineralogy), heavy mineral separation, heavy mineral chemistry, heavy mineral morphology, bulk geochemistry, petrography and U-Pb dating of zircon grains are discussed and these results are combined and discussed in order to address the objectives of the present study are concluded in chapter 4. Conclusions and possible area of research has been recommended for the future study are being discuss in Chapter 5.

CHAPTER 2

LITERATURE REVIEW

2.1 Introduction

In this chapter, a thorough literature review has been carried out and reported systematically on various methodology adopted here and previous research in the study area and its surroundings to find out the research gap. Based on the literature review, the aim of this study was set to infer the provenance and tectonic settings of Neogene clastic sediments of the Tukau Formation using mineralogy, petrography and geochemistry results.

2.2 Provenance

Provenance is important in understanding paleogeography and to reconstruct the sediment pathways in the past (Weltje and Eynatten, 2004; Garzanti et al. 2007). It is already known that sediments are transported miles away from their primary sources. During transportation, sediment is abraded and chemically weathered depending on transport mechanisms and climate; it is also fractioned according to grain size, shape, and density until it reaches the depositional basin (Alekseevskiy et al., 2008). The provenance area is divided into four major types; stable cratons, basement uplifts, magmatic arcs and recycled orogens based on petrography (Dickinson, 1985). Various provenance terranes will yield detritus of a particular composition (Tucker, 2001). Similarly, Roser and Korsch (1986) have proposed a discrimination diagram using the major oxide concentrations of the sediments and sedimentary rocks to discriminate the sediments' origin from four different provenance areas. The four major provenance area are 1) felsic igneous provenance, 2) intermediate igneous provenance, 3) mafic igneous provenance and 4) quartzose sedimentary provenance (**Figure 2.1**). This plot is still being used to distinguish the provenance area by the researchers.

In a provenance study, aspects such as source rock, relief and climate in the source area, tectonic setting, transport history, and diagenetic modifications are very important (Schieber, 1992). These factors may control the amount and rates of sediment delivery to the drainage basin and to sediment transporting systems. Sediment composition is also affected by the modifications of source rocks during the transportation processes (Kutterolf et al., 2008). The complexity of the

processes involved implies that largely similar sediment may be produced from different sources as well as dissimilar sediments may be produced from similar source rocks (von Eynatten and Dunkl, 2012).

The current approaches for assessing provenance often involves integrated methods of the whole-rock geochemistry, petrography, dating of detrital minerals, heavy minerals such as rutile, chrome spinel, tourmaline, garnet and zircon chemistry (eg: Schieber 1992; McLennan et al., 1993; Morton and Hallsworth, 1994; Aseidu et al., 2000; Zack et al., 2004; Kemp et al., 2006; Zack et al., 2011; Nie et al., 2012; Eynatten and Dunkl, 2012; Garzanti et al., 2013; Um et al., 2013; Aparicio Gonzalez et al., 2017; Mounteney et al., 2018). Thus, being able to recognize variations in sediment provenance in an environment where the material does not show obvious lithological or elemental changes can be very important in determining events in the geological past (Haughton et al., 1991; Diskin et al., 2011; Garzanti, 2016).

2.3 Tectonic Settings

Ristau (2013) states plate tectonics' theory is closely related with the history, motions, and the tectonic plate's activities. The effects of tectonic activity may deviate and recombine transportation routes for sediments, detritus and minerals in different depo-centres at different times (De Wit et al., 2000). Geochemical signatures in sediments are associated with the processes caused by plate tectonic movement, the distinction in provenance characteristics and sedimentary processes (Oni et al., 2014).

Provenance and depositional basins of sandstones can be linked with their tectonic settings based on the detrital modes (Dickinson and Suczek, 1979; Dickinson et al., 1983). The relationships between tectonic settings and detrital modes such as the presence of quartz also had been shown through earlier studies conducted by Crook (1974) and Schwab (1975). In those two studies, the authors found quartz-rich rocks are closely related to the passive continental margins while magmatic arcs and active continental margins are presented by poor and moderate quartz content.

On the other hand, Bhatia (1983), Bhatia and Crook (1986) and Roser and Korsch (1986, 1988) have proposed the usage of chemical compositions to discriminate between the tectonic settings for clastic sedimentary rocks. Sediment composition, diagenesis and sedimentation are all influenced by the tectonic setting of the depositional environment (Pettijohn et al., 1972; Bhatia, 1983; Chamley, 1990; (cited in Getaneh, 2002). This makes it possible to identify the geochemical signature presented by different tectonic settings within a particular geological terrain (Bhatia, 1983; Bhatia and Crook, 1986; Roser and Korsch, 1986, 1988; Rollinson, 1993).

Results gained from the geochemical analyses are usually presented in the form of discrimination diagrams. The discrimination diagrams proposed by Bhatia (1983) and Roser and Korsch (1986) were based on major elements. Several studies found that the traditional discrimination diagrams introduced by Bhatia (1983), Roser and Korsch (1986) and Bhatia and Crook (1986) did not perform competently (e.g: Armstrong-Altrin and Verma, 2005; Weltje, 2006; Ryan and Williams, 2007). Thus, Armstrong-Altrin and Verma (2005) compared both discrimination diagrams and analyses showed the diagram proposed by Roser and Korsch (1986) was preferred for determining the plate tectonic settings (**Figure 2.2**) compared to the diagram by Bhatia (1983) with a moderate positive statistical agreement (50%). Also a new discrimination diagram was introduced later by Verma and Armstrong-Altrin (2013) who utilized the major elements to differentiate the sediments originating from islands or from a continental arc, collisional or continental rift. When using analytical data, errors are unavoidable and could be misrepresented in ternary diagrams (Verma, 2015). Therefore, log-ratio transformations had been introduced by several researchers to solve the problems related to analytical data (e.g: Egozcue et al., 2003; Aitchison and Ezocue, 2005; Verma, 2005). Verma and Amstrong-Altrin (2016) tested out the existing discrimination diagrams (ie: Bhatia, 1983; Roser and Korsch, 1986) using samples from active and passive margins (which is applicable for our research) of known settings. Their findings showed an unsatisfactorily results and therefore suggested utilization of major and trace elements to build up new discriminant diagrams. Recently, Verma and Armstrong-Altrin (2016) proposed a new tectonic discrimination diagrams based on log ratio transformation and linear discrimination analysis of an extensive geochemical database from the Neogene-Quaternary siliciclastic sediments from the active and passive margin tectonic settings. In which they proposed two diagrams 1) major element based and 2) combined major and trace elements based which both

discriminate the sediments from the passive and active continental margins (**Figure 2.4a,b**). Despite all of these weaknesses, geochemical analysis still acts as a useful tool for larger scale studies for used in oil and gas exploration as well as mineral reconnaissance (Mounteney et al., 2018).

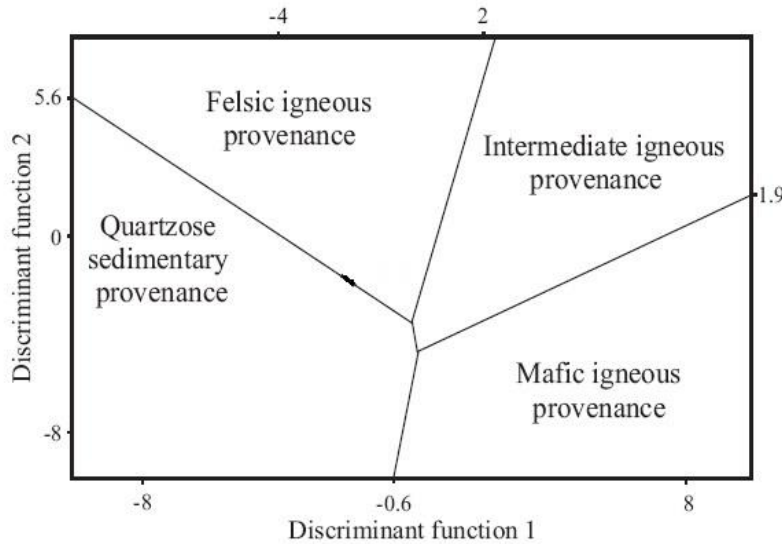


Figure 2.1. Discriminant diagram as suggested by Roser and Korsch (1986) utilizing the chemical compositions of the clastic sedimentary rock.

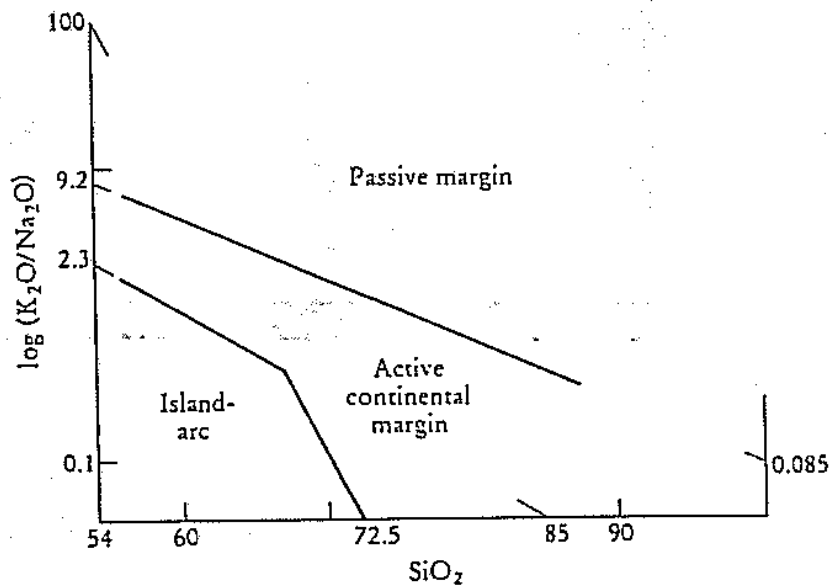


Figure 2.2. The log (K₂O/Na₂O) vs SiO₂ discrimination diagram of Roser and Korsch (1986) for sandstone-mudstone suites and showing fields for a passive continental margin, an active continental margin and an island arc.

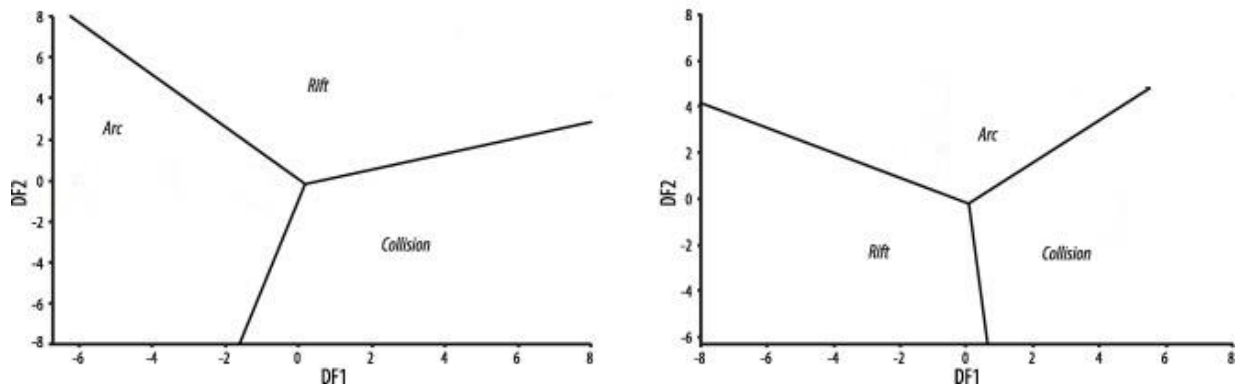


Figure 2.3. Discriminant diagram as suggested by Verma and Armstrong-Altrin (2013). The diagram is suitable to be in use for discriminating tectonic settings of older sediments as well as Neogene and Quaternary rocks. It is reliable in compare to earlier discrimination diagrams as it reduces the errors that are contributed by geological processes such as weathering and recycling activities.

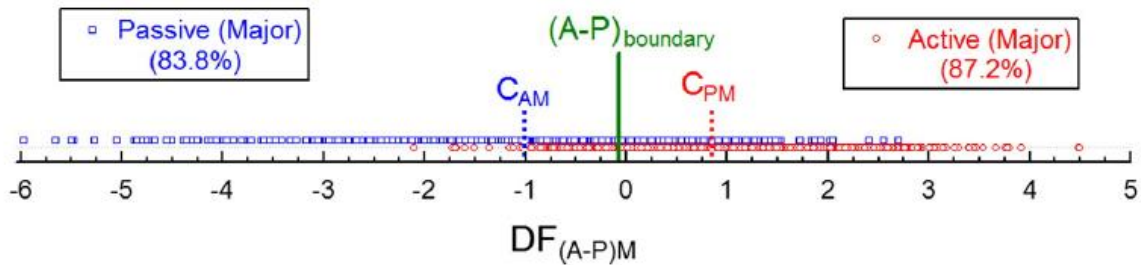


Figure 2.4a. New major element (M) based multidimensional discriminant function diagram for the discrimination of active (A) and passive (P) margin settings (Verma and Armstrong-Altrin, 2016).

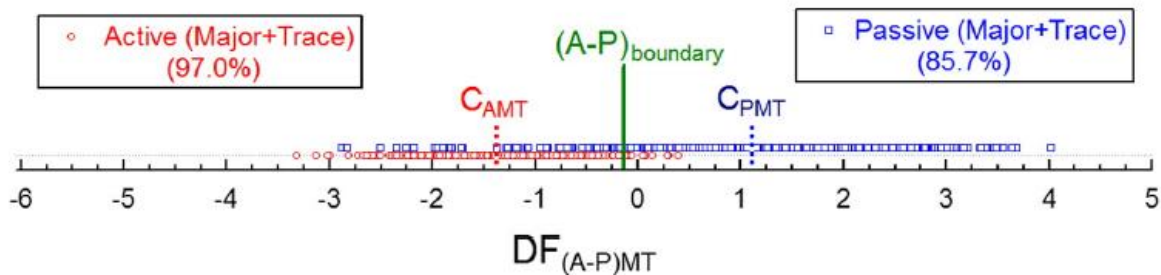


Figure 2.4b. New combined major and trace element (MT) based multidimensional discriminant function diagram for the discrimination of active (A) and passive (M) margin settings (Verma and Armstrong-Altrin, 2016).

Similar problem also might happen when we are utilizing heavy minerals for the provenance research. Heavy minerals original characteristics might be overprinted by the weathering processes that probably causing modifications to the characteristics before they get deposited in the sedimentary basin (Morton and Hallsworth, 1999). It could be even worse for provenance studies in an environment severely affected by the diagenesis processes (Morton and Hallsworth, 1994). Therefore, integrating few methods together will help to cope or reducing the errors that may arise by individual methods.

2.4 Paleoweathering

Weathering is one of the sedimentary processes that are capable of modifying original compositions of clastic sedimentary rocks apart from erosion and diagenesis processes. Indirectly, paleoweathering help in identifying the climate in the past; warm and humid climates can be shown by intense chemical weathering whilst weak chemical weathering indicate a more arid climate (Nesbitt and Young, 1982). The chemical variation in the major and trace elements can reflect the degree of weathering of the source rocks.

Observations of the enrichment of immobile elements such as SiO_2 , Al_2O_3 , TiO_2 , Rb and Ba and the depletion in CaO, Na_2O and Sr may also provide information on the past weathering processes. The parameters such as the Chemical Index of Alteration (CIA, Nesbitt and Young, 1982); the Chemical Index of Weathering (CIW, Harnois 1988); the Plagioclase index of alteration (PIA; Fedo et al., 1995); the weathering index by Parker (WIP, Parker, 1970); CIX (Garzanti et al., 2014); $\text{K}_2\text{O}/\text{Na}_2\text{O}$ (Nesbitt and Young, 1984; Lindsey, 1999); Al/Na (Selvaraj and Chen, 2006); K/Al ratio (yarincik et al., 2000); and Th/U and Rb/Sr ratios (McLennan et al., 1993) are widely used to study the degree of source rock weathering in the source area. These parameters have been used by several researchers (ie: Hurowitz and McLennan, 2005; Zimmermann and Spalletti, 2009; Wani and Mondal, 2010; Armstrong et al., 2013, 2014 2015; Nagarajan et al., 2014; 2015; 2017a) to assess the intensity of weathering in their region. For example, an increase in the Th/U ratios in sedimentary rock may suggest oxidative weathering and the presence of high kaolinite content (ie: McLennan et al., 1980; Taylor and McLennan, 1985). In a study conducted by Roddaz et al. (2006) on Neogene Amazonian sediments, higher Th/U ratios could indicate sediment sources with a minor recycling effect which may have originated from the upper granitic continental crust (Taylor and McLennan, 1985; Hassan et al., 1999; Bauluz et al., 2000). In contrast, lower Th/U could

represent changes in redox conditions or simply indicate sources with lower Th/U composition. Other researchers such as Nesbitt and Young (1984) displayed weathering trends using the Al_2O_3 - $CaO + Na_2O$ - K_2O triangular plot or more widely known as A-CN-K ternary diagram (**Figure 2.5**). The A-CN-K plot was based on the indices calculated using the formula $CIA = [Al_2O_3 / (Al_2O_3 + CaO^* + Na_2O + K_2O)] \times 100$. Weathering is characterized as intense if the values >80 while values less than 50 indicate unweathered condition (Nagarajan et al., 2015).

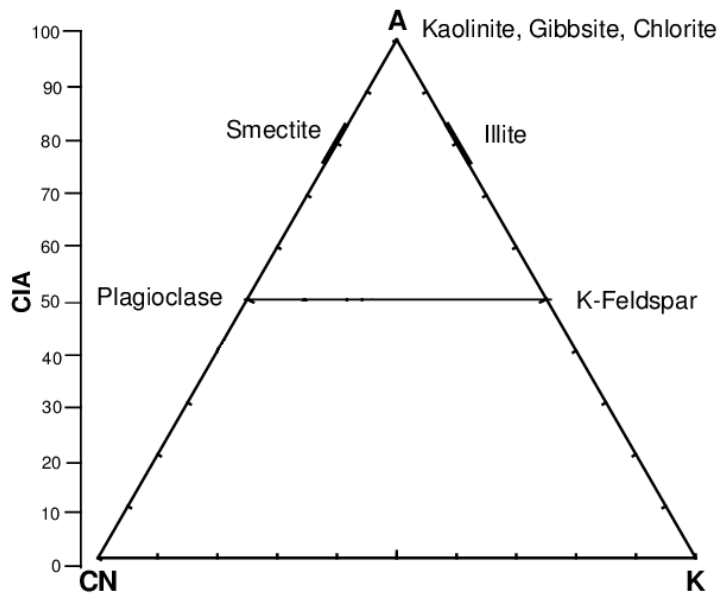


Figure 2.5 A-CN-K Ternary diagram suggested by Nesbitt and Young (1984). CIA value ranging from 70-100 is consider as moderate to high degree of chemical weathering. Meanwhile 50-70 CIA value represents low degree of chemical weathering.

2.5 Clastic Sedimentary Rocks

Clastic sedimentary rocks are made from the older fragments of pre-existing rocks such as igneous rocks, sedimentary rocks and metamorphic rocks. The two most common clastic sedimentary rocks are sandstone and mudrocks.

2.5.1 Sandstone

Sandstone comprises one fourth of the world's sedimentary rock distribution. By definition, sandstone is a type of rock made of eroded fragments from other pre-existing rocks. This rock had been known to be an important economic resource as well as an effective reservoir for oil, gas and water (Nowrouzi et al., 2014). Changes in tectonic settings or modifications of provenance terranes will be reflected in the sandstone composition (Dickinson, 1985), making it an important group of clastic sedimentary rocks for provenance study. In addition, sandstones are regarded as sensitive indicators for weathering and as a provenance of source area terranes (Roser and Korsch, 1986; Goetze, 1998; Cullers, 2000; Getaneh, 2002; Ohta, 2004; Huntsman-Mapilaa et al., 2005; Rahman and Suzuki, 2007 a; Tijani et al., 2010; Armstrong et al., 2013; Nowrouzi et al., 2014). The composition of the sandstone provides clues to understand the provenance, paleocurrents and depositional environments (Pettijohn, 1975). Until now, the relationship between tectonic setting and sandstone composition is mainly based on framework modes (Bhatia, 1983).

Currently, sandstone mineralogy has been adapted into the study of petrography (Refer to 2.6.1). Sandstone petrography has been used widely to infer the provenance and tectonic settings (i.e: Dickinson, 1970; Hossain et al., 2010; Saminpanya et al., 2014; Malaza et al., 2016) due to its very straightforward approach (Schieber, 1992). Provenance information is extracted through detailed observations of the compositional and textural features of the sandstones (Schieber, 1992). Studies have been conducted using the detrital modes of sandstones (mineralogy and geochemistry) to infer provenance and tectonic settings at different stratigraphic intervals as Precambrian (Schieber, 1992; Osae et al., 2006; Nagarajan et al., 2007a,b); Paleozoic (Cawood, 1983; Dickinson et al., 1983; Li et al., 2016; Bassis et al., 2016), Mesozoic (Saigal et al., 1988; Asiedu et al., 2000; Caja et al., 2007; Armstrong et al., 2013; Rodrigues and Goldberg, 2014) and Cenozoic (Maravelis and Zelilidis, 2009; Jalal and Ghosh, 2012; Van Hattum et al., 2006; 2013; Nagarajan et al., 2015; Ramkumar et al., 2018). As for geochemical study, researchers have utilized the chemical composition of the sandstone to relate it to the tectonic setting of the sedimentary basins (ie: Zhiming et al., 2013; Tawfik et al., 2015).

2.5.2 Mudrock

Mudrock is the term given for any rock made up of silt and/or clay. Mudrock exists throughout most of the major sedimentary environments. Despite their abundance, limited studies had been conducted on these rock types in comparison with sandstone and limestone (Potter, 2003). Interestingly, clues about the ancient depositional environment and how it has changed throughout geologic time might be reflected in the mudrocks' composition.

Sandstone can provide valuable information about tectonics and the transportation history of the sediments. In return, mudrocks complement the information gained from the assessment of sandstone by providing clues on the past oxygen levels, paleoclimates and depositional environments (Potter, 2003). The application of using mudrocks for the study of provenance also allows us to compare whether the sandstone units and mudrocks units derived from the same source had undergone same transportation modes and others questions related to the depositional environment (Potter et al., 2005). For example, Nesbitt et al. (1996) has suggested that elements are being transported and deposited with clays. Bjorlykke (2014) mentioned that mudstones are usually described based on their physical properties through observations of the outcrops, as well as the composition of their organic matter. However, their clay mineralogy is the most important analysis as it provides clues about their transportation, deposition and compaction (Potter et al., 2005).

Therefore, reconstructing provenance using clay mineralogy is preferable for samples containing higher percentages of mud. According to Potter et al. (2005), the clay fraction had undergone; a) Chemical and mineralogical modification by the weathering and diagenesis processes, b) The distance travelled may have caused the mixing of particles from different types of sources. The mixing of the different types of sources obtained from the muds' composition will give the provenance from a wider area and time period. This is in contrast to characteristics obtained from sandstones as it reflects the data from more immediate sources. With the variety of data from these two different rock types, it allows researchers to compare the provenance information of a terrigenous section.

2.6 Petrography and Geochemical Methods

2.6.1 Petrography

The petrographic modal composition of sands and sandstones contain information on composition and the texture of polycrystalline grains, which is useful for provenance studies as it can be linked to the parent-rock assemblages in the source area. The history of petrography began in 1828 by the Scottish physicist William Nicol. He invented a technique (called Nicol prisms) to produce polarized light by adding prisms made of Iceland Spar (calcite), which would then convert an ordinary microscope into a polarizing microscope. The development of petrography as a field of study intensified during the 1840s with the introduction of thin sections by Sorby (1880) and other researchers. The method later became the standard method for studying rocks.

In petrography, the point-counting method is a standard procedure for estimating the framework composition of sandstones (Dickinson, 1985). Dickinson also suggested the usage of the point-counting method particularly for provenance determination for samples having comparable grain sizes. Several point-counting methods have been introduced in the past to meet different research objectives. For the Glagolev-Chayes method, the counting usually includes roughly 300 to 600 points in a thin section (Chayes, 1949, 1956). The Glagolev-Chayes method was adapted by two different sedimentary petrography schools of thought, later two sets of classification schemes were introduced, the Indiana method and the Gazzi-Dickinson method.

The Indiana point-counting method discussed in Suttner (1974) and Suttner et al. (1981) is suitable for analyzing provenance, transport history and post-depositional modifications. The basic criteria for the Indiana method were based on the formalization of traditional sedimentary-petrographic classification systems, but was later developed to identify changes in sandstone composition due to weathering and transportation. Meanwhile, two separate researchers; Gazzi (1966) and Dickinson (1970) developed the Gazzi-Dickinson method with the same purpose, i.e. to minimize the effects of grain-size variations on sandstone composition.

The Indiana and Gazzi-Dickinson methods share two similarities: a) both methods formed the ternary diagrams based on the percentage of quartz, feldspar and lithic fragments observed. The Indiana method labeled them as QFR whilst the Gazzi-Dickinson method categorized them as

QFL, and b) Carbonate fragments are not taken into account in either schemes and labeled as “lime clasts” in the Gazzi-Dickinson method.

2.6.1.1 Quartz

Quartz was first used to assess provenance by Mackie (1896) through the observation of quartz inclusions. Later, the usage of quartz as provenance indicators was expanded by Krynine (1940, 1946) and Folk (1974). Both authors utilized the quartz’s undulatory extinction and polycrystallinity properties in order to classify them from their presumed parent rocks. The utilization of quartz for the study of provenance has also been discussed in Todd and Folk (1957) and Voll (1960). Blatt (1967a, b) had reviewed the classification presented by Krynine’s in 1940s using detrital quartz. Quartz had also been used to assess the mineralogical maturity of sedimentary rocks. Sediments containing higher proportions of quartz grains are considered mineralogically mature. Experiments on maturity in the past were conducted by targeting several groups of minerals (ie: Cozzens, 1931; Friese, 1931; Woodruff, 1937; Thiel, 1940).

Quartz has been used recently by researchers in their studies in Northern Borneo for assessing provenance (eg: Nagarajan et al., 2015), porosity and permeability (eg: Ben-Awuah and Eswaran, 2015). However, the identification of quartz as the main composition in sandstone was made indirectly using chemical approaches. For example, Nagarajan et al. (2015) adapted the X-ray diffraction (XRD) method to identify the mineralogy of the sandstone of the Sibuti Formation and used petrography for identifying the sandstones of the Lambir Formation (Nagarajan et al., 2017a). In another study from the Baram Delta, conducted by Ben-Awuah and Eswaran (2015), the quartz was identified by the Energy-dispersive X-ray spectroscopy (EDX) method. The researchers conducted a thin section analysis; however, their observations focused more on the texture since the research was designed to determine the quality of a reservoir affected by bioturbation activity. In regards to the petrography of Neogene sandstones from Northern Borneo (Miri region) this very limited study utilized quartz from onshore outcrops which had become an additional objective for conducting this particular research study.

2.6.1.2 Feldspar

The function of feldspar as a guide for provenance studies was generally not seen as equally important as quartz. This is simply because in contrast with quartz, feldspar components will

gradually decrease as the mineralogical maturity increases. Therefore, this observation might not be applicable for sediments that are derived from feldspar-poor terranes (Pettijohn, 1975).

However, there have been some studies where feldspar had been proven to be useful for provenance identification. Pittman (1963) suggested several types of feldspar may originate from different tectonic environments. For example, plagioclase feldspar has been used as an indicator of provenance in sedimentary rocks. Plagioclase feldspar naturally exists as an unstable component and is prone to weathering processes. The unstable characteristics allowed plagioclase feldspar to become more useful in studying younger rock sequences and in rapid deposition cases (Pittman, 1970). In his papers, Pittman (1963, 1970) has applied the twinning and zoning properties of plagioclase feldspar for the study of provenance. In several cases, the abundance of plagioclase feldspar can be associated with first-cycle materials and this has been supported by Kuenen (1959) and Folk (1959), as the plagioclase feldspar was found to be very scarce in second-cycle materials. Still, the usage of plagioclase feldspar for the study of provenance has been limited to specific situations. For example, the variation in terms of potential sources had resulted in the failure of Simonen and Kouvo (1955) in determining the source of plagioclase in the Finland region.

Based on the potassium (K) composition in plagioclase feldspars, Trevena and Nash (1981) separated both volcanic and plutonic source rocks. Their findings showed alkali feldspar originating from volcanic sources are more sodic than albite, while alkali feldspar with a potassic composition $> 85\%$ are plutonic-metamorphic in origins. Later, Maynard (1984) simplified the classification made by Trevena and Nash (1981) by dividing into high and low potassium (K) content. Maynard's classification was more effective because he concluded a high-K category should be considered as volcanic in origin, whilst a low-K category is of plutonic-metamorphic origins. In addition, Maynard (1984) also stated the sediments derived from island arcs are rich in Ca-plagioclase whilst sediment from passive continental margin are rich in Na-rich plagioclase (ie: albite).

2.6.1.3 Rock Fragments/Lithic Fragments

Apart from quartz and feldspar grains, rock fragments are another component helpful in provenance studies. Rock fragments or lithic fragments are defined as pieces of other rocks having been eroded down to sand size through sedimentary processes, are present as sand grains in

sedimentary rock, and can be derived from existing sedimentary, igneous and metamorphic rocks. For example, provenance of sandstone can be determined if the rock fragments found in the rock refer to a specific source area (Tucker, 2001). Therefore, rock fragments have a higher value in determining the provenance since they originated from the parent source rock (Boggs, 1968). The importance of rock fragments for deciphering provenance also has been mentioned in Potter (1978) and Dickinson and Suczek (1979).

However, there are some difficulties in utilizing rock fragments for provenance studies. This is often due to their smaller grain size, which has caused the identification of parent-rock more difficult. Usually, rocks are identified in the field and hand samples mainly based on the texture, structure, mineral composition and geologic occurrence. The likelihood of observing these properties decreases when the grain size is reduced due to breakage during transportation and depositional processes.

2.6.2 Quantitative Mineralogy

Quantitative Evaluation of Minerals by Scanning Electron Microscopy (QEMSCAN) is a combined techniques of scanning electron microscopy (SEM) and energy-dispersive X-ray (EDX) spectra. The basic concept of QEMSCAN uses the energy dispersive X-rays and/by identification based on the backscattered electron images which generate mineral maps (based on the mineralogical phases). The chemical composition captured from the x-ray and backscattered electrons allowing these mineralogical phases to be identified (Gottlieb et al., 2000; Butcher et al., 2010). The texture and the mineral associations can often be obtained from the mineral maps. QEMSCAN also produces results on quantitative mineralogy and grain sizes of the minerals. As for the mining industry, the usage of QEMSCAN allows the minerals associated with the economically valuable minerals to be identified and quantified (Lotter et al., 2011).

Generally, the QEMSCAN technique is often used together with other analytical techniques such as X-ray diffraction (XRD), scanning electron microscope-energy dispersive spectrometry (SEM-EDS) and optical petrography. Utilizing all these methods together can produce comprehensive results for provenance studies. Mining companies may use the data collected for designing their ore processing and recovery processes.

2.6.3 Bulk Rock Geochemistry

Successful studies using geochemical methods involving igneous rocks (eg: Pearce and Cann, 1973; Winchester and Floyd, 1977; Wood et al., 1979; Bailey, 1981) have led to the extension of the methods' utilized in sedimentary rocks (eg: Bhatia, 1983; Bhatia and Crook, 1986) especially trace and major elements. The geochemical approach allows a large sample number to be analyzed at a faster rate. In comparison with standard optical microscopy, the geochemical method gives multiple results without undermining the final interpretation. REE quantification is a good example of an effective geochemical method (McLennan et al., 1989; 1990; Mounteney et al., 2018).

In current practice, the relationship between sandstone composition and tectonic settings has been established using the framework mode, however, there are cases where the petrography method is not suitable for fine-grained sandstone and mudrocks (mudstone and shale) and bulk chemistry is a more effective technique to analyze them (Blatt, 1983; Haughton et al., 1991; Totten et al., 2000). As mentioned earlier (chapter 1), several factors may affect source rock compositions such as chemical weathering, sorting and diagenesis (McLennan, 1989; Weltje and von Eynatten, 2004) and is reflected in the form of chemical compositions.

Major and trace elements of mudrocks (mudstone and shale) have been widely observed to constrain the provenance and tectonic settings (ie: Cullers, 1994, 2000; McLennan et al., 1993; Pantopoulos and Zelilidis, 2011; Armstrong-Altrin et al., 2013). Chemical weathering intensity, maturity, provenance, the recycling effect and sediment type may be evaluated from the major and trace compositions (Nesbitt and Young, 1982, 1984; Taylor and McLennan, 1985; Wronkiewicz and Condie, 1987; Cullers et al., 1988; Herron, 1988; Roser and Korsch, 1988; Condie, 1993; McLennan et al., 1993; Cox et al., 1995; Gaillard et al., 1999; Borges et al., 2008; Lupker et al., 2012; Garzanti et al., 2013b, 2016; Garzanti and Resentini, 2016; Hossain et al., 2017; Nagarajan et al., 2017a).

Bhatia (1983) mentioned that among the commonly used discriminating parameters are $\text{Fe}_2\text{O}_3 + \text{MgO}\%$, and the $\text{Al}_2\text{O}_3/\text{SiO}_2$, $\text{K}_2\text{O}/\text{Na}_2\text{O}$ and $\text{Al}_2\text{O}_3 / (\text{CaO} + \text{Na}_2\text{O})$ ratios. Fe and Ti were found to have low immobility and low residence time (Holland, 1978). Quartz enrichment particularly in the sandstones is monitored by assessing the $\text{Al}_2\text{O}_3/\text{SiO}_2$ ratio (Bhatia, 1983). These discriminants are used to identify the tectonic settings. For examples, sandstones originating from

an oceanic island arc will show higher $\text{Fe}_2\text{O}_3 + \text{MgO}\%$, $\text{TiO}_2/(\text{Al}_2\text{O}_3/\text{SiO}_2)$ ratios with lower $\text{K}_2\text{O}/\text{Na}_2\text{O}$ and $\text{Al}_2\text{O}_3/(\text{CaO} + \text{Na}_2\text{O})$ ratios. Meanwhile, sandstones from a continental island arc will have the opposite results; lower $\text{Fe}_2\text{O}_3 + \text{MgO}\%$, $\text{TiO}_2/(\text{Al}_2\text{O}_3/\text{SiO}_2)$, higher $\text{K}_2\text{O}/\text{Na}_2\text{O}$ and $\text{Al}_2\text{O}_3/(\text{CaO} + \text{Na}_2\text{O})$ ratios. Other studies such as by Floyd and Leveridge (1987) used K_2O and Rb as an indicator for identifying source rock for sandstone.

Similarly, geochemical data also can be utilized to classify the sandstone based on the chemical composition. One of the most widely used sandstone classification was proposed by Herron (1988). The advantage of using Herron (1988) is that it avoids the alkali problems as well as measures the mineral stability. The presence of alkalis (Na_2O and K_2O) in the samples can be affected by the occurrence of other components such as micas, clays and lithic fragments. These components are able to contribute to the alkalis composition as well as potassium concentration (Lindsey, 1999). Questions might rise if one eliminates the alkalis in plotting the diagram as they are quite useful in discriminating between arkoses and greywackes (see Pettijohn, 1963). Similarly, under the thin sections, there could be a confusion between wackes and arkoses borderline. However, arkoses and greywackes can be distinguished directly by calculating the ratios for $(\text{SiO}_2/\text{Al}_2\text{O}_3)$; arkose is represented by log values <1.0 and subarkose is <1.3 (Lindsey, 1999). Compositional classes of arkoses from subarkoses, sublitharenites from litharenites and sandstones can be distinguished using the Herron's designed classification system (Lindsey, 1999). The weakness of Herron (1988) classification might occur in distinguishing litharenite and sublitharenite, however, this problem also experienced by other classification diagrams (eg: Pettijohn, 1963; Blatt et al., 1972). The variations in the answers when it comes to lithics are expected as each fragment is having variation in term of composition. There are several other geochemical classification available such as the one introduced by Blatt et al. (1972). However, their classification diagram did not emphasize on classifying the sandstone further into different classes as introduced by Folk (1965) or Pettijohn (1975). Instead, the classification divides them into sodic sandstones, potassic sandstones and ferromagnesian sandstones. This classification is rather difficult to compare with data gained from petrographic observation.

2.6.3.1 Major Elements

The usage of major elements in identifying the tectonic settings has been discussed by Schwab (1975), Bhatia (1983), and Roser and Korsch (1986). Due to the effects of sedimentary

processes, major elements are subjected to change in their composition as well. For example, the enrichment of SiO_2 in sedimentary basins will show a depletion of Na_2O and CaO in sandstone compared to the source rock composition. In a region controlled by the tectonic setting, major element chemistry is applicable in inferring the provenance type and weathering conditions (Bhatia, 1983). However, according to Maynard et al. (1982), it is easier to differentiate the sands from fore-arc basins and passive margins based on major elements distributions, but this might be difficult for other tectonic settings. Recent publications have utilized major elements for provenance studies (ie: Kroonenberg, 1994; Zimmermann and Bahlburg, 2003; Armstrong-Altrin et al., 2004; Castillo et al., 2015; Bassis et al., 2016; Ramachandran et al., 2016; Hernandez-Hinojosa et al., 2018; Tiju et al., 2018).

2.6.3.2 Trace Elements

The usage of trace elements allows the categorization of an igneous source to be identified as either relatively mafic or felsic easily. Low-mobility trace elements (ie: La, Th, Y, Zr, Ti, Co and Ni) are suitable for discriminating the sandstones formed in an oceanic island arc, continental island arc, an active continental margin or a passive continental margin settings (Bhatia and Crook, 1986).

Amongst the trace elements, Nickel (Ni) and Chromium (Cr) are considered important as they are abundant in ultramafic and mafic rocks and scarce in felsic rocks. Therefore, they are good indicators of ophiolitic sources and might indicate an arc-continent collision in the source area (ie: Totten et al., 2000). Zirconium (Zr) in contrast to Ni and Cr is more abundant in felsic rocks (Potter et al., 2005, p.167). This ensures the proportions of mafic materials in the source are quantified using Ni/Zr or Cr/Zr plot. However, the usage of Ni in the bivariate plots should be used carefully as the elements can be altered by weathering and the diagenesis processes due to having less solubility properties.

Other elements such as Thorium (Th) and Scandium (Sc) are also chosen as a good indicator for sedimentary provenance due to their insolubility (Potter et al., 2005, p.167). In a study by Pe-Piper et al (2008), Thorium (Th) was found to be useful in discriminating between mudrocks from different parts of the basin in comparison to other trace elements. These elements are often presented in the form of bivariate plots (ie: Th/Sc against Sc or Cr/Th against Sc/Th) to detect the existence of mixing processes in sediments (Condie and Wronkiewicz, 1990; McLennan

et al., 1990; McLennan and Taylor, 1991). Higher Th/Sc ratios along with an increase of La/Lu and Eu anomalies (Eu/Eu*) suggest felsic rocks as the dominant source, on the other hand, lower ratios indicate mafic rock origin (Ershova et al., 2015). The reliability of trace elements in comparing source areas for sandstones has been examined by Von Eynatten et al. (2003a).

2.6.3.3 Rare Earth Elements (REE)

Another important component of trace elements are Rare Earth Elements (REE). Rare Earth Elements (REE) exist in clastic sedimentary rocks originating from its provenance (Fleet, 1984; McLennan, 1989). In other words, REE composition is being controlled by the sediment provenance (Taylor and McLennan, 1985; Condie, 1991; Yang et al., 2002; Song and Choi, 2009). REE are known to be relatively insoluble under most geological conditions, which allows REE to be used as provenance tracers (Rollinson, 1993). They exist in very low concentrations (ranging from 10×10^{-7} to 10×10^{-2}) in river and seawater (Potter et al., 2005).

The reliability of REE has been acknowledged and used as provenance indicators by several authors (ie: Taylor and McLennan, 1985; McLennan, 1989; Wronkiewicz and Condie, 1989; McLennan et al., 1995; Suzuki et al., 2000; Munksgaard et al., 2003; Rahman and Suzuki, 2007; Dou et al., 2010; Um et al., 2013, Ramkumar et al., 2018). REE is more reliable compares to heavy mineral, as heavy minerals sometimes unable to discriminate between opaque and transparent minerals; for example, optically it is difficult to identify chrome-spinel from other minerals (Mounteney et al., 2018).

2.6.3.4 Heavy Minerals

As mentioned earlier in the introduction, heavy minerals are among the components useful in deciphering the provenance. Sediments containing heavy minerals from different source areas are easily distinguishable, as heavy minerals exist in specific source rocks (Morton and Hallsworth, 1999; Sevastjanova et al., 2012). In general, heavy minerals can be classified into either the transparent group (ie: apatite, garnet, monazite, staurolite, tourmaline, rutile, and zircon) or the opaque (ie: chromite, goethite, hematite, ilmenite, leucoxene, magnetite and pseudorutile) group (Pettijohn et al., 1973; Kettanah and Ismail, 2016).

The importance of heavy minerals in provenance studies such as tourmaline and chromite spinel has been briefly discussed in Chapter 1 (Introduction). Other major heavy minerals such as apatite, rutile and zircon also play an important role in provenance studies (ie: von Eynatten and Gaupp, 1999; Asiedu et al., 2000; Morton et al., 2005; Bojar et al., 2010; Olivarius et al., 2014; Krippner et al., 2016). Detrital zircon is among the commonly used heavy minerals as it can be used in estimating the age of the source rocks (ie: Carter and Bristow, 2003; Jacobsen et al., 2003; Rahl et al., 2003; Wang et al., 2016). Meanwhile, presence of rutile may indicate sources from medium to high grade metamorphic rocks (Force, 1980) or indicate their association as an accessory mineral in granites, eclogites, gneisses, schists and pegmatites (Shi et al., 2016).

However, the occurrence and ratios of the heavy minerals can be altered by the sedimentary cycles (Morton and Hallsworth, 1999). Thus, any heavy mineral ratios differences may not represent different sources of origin but signify more about the sedimentary cycle processes. This is because a particular environment and climate may strongly affect the stability of heavy minerals (Pettijohn 1941; Morton and Hallsworth, 1999; Velbel, 2007; Ando et al., 2012; Morton, 2012; Garzanti et al., 2013). Precautions can be taken to cope with ratio variations; any heavy mineral analysis related study should include all grain size fractions. Sedimentary cycles can cause segregation and sorting of grains as they are transported from the source area to the depositional basins (Morton and Hallsworth, 1999; Garzanti et al., 2009; Krippner et al., 2015, 2016). World wide, studies on heavy minerals are not limited to deciphering provenance. Heavy mineral analysis also applied in forensic science (ie: Smale and Trueman, 1969; Isphording, 2007; Palenik, 2007), the mining industry (ie: Belousova et al., 2002; Nowicki et al., 2003; Salama et al., 2016), in the correlation of strata with limited or no fossils and in the reconstruction of source to sink sediments. By considering heavy minerals, this study gives new insights into deciphering the provenance of sediments.

2.6.3.5 Zircon Dating

Detrital zircon Uranium-Lead (U-Pb) dating analysis is not new in the field of provenance studies. and has proven to be one of the most powerful tools in inferring provenance for sedimentary rocks (eg: Sevastjanova et al., 2010). U-Pb dating analyses were originally aimed to be used in radiometric dating methods for igneous and metamorphic rocks. Unfortunately, several geographic

areas, for example Northwestern Borneo, contain a limited number of igneous or metamorphic rocks, which can be used for dating analyses. Thus, researchers have been applying this method for dating the deposition of sedimentary rocks. The usage of detrital zircon to constrain the depositional age of clastic sedimentary rocks has been widely studied by researchers (eg: Yamashita et al., 2000; Xiangyang and Mann, 2014; Zhong et al., 2015). Several researchers even used the method to evaluate the time of deposition of calcretes (eg: Wang et al. (1998). Meanwhile, the reliability of detrital zircon has been discussed in several papers (eg: Brugiuiier and Lancelet, 1997; Kosler and Sylvester, 2003; Federico et al., 2004).) The method of dating detrital zircons has been a useful tool in basin analysis studies, for the determination of the time of sediment. On the Island of Borneo, zircon U-Pb has been used in some recent studies for reconstructing provenance, for determining tectonic settings and for the mining exploration of diamonds (eg: Witts et al., 2012; Kueter et al., 2016; White et al., 2016; Breitfield et al., 2017; Galin et al., 2017).

2.7 Status of research in Northern Borneo

The full mineralogical and geochemical characteristics of the Tukai Formation and several surroundings formations are not fully investigated. Existing literature published from Sarawak region showed less attention being given on the geochemistry, provenance and paleoweathering on onshore clastic sediments. Tectonic interpretation and reconstructions are made on computer-based, tectonic modelling and seismic data with less involvement in the field studies (i.e Mat-Zin and Swarbrick, 1997; Singh et al., 2009; Cullen, 2010; Morley et al., 2008; Vijayan et al., 2013). Among reviewed published literature, main focus has given on stratigraphy (eg: Morrison and Lee, 2003; Kosa, 2015), structural geology (eg: Morley et al., 2008;), depositional tectonic settings (eg: Lim and Mohd Shafea,1994; Abd Rahman et al., 2014; Collins et al., 2017), marine geophysical survey (eg: Zampetti et al., 2004) , faunal assemblages and petroleum geology (eg: Keij and Harcourt, 1965; Wan Hasiah, 1999; Ingram et al., 2004; Ali and Padmanabhan, 2014; Togunwa et al., 2015; Collins et al., 2017) and little studies have concentrated on the provenance of the Neogene sediments (Nagarajan et al., 2014, 2015 and 2017a, c).

Current research pattern showed more interest being put on going further onto the offshore of Sarawak and less exposure for the formation available onshore. This is mostly driven by ongoing researches going for the oil and gas exploration and also the inaccessibility of onshore outcrops due to the thick forests. For example, current research trend focuses on understanding Baram Delta,

Dangerous Ground, Northwest Borneo Trough, Central Luconia Basin and carbonate platforms and deep sea sediments of South China Sea (eg: Lambiase et al., 2002; Zampetti et al., 2004; Morley et al., 2008; Abdul Rahman, et al., 2014; Ben-Awuah and Eswaran, 2015; Kosa, 2015; Togunwa et al., 2015; Liu et al., 2016 (references there in); Ben Awuah et al., 2017; Hall and Breitfeld, 2017).

For Northwest Sarawak, several notable publications such as stratigraphic scheme for Sarawak Basin was proposed by Mat-Zin and Tucker (1999), facies distribution and sedimentary processes in modern Baram Delta and its implications on sandstones reservoirs was discussed by Lambiase et al (2002), normal fault evolution in siliciclastics sequence for Miri Formation was discussed by Van Der Zee and Urai (2005), comparison between reservoir characters of Miri Formation and Nyalau Formation was made by Jia and Rahman (2009), Neogene organic-rich sediments on hydrocarbon and source rock potential by Togunwa et al. (2015), morphotectonic analysis on Rajang and Baram basins (Mathew et al., 2016) and geochemistry of offshore Miocene sedimentary rocks (Ben Awuah et al., 2017).

The scenarios had been changing recently with many researchers focused their research in North West Borneo sediments, particularly over the past 4-5 years (2013-2018). Some publications were made from this are (ie: Lambiase and Cullen, 2013; van Hattum et al., 2013; Nagarajan et al., 2014, 2015, 2017a,c; Galin et al., 2017). Based on the literature review, limited number of research studies have been carried out on the petrography and geochemical signature of North West Borneo sediments and in Sarawak as overall. Only by recently, we can see some researchers started to explore the onshore Sarawak for the study of provenance and tectonic setting (ie: Ferdous and Farazi, 2017) and interior Sarawak focusing on Rajang Group (ie: Galin et al., 2017).

In comparison with the other two formations (Lambir Formation and Liang Formation), it is clearly showed that few researches have been conducted on Tukai Formation. Several researches had been conducted involving Lambir Formation particularly in the field of paleo-depositional environment, provenance, paleoweathering, and tectonic settings (ie: Ali and Padmanabhan, 2014; Nagarajan et al. 2017a).

As for Tukai Formation, limited published papers related closely to the formation. For example, preliminary geochemical study by using a limited data set (concentrated on lower part of

Tukau Formation), Nagarajan et al. (2014), has shown that the clastic sediments of the Tukau Formation are mainly derived from felsic source region and they were deposited in a complex tectonic setting. This is later followed by follow-up studies by Nagarajan et al. (2017). Their findings can be relatable to the results obtained by Hall and Nichols (2002) which also showed that the Neogene sediments in Borneo contained some basement rocks composition in the clastic sediments. This is further supported by studies that throughout Cenozoic, the recycle orogenic source patterns have been observed in the clastic sediments (ie: van Hattum et al., 2006; Tanean et al., 1996). The contribution of sediments from ophiolites and or from some mafic suits from the source region raises the question on how and when the formation formed. Hence, it might indicate that the Tukau Formation may hold the same provenance and tectonic settings as the other Neogene sediments would be premature as each provenance, geography and their plate tectonic location probably differs which affecting their stratigraphic sequences (Beddoes,1981). In a separate study by Togunwa et al. (2015) on source rocks implications and hydrocarbon generative potential, it was found that Total Organic Carbon (TOC) is more than 1% in coal/organic layers interbedded within sandstone which indicate that the organic layers inderbedded within the sandstones of the Tukau Formation have good source potential. Their findings also concluded that the kerogen type for Tukau Formation is Type III. However, the rocks belong to Neogene period (Lambir, Miri and Tukau Formations) has not been subjected to enough temperature to generate hydrocarbons.

Overall, it is very clear that very few studies have concentrated on the geochemistry of the Neogene clastic sediments in order to address their, provenance, weathering, and tectonic settings and rarely on mineralogy. Thus, this research work is proposed on minerogical, petrographical and geochemical studies on North West Borneo sediments (the Tukau Formation).

CHAPTER 3

RESEARCH METHODOLOGY

3.1 Introduction

This chapter outlines the methodology used in completing the research. All sample collections, preparations and analysis methods are included in this chapter.

3.2 Research Methodology

The methods used throughout this research were a combination of mineralogy, petrography and geochemistry (bulk geochemistry, mineral chemistry and U-Pb geochronology). The combined methods have been widely used worldwide for provenance studies (ie: Schieber, 1989; Kutterolf et al., 2008; Pantopoulos and Zelidis, 2012; Perri et al., 2013; Nowrouzi et al., 2014; Ershova et al., 2015; Kyaw Linn et al., 2015; Madhavaraju et al., 2017). Combining data from various methods can yield more valuable information to elucidate the provenance, paleoclimate, and sedimentary environments (ie: Perri and Ohta, 2014). Furthermore, applying both methods allowed for assessing the agreement between the two approaches and finally, refining the knowledge on the Tukai Formation. Each step taken for each of the methods has been explained separately in this chapter.

3.3 Sample Types and Sampling

Sampling plays an important part for any lab analysis procedure involving the process of collecting data. The chosen sampling technique depends on the materials, availability of equipment, the sampling environments and the objectives of the study (i.e. Camuti et al., 1999). For this study, sandstones, siltstones, mudstones and some shales have been used from the Tukai Formation. The samples were collected from the exposed outcrop of the Tukai Formation based on their lithological variation and stratigraphic thickness. Fresh clastic sediments were collected using a modified hand core pipe, kept inside a sealed plastic bag and labeled immediately after sampling. In total, 5 outcrops were selected in which 4 of them has been exposed continuously with possible access but the 5th outcrop is stratigraphically located on the top of others with some interval. These outcrops are well exposed in the Bakam and Brick Valley of Sg.Rait region. 100 sediment samples

were collected from the upper Tukau Formation located in the NW Sarawak, East Malaysia. Later, in the lab, the samples were further divided into consolidated and unconsolidated types.

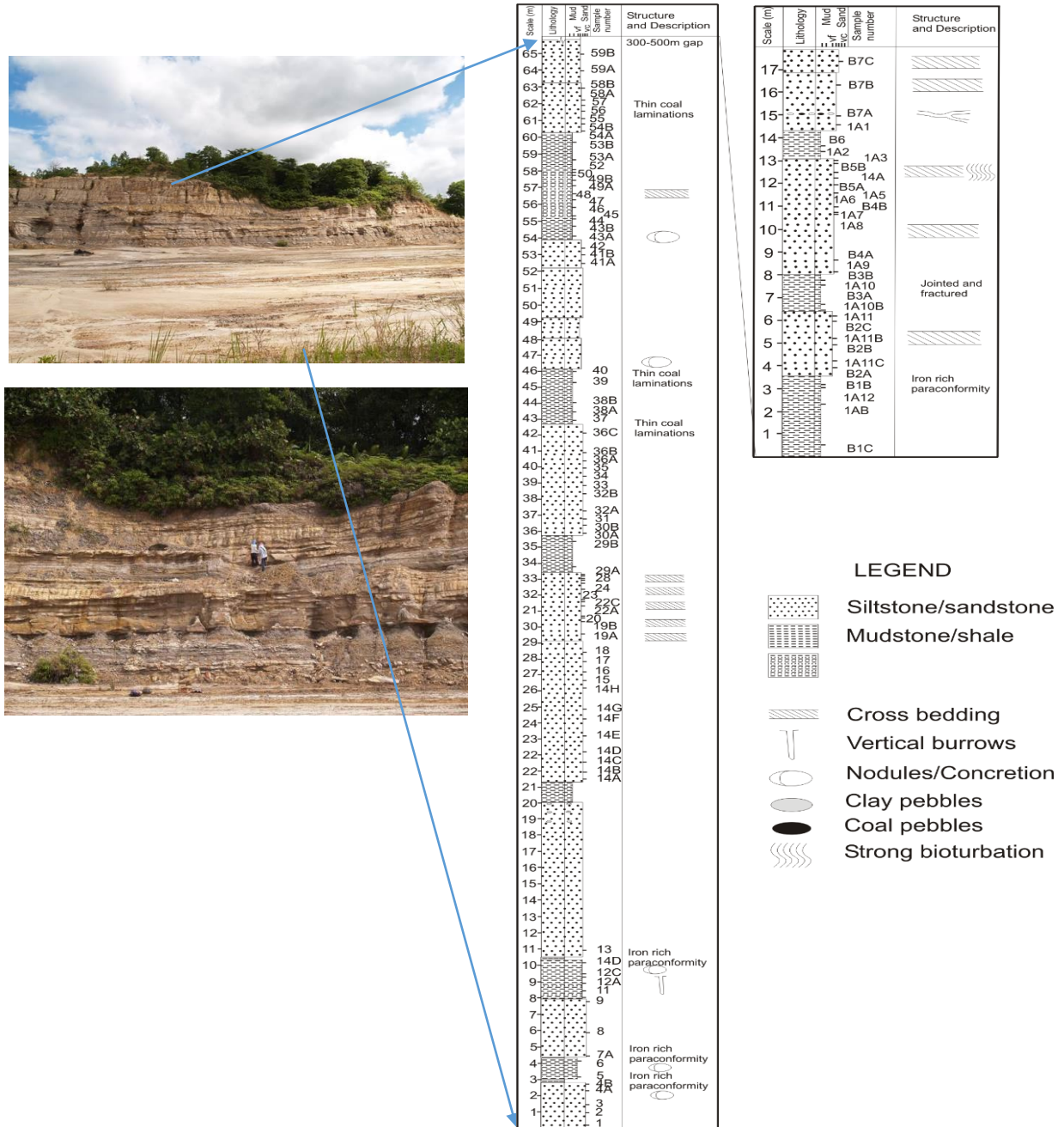


Figure 3.1 Stratigraphic log and sample position from the Tukau Formation exposed near the Brick Valley of Sg.Rait region (the outcrops exposed near Sg.Rait region is shown in the photos) Credit: Dr. Franz Kessler.

3.4 Petrography

Sandstone was the primary sample for the petrography analysis. The petrography method used in the sample preparation was modified from Hirsch (2012) and requires the availability of particular equipment and materials. Equipment required for the sample's preparation include an Ingram-WARD trim saw with grinder and a Hillquist polishing machines are available in the Sedimentology Lab, Curtin University, Malaysia.

3.4.1 Thin Section Preparation

The first step for the thin section preparation was to dry the samples using a laboratory oven. This drying method is suitable for this research purpose with the assumption was the sediment samples contained a low percentage of expanding clay content and no soluble minerals are being investigated (Drees and Ulery, 2008). For their research, no clay properties were being investigated, therefore, the effect could be ignored. Samples were left to dry in an oven set at 40°C for roughly 8 hours to eliminate any moisture content. A temperature set at 40°C helps in minimizing the effects of sample shrinkage and crackings. Drying the samples at this temperature will allow any organic content to be retained and can be used later for other investigations. After completely drying, the samples were later impregnated with 50ml of part A (Resin), 50ml of part B (Hardener) and 25ml of acetone. The samples were left to harden for roughly 3 hours (on a heating plate) with a temperature of < 80°C. Hardened samples were cut using the trim saw into a slab roughly 2 cm x 3 cm for each of the samples. One side of the slab was labeled while the other side of the slab was flattened and lightly polished on a glass plate with 1000 grit carborundum powder. After flattening and polishing the slab, they were dried for four to five hours in an oven with a temperature of around 100°C. After drying, the glass slide was glued to the lapped surface using epoxy glue (Loctite Hysol 0151). The sample was allowed to set overnight to ensure the sample was satisfactorily glued to the slide. Later, using the thin section saw, the slab was cut close to the slide. The thickness of the slab was maintained at 3mm. A finished thickness of the slab was achieved by lapping the section by hand on a glass plate with 1000 grit carborundum powder. Detailed steps on the thin section preparation can be refer to **Appendix 2.0**.

3.4.2 Petrography Laboratory Analysis

Point counting using the modified Gazzi-Dickinson method was adopted for this petrographic analysis. A total of 300 points per thin section were analyzed (Osae et al. 2006). If the sandstones are well-sorted with medium grains, only the grains with diameters in the range of 0.20 to 0.60 mm were counted (eg. Cox & Lowe, 1996). Later, the counted points were summed up in a table and used for quantitative compositional analysis. The quartz, feldspar and lithic fragments ratio was used to classify the sandstones and to trace the provenance and tectonic setting (Dickinson, 1970; Folk, 1974).

3.5 Sedimentary Textures

The sedimentary textures were observed in terms of grain size and shape.

3.5.1 Measuring grain size

The selected method in determining the grain size was based on the size of the particles (as seen with the naked eye and with the help of a grain size chart) and the state of the consolidation. Most of the samples collected from the Tukai Formation were poorly consolidated and some were in an unconsolidated state due to high fragility. Thus, the determination of the grain size and sorting were interpreted based on a visual inspection using a binocular stereomicroscope and a polarizing microscope and with the help of sediment grain size scale (**Figure 3.2 and 3.3**).

The grain size was first estimated using the grain size chart while observed under the binocular stereomicroscope. The grain size was later confirmed with a similar measurement made using the thin sections using a polarizing microscope (NIKON 50i Eclipse) fitted with an ocular micrometer.

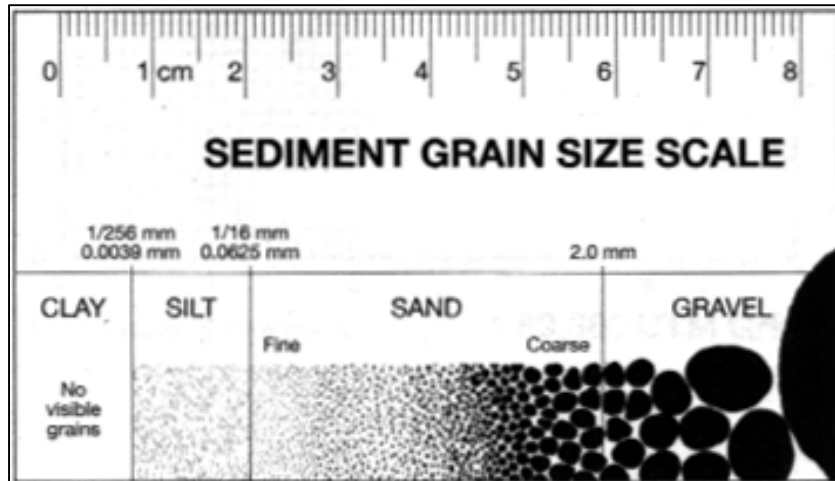


Figure 3.2 Example of grain size scale for rough grain size estimation

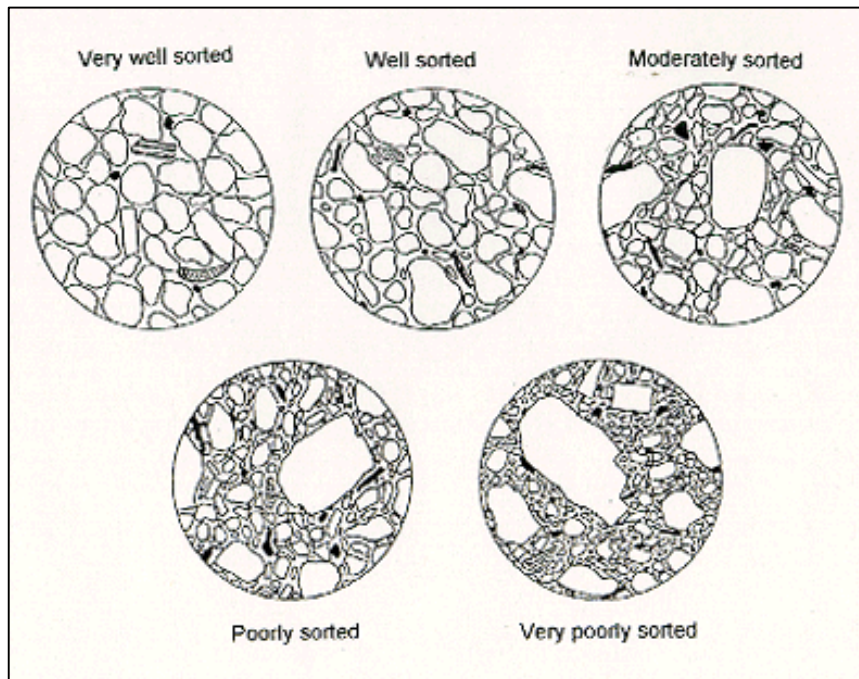


Figure 3.3 Example of grain size visual sorting estimating chart

3.5.2 Grain Shape

As discussed in Chapter 2, grain shape can be described by its form, roundness and surface textures. For this research, only the roundness parameter was taken into consideration. The estimation of the particle roundness was aided by the use of a visual estimation charts as proposed by Powers (1953) and shown in Figure 3.4.

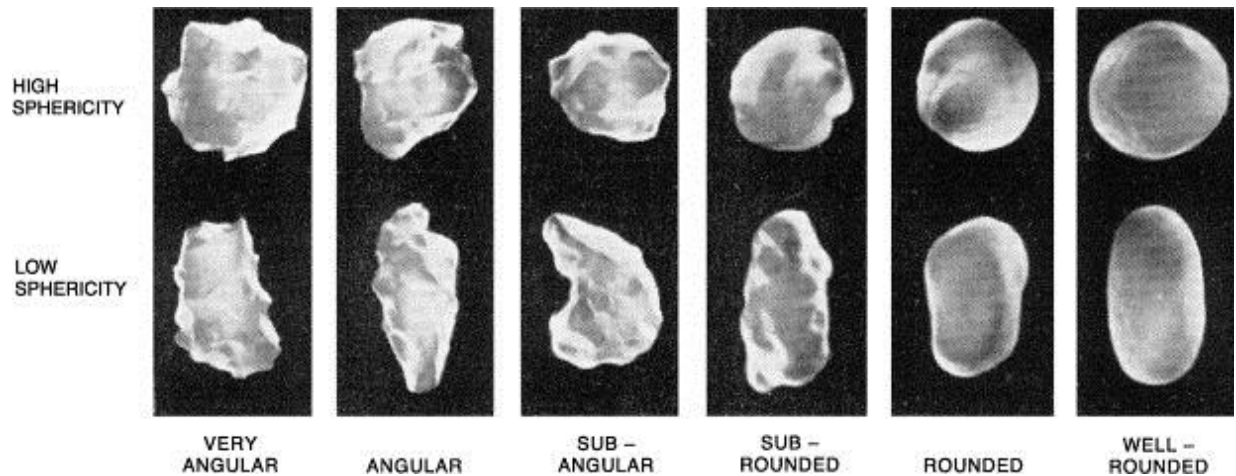


Figure 3.4 Example of grain images for estimating the roundness of sedimentary particles (Powers, 1953).

3.6 Mineralogy and Mineral Chemistry

20 samples (11 sandstones; 7 mudstones and 2 mixed/interbedded rocks) were analysed to determine their advanced reservoir quality, which involved bulk mineralogy, clay mineralogy, heavy mineral analysis and mineral chemistry. All 20 samples were analysed under the QEMSCAN and 7 samples were later analysed under the XRD. Heavy minerals were segregated from 4 selected samples which later were analysed for their chemistry and captured in images. Out of the 4 samples, one sample was discarded due to insufficient heavy minerals.

The QEMSCAN system is an automated scanning electron microscope-based system that locates and mineralogically maps materials using a combination of backscattered electron and characteristic X-ray signals providing unbiased chemical-mineralogical data. Although typically used for analysis of inorganic solids such as rocks, the QEMSCAN mineral analysis system is also well suited to analysing virtually any chemically distinct material whether biogenic (e.g. diatoms, foraminifera etc) or inorganic (i.e. sediment or precipitates). The instrument captures the images (elemental signatures) of the particulates (or areas) within the sample and thus provides not only an indication of the chemistry and mineralogy of the materials present, but also the textural characteristics of the sample.

3.6.1 QEMSCAN Analytical Parameters

All samples were clean, oil-free samples and prepared as 30 mm polished epoxy resin blocks without any prior treatment. They were first resin-impregnated and then cut to size prior to becoming embedded in epoxy resin. Later, they were mineralogically mapped using a fieldimage technique. This analytical methodology scans an electron beam over the field of view at a pre-determined beam-stepping interval, which depends on the sample texture and grain size. In this study, a 10 µm step interval was used for coarser lithologies. At each step, a combination of BSE and X-ray signals were used to create a mineralogical image of the sample.

3.6.1.1. QEMSCAN Data Processing

Using the QEMSCAN image analysis software (iDiscover), all of the images were processed in order to optimize the reported mineral list to the samples measured and may include mineral species, biogenic species, man-made materials and precipitates. Multiple mineral lists (**Table 3.1**) can be used to define the mineralogy of samples and simplify reporting.

3.6.2. X-Ray Diffraction (XRD)

X-ray diffraction analysis is a material identification methodology that uses the characteristic crystal structure of a material to make a positive phase identification. This methodology is therefore well suited to the analysis of minerals and other crystalline solids. However, as the methodology relies on the measured materials having a crystal structure, amorphous or poorly crystalline material may not be identified or may be subject to some detection limits. In this study, the primary aim of the XRD analysis was to determine the clay species mineralogy of the samples and in particular, identify the presence of swelling clay (e.g. smectite), and provide an indication of crystallinity and interlayer ordering. First, samples were hand crushed allowing 90 % of it to pass through a 710 µm sieve and the resulting material split into two aliquots; one for whole rock analysis and the second for clay speciation analysis.

Table 3.1 Description of the mineral categories reported in this study with QEMSCAN and combination with BSE and X-ray signals

Mineral	Description
Quartz	Silica group of minerals (e.g. quartz, cristobalite, etc). Includes opal and chert.
K Feldspar	K-rich alkali feldspar including orthoclase, sanidine & microcline.
Albite	Na-rich plagioclase compositions such as albite. May also include Na-rich alkali feldspar compositions. May include analcime and / or specific zeolite compositions where present.
Calcic Plagioclase	Calcic plagioclase compositions ranging from oligoclase to anorthite. May include specific zeolite compositions where present.
Muscovite	Muscovite and Al-rich white mica such as sericite.
Biotite	Biotite and phlogopite. May include specific compositions of glauconite (minor-trace amounts).
Kaolinite	Kaolinite group such as dickite, halloysite & kaolinite ss.
Chlorite	Chlorite group minerals such as chamosite, clinochlore, etc. May include specific compositions of garnet and/or tourmaline. May also include staurolite and specific compositions of volcanic glass.
Calcareous illitic clays	Illite and illite-dominant illite-smectite finely intermixed with calcite. May include specific mixtures of calcite, kaolinite and illite.
Calcareous Fe illitic clays	Ferroan illite and illite-dominant illite-smectite intermixed with calcite. May include specific mixtures of calcite, kaolinite and illite.
Illite & illite-smectite	Illite and illite-dominant illite-smectite. May include specific mixtures of kaolinite and illite.
Fe-Illite & illite-smectite	Ferroan illite and illite-dominant illite-smectite. May include specific mixtures of kaolinite and ferroan illite or Fe oxides.
Calcite & Aragonite	Calcite, aragonite, etc.
High Mg Calcite	High magnesium calcite.
Dolomite	Non-ferroan dolomite.
Ferroan Dolomite	Ferroan dolomite. Fe is typically present in quantities exceeding 5 wt %.
Fe Oxide & siderite	Fe Oxides such as magnetite and hematite. May also include Fe hydroxides and carbonates such as goethite and siderite.
Pyrite	Pyrite and marcasite.
Sphalerite	Sphalerite and other Zn-bearing sulphides / sulphates.
Barite	Barite and celestine.
Rutile & Ti Silicates	Ti-Oxides such as rutile or anatase. May include altered (Fe-poor) ilmenite. Any Ti silicates such as titanite have been included in this category for brevity.
Tourmaline	Mg-Fe tourmaline (e.g. dravite / schorl). May also include certain compositions of chlorite.
Apatite	Apatite, hydroapatite and bone. May also include Ca-phosphate pellets.
Zircon	Zircon. May include Hf-bearing zircon and Zr-bearing hafnon.
Monazite	Monazite.
Xenotime	Xenotime.
?Florencite	Ce Al Phosphates including florencite.
Chromite	Chromite and chrome spinel. Compositional analysis indicates that most grains are Al- and Mg-bearing.
<i>Epidote</i>	<i>Epidote, zoisite and piedmontite. May include specific compositions of Fe-rich amphibole.</i>
Amphibole / Clinopyroxene	Amphibole and pyroxene. Includes Fe-rich varieties such as actinolite and Mg-rich varieties such as magnesiohornblende and augite.
Andalusite	Andalusite. May include kyanite and sillimanite if present. Optical analysis indicates that the majority of grains are andalusite.
Garnet	Garnet. Compositions are variable but predominantly Fe-rich (almandine) and Mn-rich (spessartine).
Ilmenite	Ilmenite.
Ca Sulphate	Ca sulphates such as gypsum and anhydrite.
Undifferentiated	Undifferentiated mineral phases (trace quantities).

3.6.2.1. Whole Rock Geochemistry

The aliquot for whole rock analysis was milled and a known quantity of an internal reference standard was added (in this case, fluorite). The addition of an internal standard served to quantify amorphous material and is also used for quality control. After the internal standard was added, the samples were micronized and the resulting homogeneous powder analysed by XRD. The phases present in each sample were then identified and quantified by the Rietveld Refinement method. Where required, the amorphous content was also estimated by reference to the internal standard.

3.6.2.2. Clay Speciation

For clay speciation analysis, clays were first concentrated through a combination of ultrasound and centrifugation. The resultant concentrated clay fraction was analysed and then repeatedly analyzed after progressive glycolation and heat treatments (heated to 400°C and 550°C). Different heating temperatures caused the layers of the clay to collapse and produced different peak positions. The types of clay presents in the sample were being identified based on the peak positions produced during the analysis.

3.6.3 Heavy Mineral Separation and Analysis

The heavy minerals were concentrated using a heavy liquid separation technique. The resulting heavy mineral concentrate was then analysed using a combination of techniques to provide an indication of sediment provenance. The measuring instrument used to analyse the heavy mineral concentrates included scanning electron microscopy (SEM), optical microscopy and QEMSCAN. In order to provide additional detail, compositional data were collected for a range of minerals such as chromite, zircon, rutile, apatite, tourmaline and garnet grains.

Whole rock samples were dried, weighed then crushed to a 150 µm size. All samples were then wet screened at 20 µm. Both fractions (+20 and -20 µm) were dried and weighed. The +20 µm material was subjected to heavy liquid separation using TBE with a specific gravity of 2.96 g/cm³. Sediments were washed with acetone, then dried and weighed. All material fractions were

retained for subsequent analysis. The heavy mineral concentrates were then prepared as grain mounts for SEM / QEMSCAN analysis by sprinkling grains onto a 30 mm diameter stub covered with adhesive carbon tape. A conductive carbon coating was applied prior to analysis. A subsample was also examined optically to validate the SEM / QEMSCAN data. Subsequently, loose grains were mounted on a glass slide and observed under both reflected and transmitted light using a standard petrographic microscope.

3.6.3.1.SEM Imaging Parameters

Samples were imaged under high vacuum using a combination of a secondary electron signal (Primarily for topographic / morphological analysis) and a backscattered electron signal (primarily compositional analysis). Grain types were identified based on backscatter electron brightness and qualitative EDS spot chemical analysis. Detailed, quantitative EDS spot analyses of selected grains, typically chromite, tourmaline and garnet were also undertaken. A range of accelerating voltages (from 15 kV to 25 kV; typically 25 kV) and beam currents were used during imaging in order to maximize image quality and optimize EDS spot analysis.

3.6.3.2.QEMSCAN parameters

Heavy mineral concentrates were analysed using the QEMSCAN to determine the heavy mineral phases present. The samples were analysed using a similar methodology to that outlined above under *QEMSCAN Analytical Parameters* using a beam stepping interval appropriate for the grain size of the sample but typically either 5 (for fine grained samples) or 10 μm (for coarser grained samples). In addition to the heavy minerals of interest, other dense minerals were also present in the heavy mineral concentrates e.g. pyrite and siderite. As these phases are primarily authigenic, they were excluded from the data set. In order to minimise bias from the different grain sizes in the heavy mineral grain species, all data were presented as normalised grain counts i.e. the number of grains of a specific mineral expressed as a percentage of the total number of grains measured.

3.7 Geochemical analysis

100 sediment samples were collected from the Upper Tukai Formation in the NW Sarawak, East Malaysia. Among these 100 samples, 63 fresh or unweathered rocks samples were selected for geochemical analyses (i.e. determination of major, trace and rare earth elements) based on the lithology and locality in the stratigraphic column. These selected samples were oven dried at 40°C, homogenized and subsequently ground to a 230 mesh using an agate mortar. The oxides of 10 major elements (Si, Al, Ti, Fe, Ca, Mg, Na, K, Mn and P) were measured in fused discs following the methods of Verma et al. (1996) and Lozano and Bernal (2005) in a Siemens SRS 3000 wavelength dispersive X-ray Fluorescence (XRF) spectrometer. The precision of the analysis is ~10% for both major elements (Roy et al., 2010; Nagarajan et al., 2014). Trace and rare earth element (REE) analysis was carried out with 50 samples at the Activation Laboratories Limited, in Canada using a Code 4LITHO (11+) Trace Element Fusion ICP/MS (WRA4B2) package. The most effective fusion technique was employed with a lithium metaborate/tetraborate fusion for the trace and REE analyses. The resulting molten bead was rapidly digested in a weak nitric acid solution and measures were taken to ensure ensure the entire sample was dissolved. Further analyses were carried out using ICP and ICPMS. Certified reference materials NIST 694, W-2a, NCS DC70014, LKSD 3 were used to ensure the accuracy and precision of the geochemical analysis. The accuracy and precision for the analysis was better than $\pm 5\%$. The list of the elements analyzed, the detection limits and instrument details are summarized below (**Table 3.2**).

Table 3.2 List of elements analyzed, unit, detection limit and instruments details

Analyte Symbol	Unit Symbol	Detection Limit	Analysis Method
SiO ₂	%	0.01	XRF
Al ₂ O ₃	%	0.01	XRF
Fe ₂ O ₃ (T)	%	0.01	XRF
MnO	%	0.001	XRF
MgO	%	0.01	XRF
CaO	%	0.01	XRF
Na ₂ O	%	0.01	XRF
K ₂ O	%	0.01	XRF
TiO ₂	%	0.001	XRF
P ₂ O ₅	%	0.01	XRF
LOI	%	0.1	XRF
Be	ppm	1	FUS-ICP
V	ppm	5	FUS-ICP
Ba	ppm	3	FUS-ICP
Sr	ppm	2	FUS-ICP
Y	ppm	2	FUS-ICP
Zr	ppm	4	FUS-ICP
Cr	ppm	20	FUS-MS
Co	ppm	1	FUS-MS
Ni	ppm	20	FUS-MS
Cu	ppm	10	FUS-MS
Zn	ppm	30	FUS-MS
Ga	ppm	1	FUS-MS
Ge	ppm	1	FUS-MS
As	ppm	5	FUS-MS
Rb	ppm	2	FUS-MS
Nb	ppm	1	FUS-MS
Mo	ppm	2	FUS-MS
Ag	ppm	0.5	FUS-MS
In	ppm	0.2	FUS-MS
Sn	ppm	1	FUS-MS

Table 3.2 (contd...) List of elements analyzed, unit, detection limit and instruments details

Sb	ppm	0.5	FUS-MS
Cs	ppm	0.5	FUS-MS
La	ppm	0.1	FUS-MS
Ce	ppm	0.1	FUS-MS
Pr	ppm	0.05	FUS-MS
Nd	ppm	0.1	FUS-MS
Sm	ppm	0.1	FUS-MS
Eu	ppm	0.05	FUS-MS
Gd	ppm	0.1	FUS-MS
Tb	ppm	0.1	FUS-MS
Dy	ppm	0.1	FUS-MS
Ho	ppm	0.1	FUS-MS
Er	ppm	0.1	FUS-MS
Tm	ppm	0.05	FUS-MS
Yb	ppm	0.1	FUS-MS
Lu	ppm	0.04	FUS-MS
Hf	ppm	0.2	FUS-MS
Ta	ppm	0.1	FUS-MS
W	ppm	1	FUS-MS
Tl	ppm	0.1	FUS-MS
Pb	ppm	5	FUS-MS
Bi	ppm	0.4	FUS-MS
Th	ppm	0.1	FUS-MS
U	ppm	0.1	FUS-MS

3.7.1 U-Pb Geochronology of Zircons

Three samples were selected for U-Pb dating of zircons based on the mineralogy studies which were collected from the lower part of the Tukai Formation adjacent to the stratigraphical boundary with the Lambir Formation. After initial preparation, zircons were concentrated, subsequently embedded in epoxy resin and polished before being subjected to laser ablation analysis. The internal features were studied under cathodoluminescence by a using scanning electron microscope and selected grains for each samples studied are shown in **Figures 3.5 to 3.7**.

While performing the offline data reduction using VizualAge identifying the longest possible integration that yields a concordant point with overlapping $^{206}\text{Pb}/^{238}\text{U}$, $^{207}\text{Pb}/^{235}\text{U}$ and $^{207}\text{Pb}/^{206}\text{Pb}$ ages was attempted. If necessary, a common-Pb correction was also applied, in which case integrations were chosen that yielded a concordant 204-corrected ellipse. A minimum of 60 zircon grains were used for the U-Pb dating. Zircon U-Pb dating was carried out using a Resonetics

RESOLUTION M-50 series 193nm excimer laser ablation system equipped with a Laurin Technic Pty S-155 ablation cell. Ablation was conducted in a mixed He (300 mL/min) and Ar (930 mL/min) carrier gas and mixed with N₂ (2 mL/min) downstream of the cell. Contamination at mass 204 from Hg in the carrier gases was <150cps. All data were collected using a 36 µm Ø laser crater, a repetition rate of 3 Hz, and laser fluence of 3 J/cm². The data were standardized against FC1 zircon (1099 ± 2 Ma) which was analyzed at least 16 times per run and distributed evenly throughout the sequence. Each ablation was 30 seconds in duration and was preceded by 30 seconds of background collection. Ablated aerosol was transferred to the ICP-MS using nylon tubing with an in-line ‘squid’ smoothing device connected immediately before the junction with an ICP-MS torch. Isotope intensities were measured using an Agilent 7700x quadrupole-ICP-MS operated in ‘auto’ detector mode: sensitivity and P/A factors were tuned by rastering across a NIST610 glass before the start of each run. A second external rotary pump was used to enhance sensitivity.

The ICP-MS method measured ⁹⁰Zr, ²⁰²Hg, ²⁰⁴Pb, ²⁰⁶Pb, ²⁰⁷Pb, ²⁰⁸Pb, ²³²Th and ²³⁸U with a total quadrupole sweep time of 0.26 seconds. The background corrected ²⁰²Hg ion beam measured during ablation was used to peak strip any small excess ²⁰⁴Hg from the ²⁰⁴Pb signal using the ²⁰²Hg/²⁰⁴Hg measured on the gas background. The magnitude of this correction was typically insignificant. The data were reduced offline using VizualAge (Petrus and Kamber 2012) and Iolite v2.5 (Paton et al. 2011) running as plugins in Wavemetrics Igor Pro 6.23. Concentration data were calculated relative to NIST610 (distributed throughout the sequence) and using the Iolite trace-elements “internal standardization” data reduction scheme. An estimated value of 44 wt% Zr in zircon was used as the internal standard composition. Common-Pb was corrected (if necessary) using the background-corrected and Hg-interference corrected ²⁰⁴Pb intensity, a common-Pb composition based on Kramers and Tolstikhin (1997) Pb-Pb evolution curve and an estimate of the age of the zircon based on the uncorrected ²⁰⁶Pb/²³⁸U age. This correction method is suitable for grains with modest common-Pb content and minor Pb-loss. The %Pb* estimate reported in the data tables was taken from the Andersen (2002) routine implemented in VizualAge.

The Plešovice zircon standard from the Bohemian Massif, Czech Republic, provided by Jiří Sláma (Bergen) was used in this study. This zircon has a concordant U–Pb age with a weighted mean ²⁰⁶Pb/²³⁸U date of 337.13 ± 0.37 Ma (ID-TIMS, 95% confidence limits) taken from Sláma et al. (2008). This material is locally affected by minor recent Pb-loss.

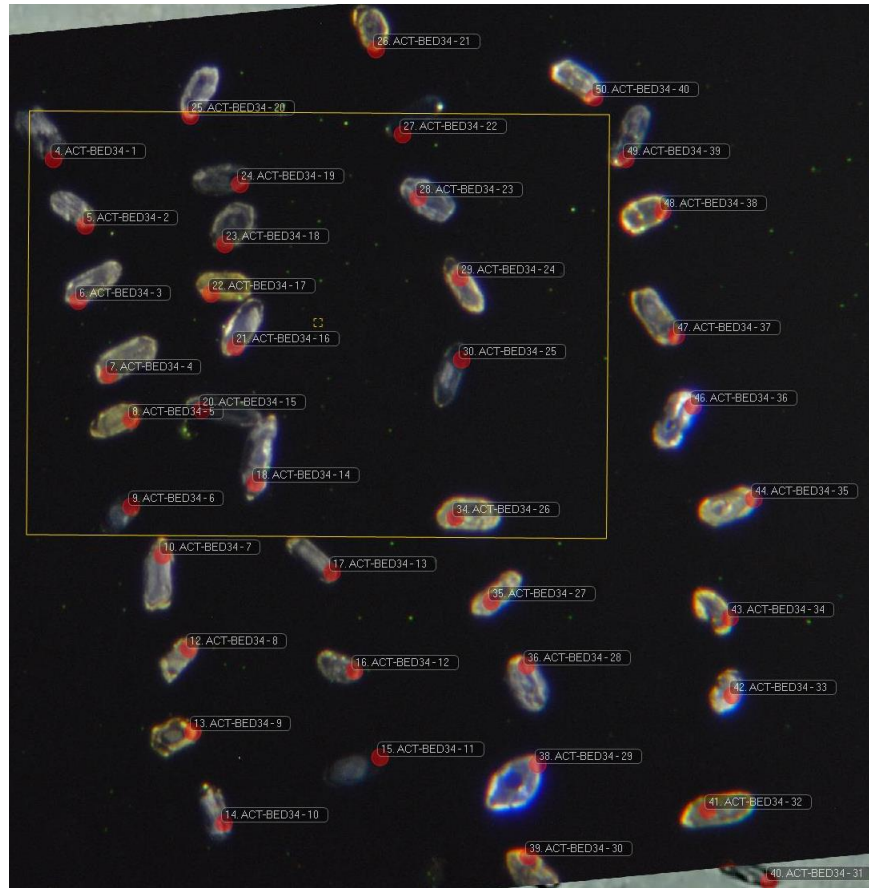


Figure 3.5 Cathodoluminescence images of selected zircon grains from Sample 1 (the age measured part is shown on the grains)

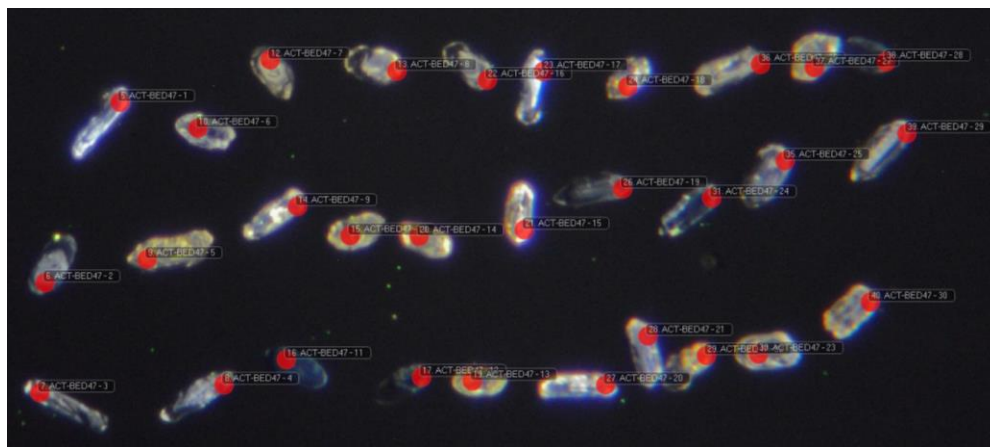


Figure 3.6 Cathodoluminescence images of selected zircon grains from sample 2 (the age measured part is shown on the grains)

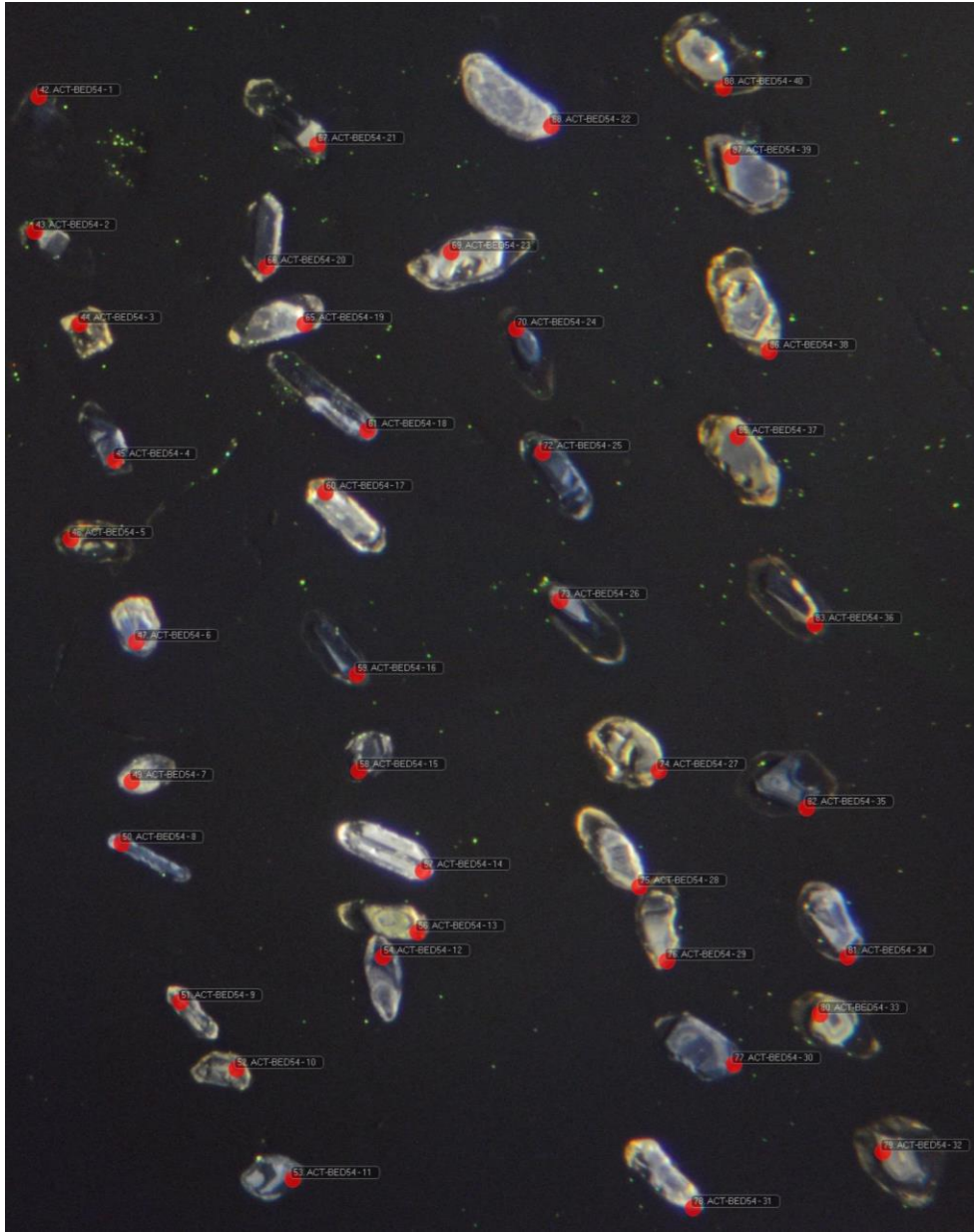


Figure 3.7 Cathodoluminescence images of selected zircon grains from Sample 3 (the age measured part is shown on the grains)

CHAPTER 4

RESULTS AND DISCUSSIONS

4.1 Introduction

The aim for this chapter is to report on the results obtained from various analyses such as bulk mineralogy by QEMSCAN and clay mineralogy by XRD, heavy mineral analysis, heavy mineral chemistry, bulk geochemical analyses and petrological study in order to elucidate the paleo-weathering, provenance and tectonic setting of the sediments of the Tukau Formation.

4.2 Results

4.2.1. Petrography

Overall, 30 sandstone samples were studied for the petrographic features. However, only 26 sandstones samples were fully observed due to thin section conditions. The Tukau formation sandstones can be grouped into two categories; a. medium grained and b. fine grained. Most of the sandstones are predominantly consisting of quartz and lithic fragments with minor amount of other minerals such as feldspars, mica, zircon and opaque minerals.

Petrographically, the studied sandstones can be classified into quartz arenite, and sublitharenites. The classification of the sandstones was identified using Folk (1974) classification method (**Figure 4.1**). This classification is based on the amount of quartz, feldspar and rock fragments and plotted in the ternary diagram. From the observations of 26 sandstone samples, Tukau sediments can be divided into two main categories; sub-litharenite and quartz arenite. The sandstones generally showcased fine-medium to coarse grained, angular to sub-rounded, low to high sphericity and moderate to poorly-sorted (**Figure 4.2**). Monocrystalline quartz (Qm), polycrystalline quartz (Qp), and rock fragments are the main framework grains found in the samples (**Figure 4.2a-1**). Generally, quartz dominates the framework in comparison to rock fragments and feldspar with a mean of 94% across all samples. Feldspar is only present as a minor constituent with alkali feldspar in dominant. The higher amount of alkali feldspar could be due to their highly resistance towards weathering compared to plagioclase series. The presence of alkali feldspars dominating the sample also indicates that the sources probably originated from granite

or gneiss rocks. The results of point counting method for consolidated and unconsolidated samples (n=26) are shown in **Table 4.1**. In this data, matrix and cement were not taken into consideration due to the inconsistent of the samples (consolidated vs unconsolidated).

4.2.1.1 Quartz arenites

Out of 26 samples, 21 samples (1, 42, 54, 14D, 19A, 4B, 7A, B2C, B4A, B5A, B7C, O1B1, O5B1, O5B2, O5B6, O6B4, S2B7, S2B9, S2B11, S3B2 and S3B4) are classified under quartz arenite. Generally, all the samples are grain-supported with roundness ranging from subrounded to sub-angular. The grain sizes range between fine to medium-grained. Both monocrystalline and polycrystalline quartz are observed in the samples, in which, sample numbers 54, 19A, 4B, B7C, S2B7 and S2B9 lack in polycrystalline quartz grains. Polycrystalline quartz showing sutured boundaries is also being observed in the sample (ie: O6B4). Lithic fragments were identified as meta sandstone, meta mudstone (**Figure 4.2 a-d, f, I, k**), chert and schists (**Figure 4.2 b**). Feldspar is also present but in very minor percentage (sample numbers: 42, 14D, 54B, B2C, B4A, B7C, O1B1, O5B2, O5B6, O6B4, S2B11, S2B4, S3B2 and S3B4). Meanwhile, mica (muscovite and biotite) also present in the samples (ie: S3B2, S2B11, O5B2) but is relatively lower in percentage (**Figure 4.2b, c, h**). In consolidated samples (O1B1, O5B1, O5B2, O5B6, O6B4, S2B7, S2B9, S2B11, S3B2 and S3B4), the cement is identified as iron oxide (**Figure 4.2i**).

4.2.1.2 Sublitharenites

Out of 26 samples, 5 samples (36C, 54(B), B4B, B2A, S2B4, S3B4) are classified under sublitharenite. The samples are generally ranged between medium to coarse-grained. The cement is identified as iron oxide while the matrix are from clay materials in consolidated samples (i.e. for S2B4 and S3B4). Monocrystalline quartz dominated the samples compared to polycrystalline quartz. Lithic fragments found in these samples consists of sedimentary to meta-sedimentary rocks (eg: meta sandstone, meta mudstone, chert) and metamorphic rocks (schists) (**Figure 4.2 a-d, f, I, k**). In these samples (ie: S2B4, S3B4), micas (muscovite and biotite) were also present but in a small amount. Their presence is isolatedly across the samples. Feldspars was present as well with alkali feldspar occurring more than plagioclase group.

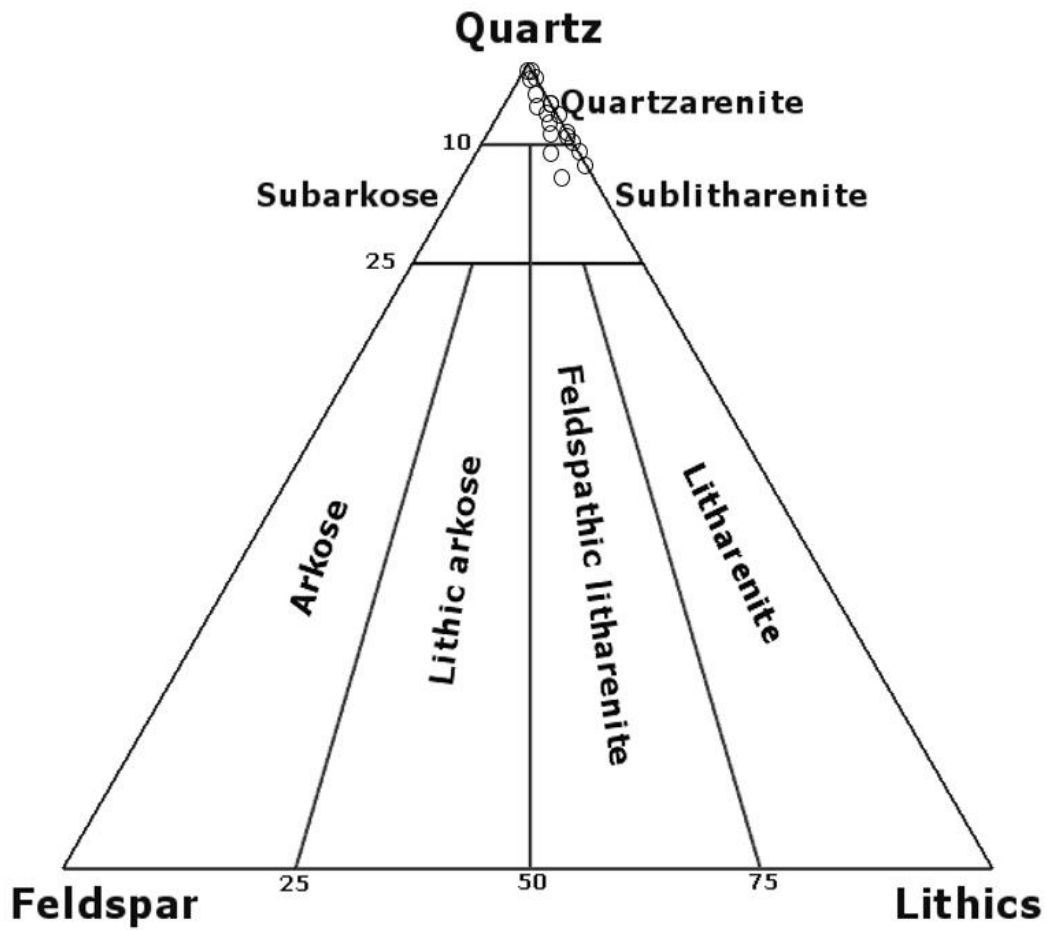


Figure 4.1 Plotted QFL Diagram after Folk (1974) for sandstone classification. Majority sample fall into quartz arenite.

Table 4.1 Modal Composition of the rocks of the study area based on QFL

Sample Number	Polycrystalline Quartz (Qp)	Monocrystalline Quartz (Qm)	Feldspar	Rock Fragments	Other Minerals	Polycrystalline Quartz (Qp), %	Monocrystalline Quartz (Qm), %	Total Quartz, %	Feldspar, %	Rock Fragments, %	Other minerals	Provenance
1	2	170	0	16	0	1.06	90.43	91.49	0.00	8.51	0.00	Recycled orogen
42	4	281	1	14	0	1.33	93.67	95.00	0.33	4.67	0.00	Recycled orogen
54	0	296	0	4	0	0.00	98.67	98.67	0.00	1.33	0.00	craton interior
14D	1	157	2	5	0	0.61	95.15	95.76	1.21	3.03	0.00	Recycled orogen
19A	0	176	0	2	0	0.00	98.88	98.88	0.00	1.12	0.00	craton interior
36C	4	258	0	38	0	1.33	86.00	87.33	0.00	12.67	0.00	Recycled orogen
4B	0	295	0	5	0	0.00	98.33	98.33	0.00	1.67	0.00	Recycled orogen
54 (b)	2	264	1	33	1	0.66	87.71	88.37	0.33	10.96	0.33	Recycled orogen
7A	4	275	1	20	0	1.33	91.67	93.00	0.33	6.67	0.00	Recycled orogen
B2A	1	270	0	29	0	0.33	90.00	90.33	0.00	9.67	0.00	Recycled orogen
B2C	1	293	3	3	0	0.33	97.67	98.00	1.00	1.00	0.00	craton interior
B4A	2	295	2	1	0	0.67	98.33	99.00	0.67	0.33	0.00	craton interior
B4B	9	261	1	29	0	3.00	87.00	90.00	0.33	9.67	0.00	Recycled orogen
B5A	3	281	1	15	0	1.00	93.67	94.67	0.33	5.00	0.00	Recycled orogen
B7C	0	281	2	17	0	0.00	93.67	93.67	0.67	5.67	0.00	Recycled orogen
O1B1	11	271	4	8	0	3.74	92.18	95.92	1.36	2.72	0.00	Recycled orogen
O5B1	12	264	3	17	0	4.05	89.19	93.24	1.01	5.74	0.00	Recycled orogen
O5B2	3	270	5	22	1	1.00	89.70	90.70	1.66	7.31	0.33	recycled orogen
O5B6	4	290	2	4	0	1.33	96.67	98.00	0.67	1.33	0.00	craton interior
O6B4	7	265	2	26	0	2.33	88.33	90.67	0.67	8.67	0.00	Recycled orogen
S2B11	0	273	1	26	4	0.00	89.80	89.80	0.33	8.55	1.32	Recycled orogen
S2B4	22	228	4	25	1	7.86	81.43	89.29	1.43	8.93	0.36	Recycled orogen
S2B7	0	218	0	3	0	0.00	98.64	98.64	0.00	1.36	0.00	craton interior
S2B9	0	298	0	2	0	0.00	99.33	99.33	0.00	0.67	0.00	craton interior
S3B2	1	292	2	5	0	0.33	97.33	97.67	0.67	1.67	0.00	Recycled orogen
S3B4	21	246	10	23	1	6.98	81.73	88.70	3.32	7.64	0.33	Recycled orogen

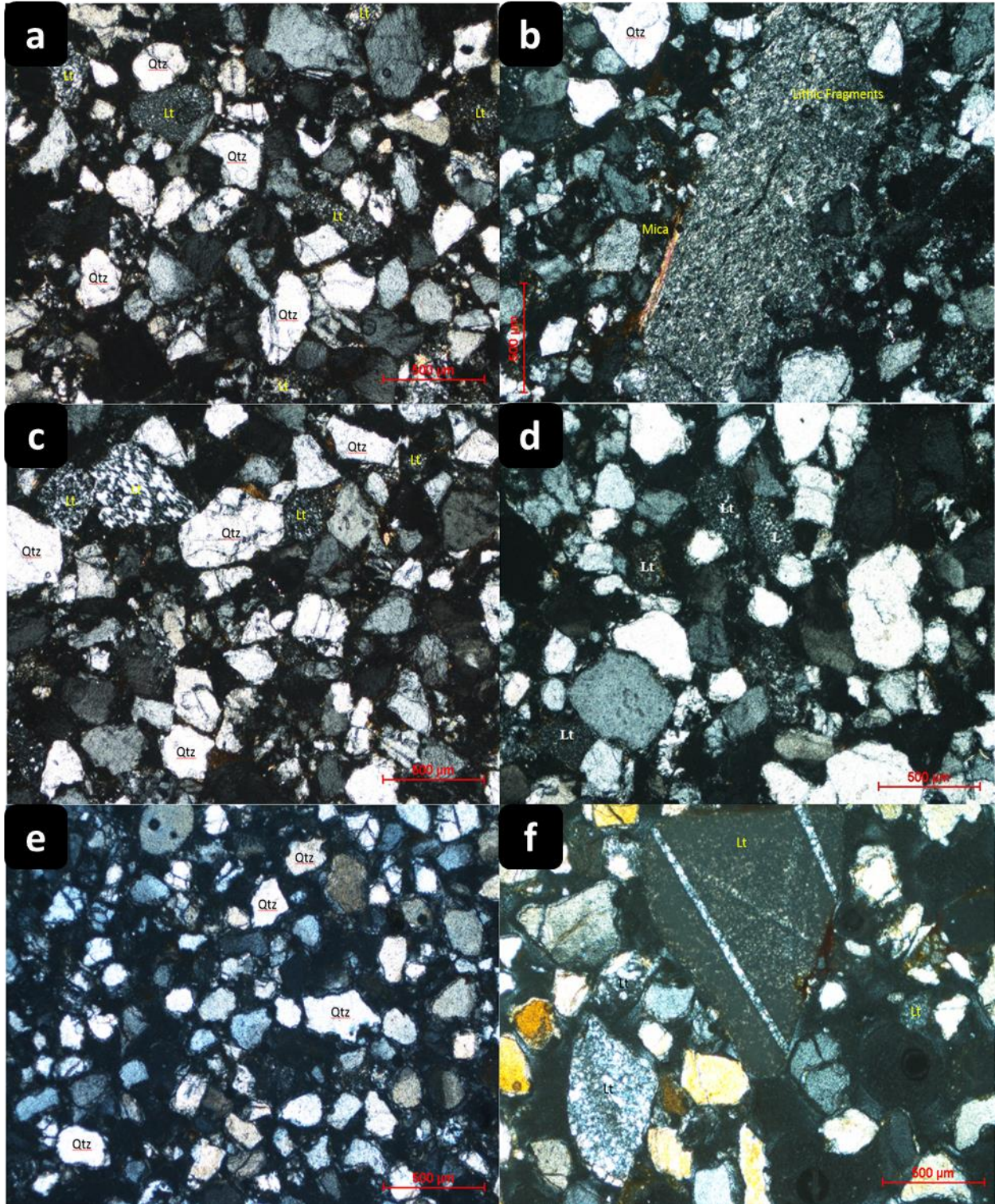


Figure 4.2(a-f): Microphotographs of the quartz arenites and sublitharenites from the Tukai Formation, NW Borneo (a,c,d,k) Abundance grain types made of quartz and lithic fragments. (b) Large lithic fragment from metamorphic origins(schist) with small mica. (f) Lithic fragments exist as larger grains in sample 54b with minor quartz veins.

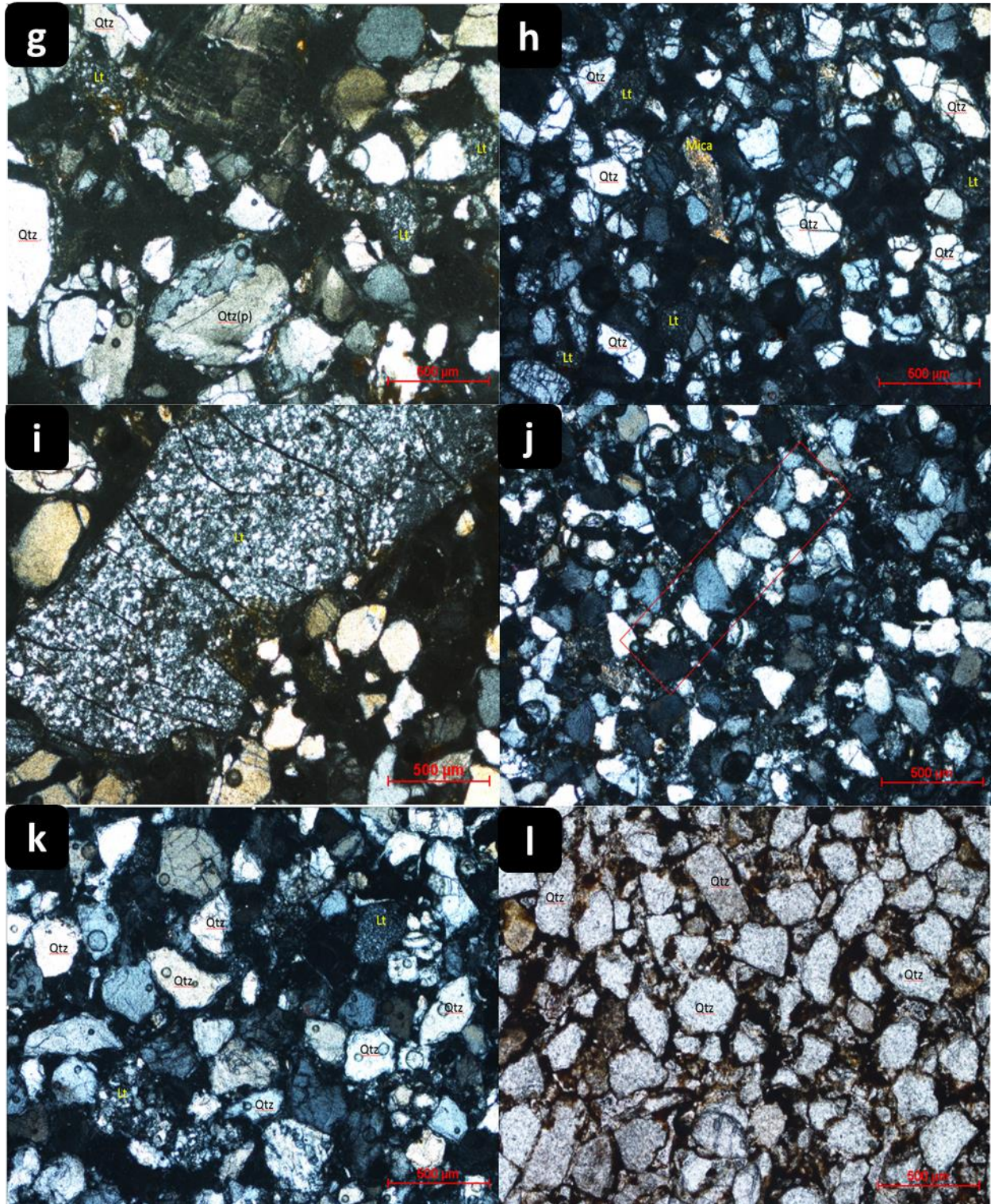


Figure 4.2(contd.): (g,h) mono and polycrystalline quartz grains, (i) a larger lithic fragment in sample 54b (j) Quartz grains show an alignment (k) Abundance grain types made of quartz and lithic fragments, (l) iron oxide cement with some clay minerals (Fe-coated) (PPL view).

4.2.2 Bulk Mineralogy

The studied Tukai samples mainly comprise of quartz as a major mineral assemblage (45.94-97.14 wt%), major to minor illite-illite-smectite clays (0.98-40.71wt%) and minor kaolinite (1.45-9.22 wt%) (**Figure. 4.3**). Chlorite is common in all the samples but the range varies from trace to minor (0.02-9.06 wt %) except two samples that show significant chlorite content as 6.28 wt% and 9.06 wt%. Plagioclase feldspars (both end members) is absent/or trace (albite=0.001-0.005 wt%) whilst K feldspar occurs as trace phase (0.005-0.91 wt%). Illite is the dominant clay mineral in the Tukai sediments and their overall association (calcareous, Fe-illite and illite & illite-smectites) ranges between 1.09 and 41.39 wt % with an average of 22.06 wt%. Other sporadic trace constituents include mica (biotite and muscovite (avg.) = 0.42 and 0.40 wt% respectively) and pyrite (0-2.25; avg. 0.23 wt%). Heavy minerals include rutile & Ti silicates, tourmaline, zircon and chromite and their total ranges from 0.11-0.36wt % with an average of 0.19 wt%. In addition to the inorganic phases, organics are also present in several samples. As organics are not routinely measured during analysis, they appear as irregular voids in the QEMSCAN images as shown in **Figure 4.3 and 4.4**.

Despite the mineralogical similarity, the Tukai samples show a range of textures and rock types as kaolinitic sandstone, laminated siltstone, and sandy siltstones. Clay cements are common within the sandstone samples. For instance, kaolinite occurs in a variety of associations including booky masses scattered throughout the pore network, intermixed with detrital clays in more argillaceous laminae, and also as rounded, grain replacive concentrations, possibly after feldspar. Illite occurs as a grain coating / pore lining cement and may also occur as a detrital phase in association with micas. In addition to clay cements, pore-filling siderite occurs in a number of samples; in these samples the siderite occurs as scattered pore-filling crystals, particularly in cleaner, more porous laminae (and possible burrows; e.g. S19) and may also form a more pervasive (albeit patchy) cement. Most of the studied samples are siltstones, often with thin fine sandstone and / or mudstone laminae. These siltstones typically comprise of medium to fine silt grade quartz and abundant illitic matrix clays. Kaolinite is normally found to be concentrated along siltstone laminae but the texture indicates that much of it is grain replacive. Graded bedding is also present in a number of samples (e.g. S03 and S07) where thin siltstone laminae grades upwards into claystone. Fe oxides and siderite are commonly concentrated along the interface between these claystone laminae and the adjacent, more porous, sandy laminae. Based on the QEMSCAN

images, the lithology can be divided into quartz arenite and range of argillaceous lithologies (mudstone and or interbedded sandstone and mudstones).

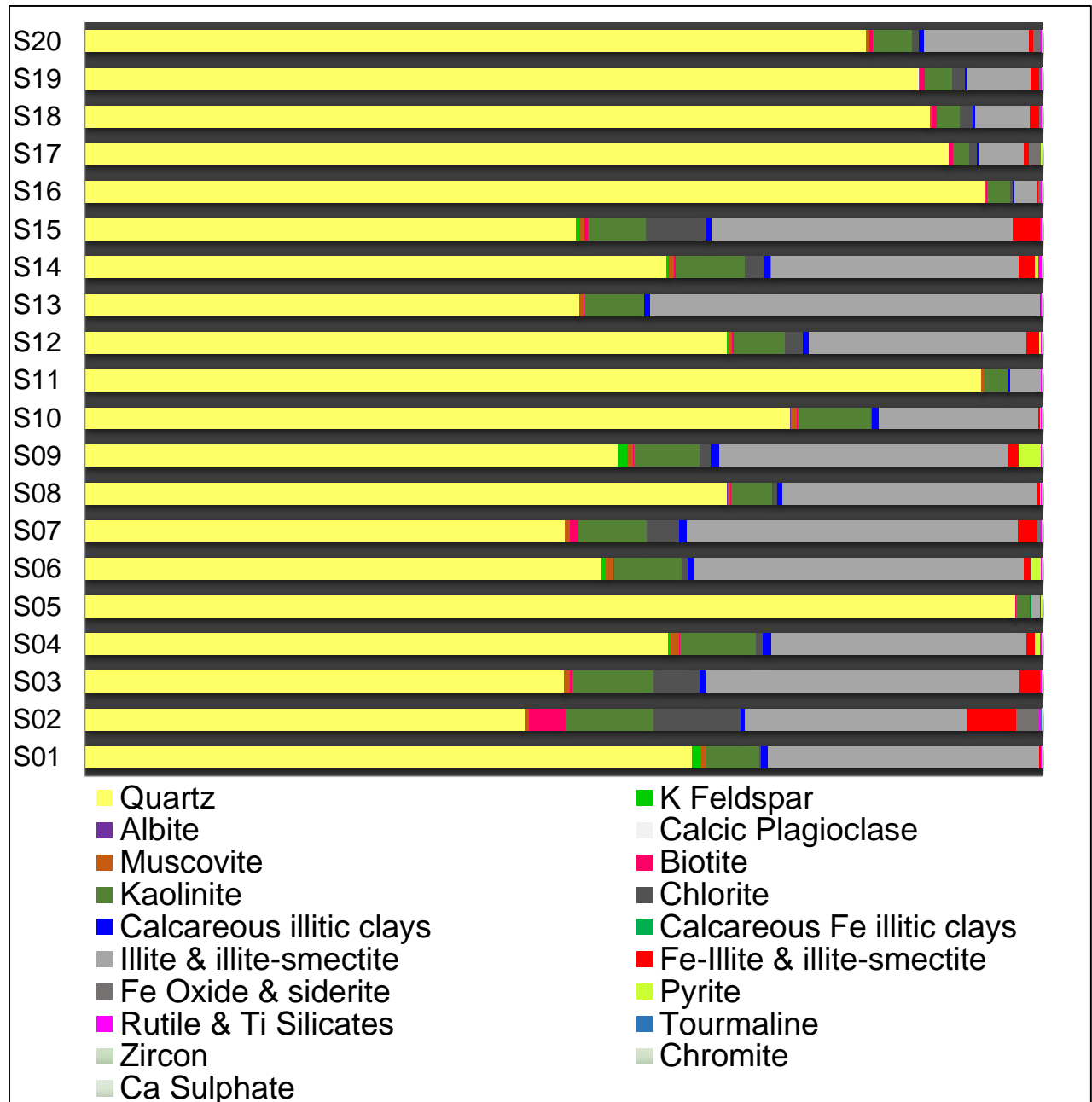


Figure 4.3 QEMSCAN modal mineralogical distributions of the Tukai clastic sediments

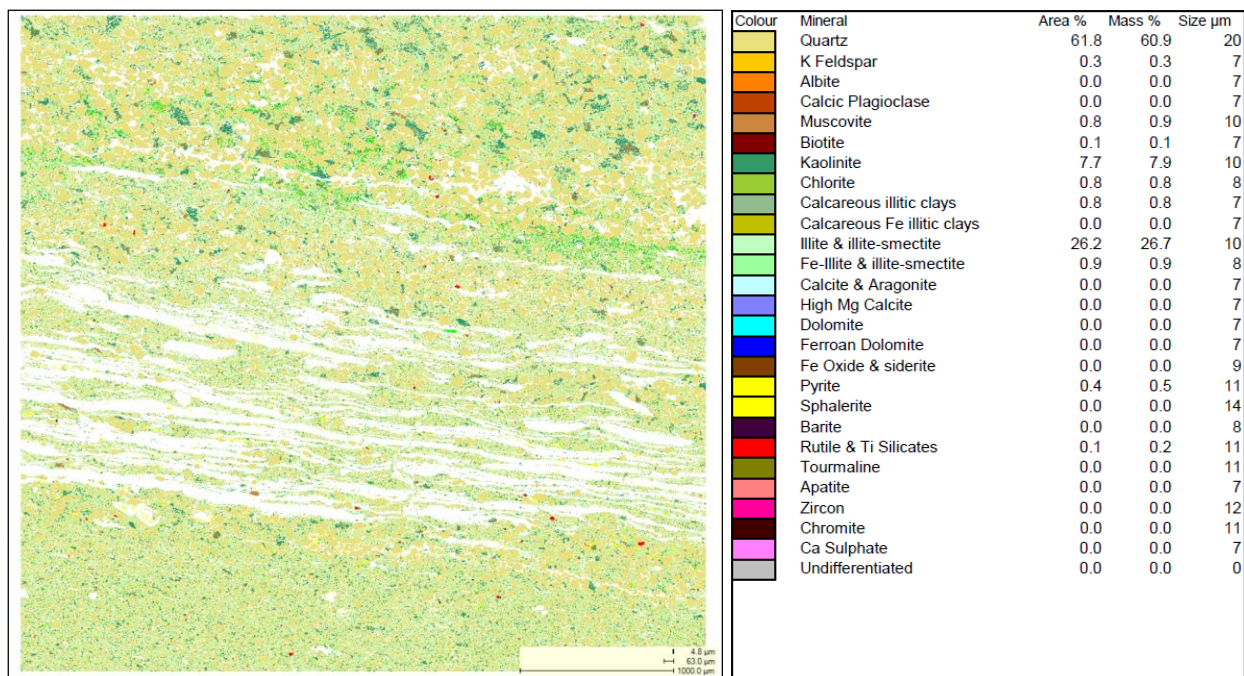


Figure 4.4 Mineralogical image of a selected area of the surface of the sample showing the distribution of the inorganic phases. The organic phases are not estimated which are blank in the image (white colour).

4.2.3 X-Ray Diffraction (XRD)

The whole rock XRD data are in accordance with the QEMSCAN mineralogy and indicate that the main species present are quartz, illitic clays and kaolinite as shown in **Figure 4.5**. Quartz is mainly associated with whole rock ($>2 \mu\text{m}$ size; 79.2-97.3 wt.%) compared to clay fraction ($<2 \mu\text{m}$ size 6.1-55.7 wt.%). Illite is the dominant clay species in both whole rock (1.85-19.1 wt.%) and the clay fraction (28.7 – 49.1 wt.%) as shown in **Table 4.2**. However, significant amount of illite in whole rock indicates that a significant proportion of the illite has a grain size greater than $2 \mu\text{m}$; often an indication of the presence of detrital illite and / or mica. Examination of the clay fraction in isolation shows that kaolinite is abundant in the clay fraction (15.2-49. wt.7%; **Table 4.2**). Again, this is in accordance with the QEMSCAN analysis which shows that kaolinite is pore-lining to filling and commonly a grain replacive authigenic phase whilst illite occurs as both a pore-lining cement and also as possible detrital material, especially in the more argillaceous laminae. Chlorite is not detected in the clay fraction suggesting that if present, it occurs in quantities below XRD detection limits (nominally 3 mass % in the fraction being measured but

strongly dependent on crystallinity). Swelling clay (smectite) is identified within the clay fraction (most notably in one sample) but these are typically present in traceable amounts (BDL – 9.6%).

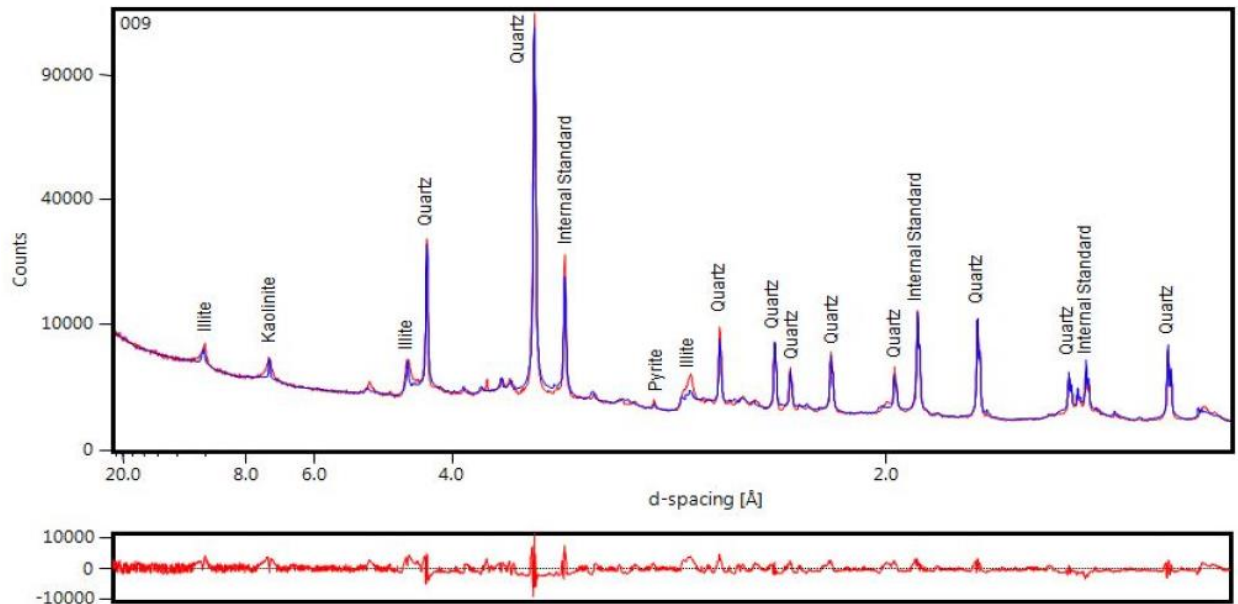


Figure 4.5. X-ray diffractogram with the main mineral peaks identified together with the Rietveld difference plot. (Sample S9)

Illite (26.2-49.1 wt. %) and quartz (6.1-55.7 wt.%) are dominating in clay fractions; kaolinite (15.2-49.7 wt.%) is present in subordinate amount as presented in **Table 4.2**. The illite crystallinity of the Tukai samples varies between moderate to poor, and most of the samples show moderate crystallinity whereas kaolinite crystallinity is mostly poor and 3 samples show moderate crystallinity.

Table 4.2 XRD results for Tukau Clastic sediments (WR=whole rock; -2 μ m = clay speciation)

Mineral/Sample No.	S01	S04	S06	S08	S09	S12	S13	
Quartz (mass %)	WR	86.69	82.95	80.69	97.33	86.69	93.07	79.19
	-2 μ m	18.4	28.3	55.7	6.1	23.6	44.3	26
Kaolinite (mass %)	WR	1.89	1.49	1.799	0.82	1.36	1.47	1.69
	-2 μ m	49.7	15.2	15.301	46	27.5	15.8	24.4
	Crystallinity	Poor	Mod	Mod	Poor	Mod	Poor	Poor
Illite (mass %)	WR	11.42	15.54	16.65	1.85	11.75	5.46	19.12
	-2 μ m	28.7	46.92	26.2	47.9	45.9	38.8	49.1
	Crystallinity	Poor	Mod	Mod	Poor	Mod	Mod	Mod
Smectite (mass %)	WR	-	-	-	-	-	-	-
	-2 μ m	Tr	9.6	-	Tr	3	0.2	0.5
Pyrite (mass %)	WR	-	-	0.86	-	0.2	-	-
	-2 μ m	-	-	2.8	-	-	-	-
Jarosite (mass %)	WR	-	-	-	-	-	-	-
	-2 μ m	3.2	-	-	Tr	-	0.9	-
Total (mass %)	WR	100	100	100.0	100	100	100	100
	-2 μ m	100	100	100.0	100	100	100	100

Tr=trace; - = not detected.

4.2.4 Heavy Minerals

Three samples out of four samples yielded significant numbers of heavy minerals (n=1966; 2449 and 5082 for S02, S07 and S14 respectively) from Tukau Formation. All three samples show a similar heavy mineral assemblage which consists of zircon, rutile/anatase with lesser quantities of chromite, ilmenite, monazite, tourmaline and garnet (**Figure 4.6 and 4.7**). Xenotime and florencite are also noted in some, but not all of the samples. The relative proportions of the mineral phases varies and ranges from rutile / anatase dominant (sample S02) to zircon- dominant (S14). Tourmaline and garnet content broadly follows that of rutile / anatase whilst xenotime and monazite content is greatest in zircon-rich samples.

	S02	S07	S14
Amphibole			
Andalusite			
Apatite			
Chromite			
Epidote			
Florencite			
Garnet			
Ilmenite			
Monazite			
Rutile / Anatase			
Tourmaline			
Xenotime			
Zircon			

Figure 4.6 QEMSCAN image grid illustrating range of grain types present within each sample

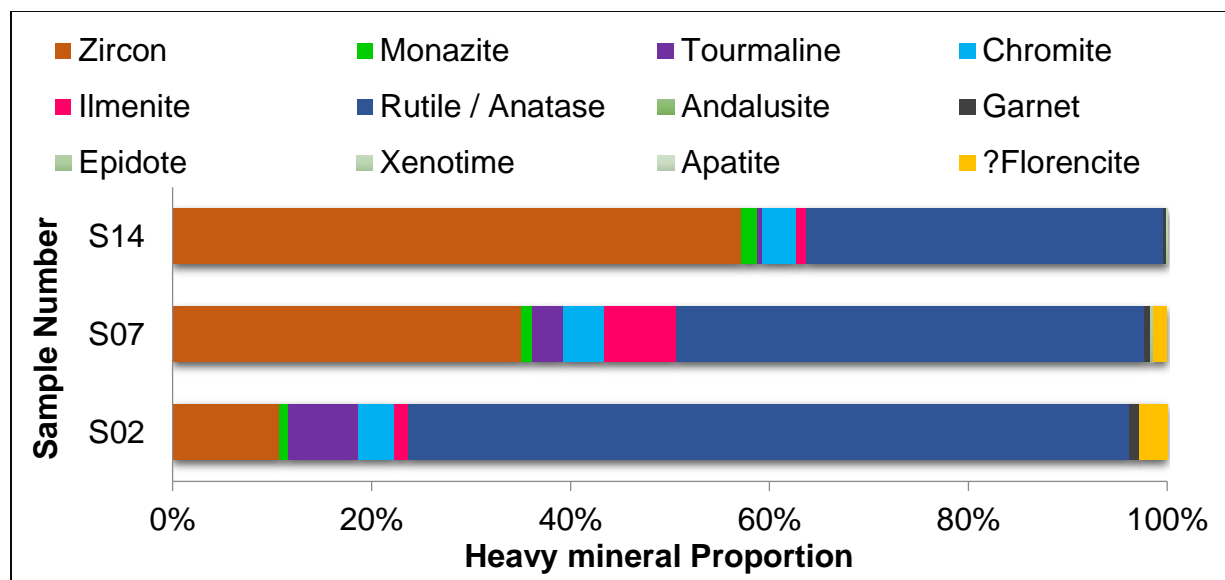


Figure 4.7. Distribution of Heavy minerals in the sediments of Tukai Formation

4.2.4.1 Heavy mineral Grain Morphology

The heavy mineral assemblages observed in Tukai sediments such as tourmaline, zircon, rutile/anatase, ilmenite, monazite chromite and garnet may be associated not only to acid-intermediate granitic rocks, but also with metamorphic rocks and even to mature siliciclastic sediments (Torres-Ruiz, et al. 2003). Presence of tourmaline and zircon in the studied samples indicate that these minerals are mainly derived from acid-intermediate igneous rocks. However presence of other heavy minerals such as rutile, chromite and garnet (in some samples) also indicates the possibility of minor contribution from mafic and regional metamorphic terrane. The textural characteristics (i.e. roundness) of zircon, chromite and tourmaline suggest a high transport distance (may be recycling processes) in addition to relatively proximal source area and/or a first cycle origin from crystalline rocks. Zircon and tourmaline exhibit a range of grain shapes from pristine euhedral crystals through to highly abraded and rounded grains. Euhedral zircon and tourmaline indicate a short-distance of transportation and derived from nearby sources (i.e. within Borneo). However, highly abraded and rounded grains of zircon suggest extensive transport and reworking (source from other than Borneo??). They might be mixed with fresh sediments which is clearly shown by the fractions of strongly rounded grains that occurred with idiomorphic or

hipidiomorphic ones. Reworking of zircon in the Tukai sediments is confirmed by Nagarajan et al. (2014) based on whole rock geochemistry from the lower part of the Tukai Formation. Zircon grain in the Tukai sediments displays a range of grain shapes ranging from pristine euhedral crystals as shown in **Figure 4.8 (a), (b), (c)** to rounded and heavily abraded grains as shown in **Figure 4.8 (a-i)**. This range of grain shapes suggests that zircon grains may be derived from several sources (of different ages) and / or may have undergone extensive transport or reworking. Some chromite grains have internal dissolution pits as shown in **Figure 4.8 (f), (g)**, possibly due to dissolution of silicate inclusions. In the weathering profile, grain fractures are filled with small amounts of hematite and goethite in some cases. The anhedral (with a pronounced conchoidal fracture for the broken ones) to angular shape of the studied chromian spinel grains indicates that the transport distance, subsequent to the weathering of the source rocks, was relatively shorter as shown in **Figure 4.8 (d), (e)**. Detrital chromian spinels were abundant in fine to very fine grained sandstones of the Tukai Formation. Chrome spinel grains are typically fractured and abraded, and are mainly rich in Al composition in addition to Mg and Fe. Backscattered electron images as shown in **Figure 4.8 (d), (f), (g)** show subhedral chromian detrital grains with evidence of dissolution, and the presence of grooves as well as indicators of corrosion on their surface suggests a high degree of chemical weathering in the depositional environment since chromian spinel is generally resistant to low-grade alteration and mechanical breakdown as shown in **Figure 4.8 (d), (f), (g)**. The observed conchoidal fractures are thought to have been formed as a result of mechanical weathering. The surface textures of chromian spinels clearly indicate the combined effects of mechanical attrition and chemical etching during the transportation and possibly prior to transportation of the mineral in the river. Immature chemical weathering of the ophiolites under highly oxidizing and alternating wet/dry conditions may have resulted in a significant amount of chromian spinel particles in the Tukai sediments which been flushed away during periods of increased humidity and deposited location in different environments. Rutile and ilmenite grains also display a variety of dissolution features as shown in **Figure 4.8 (e-i)**. Overall the mixture of euhedral and well-rounded grains of heavy minerals suggests a mixture of metamorphic/metasedimentary and granitic source areas. In addition, in the CL images of zircon, there is an exhibition of various textures for selected zircons indicating that they are derived from multiple sources.

4.3 Mineral Chemistry

Although, heavy minerals are commonly present in the accessory phase of sediments at less than <1%, they are more specific to their provenance compared to quartz and feldspar.

4.3.1. Detrital Tourmaline

The average composition of tourmaline grains from the Tukai sediments are presented in **Table 4.3**. Chemical composition of tourmalines in the Tukai sediments ranges from dravite (Mg end member) to schorl (Fe end member) (**Table 4.3**). The tourmalines are characterized by higher and various Al_2O_3 , SiO_2 and FeO concentrations: i.e. Al_2O_3 : 33.08-46.85wt%; SiO_2 :32.19-37.02 wt%; and FeO : 6.11-18.53 wt%. MgO concentrations are recorded in the range of BDL to 12.45 wt % (avg. 6.62 wt%). TiO_2 content shows significant variation as BDL to 4.38 wt% with an average of 1.51 wt%. Na_2O and CaO concentrations also show a wider ranges as BDL to 5.09 wt% (avg. 2.67 wt%) and BDL to 1.70 (avg.0.73 wt%) respectively. Tourmaline grains are mostly Fe rich with few of them are rich in Mg.

4.3.2. Detrital Chromium spinel

The results of the EDS spot quantitative analysis of Chromian spinels and stoichiometric calculations are presented in **Table 4.4**. Chromium spinels of this study are chromites except one sample where each belongs to magnesiochromite and Hercynite. The Cr_2O_3 contents range from 19.27 to 55.88 wt.%, but 83% of the grains show that Cr_2O_3 is greater than 30 wt.%. The Al_2O_3 contents range from 11.79 to 51.84 wt% with an average of 23.42 wt%. The FeO contents range from 11.84 to 35.37 wt.% (avg. 25.54 wt.%) and MgO ranges between BDL and 16.62 wt.% with an average of 7.69 wt.%. Cr_2O_3 vs Al_2O_3 and FeO vs MgO is negatively correlated. TiO_2 content is ranged between 0.44 and 2.50 wt% with an average of 1.19wt%. Total Fe was measured as FeO. The ratios of ferrous (Fe^{2+}) and ferric (Fe^{3+}) ions were calculated based on spinel stoichiometry. The parameters Mg#, Cr# and $\text{Fe}^{3+\#}$ are defined as $\text{Mg}/(\text{Mg}+\text{Fe}^{2+})$, $\text{Cr}/(\text{Cr}+\text{Al})$, and $\text{Fe}^{3+}/(\text{Cr}+\text{Al}+\text{Fe}^{3+})$, respectively. The Cr# and Mg# ratios vary between 0.20-0.74 (avg.0.55) and 0-0.71 (avg.0.35).

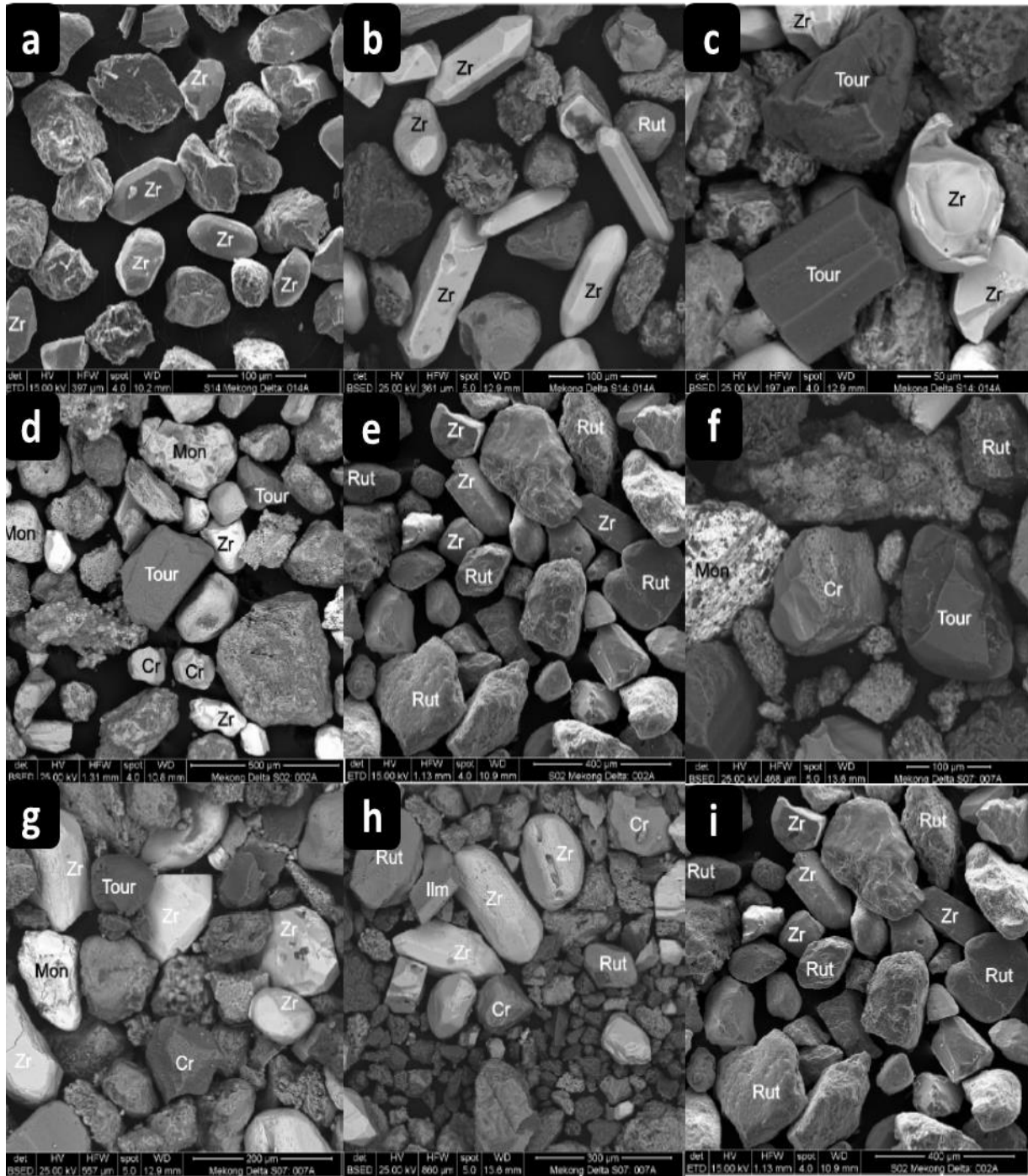


Figure 4.8 (a-i). Morphological features of heavy minerals separated from the sediments of the Tukai Formation (Zr= Zircon; Rut = Rutile; Tour = Tourmaline; Mon = Monazite; Cr = Chromian spinel; Ilm = Ilmenite)

Table 4.3 Representative composition of detrital Tourmalines from sediments of the Tukau Formation

Elements	T1	T2	T3	T4	T5	T6	T7	T8	T9	T10	T11	T12	T13	T14	T15	T16	T17
SiO ₂	36.04	32.19	37.02	34.05	36.33	33.72	34.43	36.28	34.13	33.78	33.89	35.55	33.71	35.27	34.01	34.84	34.89
TiO ₂	1.77	3.24	1.61	1.41	0.88	1.92	0.00	0.98	0.96	0.74	0.66	1.17	4.38	1.25	1.66	1.73	1.32
Al ₂ O ₃	43.84	42.88	45.23	45.33	42.73	36.03	45.45	46.85	43.00	41.91	41.89	40.25	33.08	45.26	42.36	40.69	40.07
FeO	8.83	9.91	15.48	13.40	10.47	18.53	13.76	6.54	9.47	18.11	14.92	6.40	18.15	8.07	6.11	8.66	10.16
MnO	0.00	0.00	0.00	0.00	0.00	0.00	0.00	0.00	0.00	0.00	0.00	0.00	0.00	0.00	0.00	0.00	0.00
MgO	8.70	6.72	0.00	4.82	8.65	4.67	3.60	8.61	8.06	0.00	4.19	12.45	5.64	7.11	10.65	9.52	9.23
CaO	0.81	0.73	0.67	0.99	0.95	1.63	0.00	0.75	0.75	0.37	0.34	0.58	0.54	0.78	0.90	1.70	0.00
K ₂ O	--	--	--	--	--	--	--	--	--	--	--	--	--	--	--	--	--
Atomic ratios (stoichiometric calculation based on 24.50)																	
Si (Total)	5.09	4.68	5.33	4.91	5.17	5.11	5.00	5.05	4.92	5.07	5.00	5.06	5.13	5.00	4.86	5.01	5.06
Al (Tot)	7.30	7.36	7.68	7.71	7.17	6.44	7.78	7.69	7.30	7.41	7.29	6.76	5.93	7.56	7.13	6.90	6.84
Ti	0.19	0.35	0.17	0.15	0.09	0.22	0.00	0.10	0.10	0.08	0.07	0.12	0.50	0.13	0.18	0.19	0.14
Fe	1.04	1.21	1.87	1.62	1.25	2.35	1.67	0.76	1.14	2.27	1.84	0.76	2.31	0.96	0.73	1.04	1.23
Mg	1.83	1.46	0.00	1.04	1.83	1.06	0.78	1.79	1.73	0.00	0.92	2.64	1.28	1.50	2.27	2.04	1.99
Zn	0.00	0.00	0.00	0.00	0.00	0.00	0.00	0.00	0.00	0.00	0.00	0.00	0.00	0.00	0.00	0.00	0.00
Ca	0.12	0.11	0.10	0.15	0.14	0.26	0.00	0.11	0.12	0.06	0.05	0.09	0.09	0.12	0.14	0.26	0.00
Na	0.00	1.22	0.00	0.00	0.00	1.03	0.78	0.00	1.02	1.48	1.18	1.00	1.33	0.62	1.19	0.80	1.21
K	0.00	0.00	0.00	0.00	0.00	0.00	0.00	0.00	0.00	0.00	0.00	0.00	0.00	0.00	0.00	0.00	0.00
Total	15.6	16.4	15.2	15.6	15.7	16.5	16.0	15.5	16.3	16.38	16.4	16.4	16.6	15.9	16.5	16.25	16.5
Fe/Fe+Mg	0.36	0.45	1.00	0.61	0.40	0.69	0.68	0.30	0.40	1.00	0.67	0.22	0.64	0.39	0.24	0.34	0.38
Na/Na+Ca	0.00	0.92	0.00	0.00	0.00	0.79	1.00	0.00	0.90	0.96	0.96	0.92	0.94	0.84	0.90	0.75	1.00
Na+K+Ca	0.12	1.34	0.10	0.15	0.14	1.29	0.78	0.11	1.13	1.54	1.23	1.08	1.42	0.74	1.33	1.06	1.21
X _{vac}	0.88	-0.34	0.90	0.85	0.86	-0.29	0.22	0.89	-0.13	-0.54	-0.23	-0.08	-0.42	0.26	-0.33	-0.06	-0.21
X _{vac} /Na+X _{vac}	1.00	-0.38	1.00	1.00	1.00	-0.40	0.22	1.00	-0.15	-0.57	-0.25	-0.09	-0.46	0.29	-0.39	-0.08	-0.21
Mg/Fe+Mg	0.64	0.55	0.00	0.39	0.60	0.31	0.32	0.70	0.60	0.00	0.33	0.78	0.36	0.61	0.76	0.66	0.62
Al/Al+Fe+Mg	0.72	0.73	0.80	0.74	0.70	0.65	0.76	0.75	0.72	0.77	0.73	0.66	0.62	0.75	0.70	0.69	0.68

Table 4.4 Representative Composition of detrital Chromian spinels from sediments of the Tukai Formation

Elements	CP1	CP 2	CP 3	CP 4	CP 5	CP 6	CP 7	CP 8	CP 9	CP10	CP11	CP12	Min	Max	Avg	St.Dev
SiO ₂	2.84	1.10	0.00	0.00	0.00	0.00	6.00	0.00	0.00	0.00	0.00	0.00	0.00	6.00	0.83	1.84
TiO ₂	1.51	1.14	0.94	0.90	0.85	0.98	1.79	1.37	0.94	2.50	0.44	0.91	0.44	2.50	1.19	0.54
Al ₂ O ₃	11.79	29.34	11.82	26.78	33.04	18.60	25.07	13.07	23.74	12.54	51.84	23.37	11.79	51.84	23.42	11.55
Cr ₂ O ₃	50.36	27.77	48.32	41.35	31.29	45.98	33.65	55.88	42.01	51.08	19.27	49.08	19.27	55.88	41.34	11.08
FeO	28.48	32.47	35.37	19.22	23.38	25.22	33.49	21.93	26.92	27.72	11.84	20.44	11.84	35.37	25.54	6.71
MnO	0.00	0.00	0.00	0.00	0.00	0.00	0.00	0.00	0.00	0.00	0.00	0.00	0.00	0.00	0.00	0.00
MgO	5.02	8.17	3.55	11.75	11.44	9.21	0.00	7.75	6.39	6.16	16.62	6.21	0.00	16.62	7.69	4.29
NaO	0.00	0.00	0.00	0.00	0.00	0.00	0.00	0.00	0.00	0.00	0.00	0.00	0.00	0.00	0.00	0.00
CaO	0.00	0.00	0.00	0.00	0.00	0.00	0.00	0.00	0.00	0.00	0.00	0.00	0.00	0.00	0.00	0.00
ZnO	0.00	0.00	0.00	0.00	0.00	0.00	0.00	0.00	0.00	0.00	0.00	0.00	0.00	0.00	0.00	0.00
Sum	100	100	100	100	100	100	100	100	100	100	100	100				
Si	0.10	0.03	0.00	0.00	0.00	0.00	0.20	0.00	0.00	0.00	0.00	0.00	0.00	0.20	0.03	0.06
Ti	0.04	0.03	0.02	0.02	0.02	0.02	0.04	0.03	0.02	0.06	0.01	0.02	0.01	0.06	0.03	0.01
Al	0.47	1.06	0.48	0.96	1.16	0.70	0.97	0.51	0.89	0.50	1.65	0.88	0.47	1.65	0.85	0.35
Cr	1.34	0.67	1.31	1.00	0.74	1.16	0.87	1.46	1.06	1.36	0.41	1.25	0.41	1.46	1.05	0.32
Fe ³⁺	0.000	0.146	0.169	0.002	0.069	0.090	0.000	0.000	0.001	0.023	0.000	0.000	0.00	0.17	0.04	0.06
Fe ²⁺	0.80	0.69	0.84	0.49	0.51	0.58	0.92	0.61	0.72	0.75	0.27	0.55	0.27	0.92	0.64	0.18
Mn	0.00	0.00	0.00	0.00	0.00	0.00	0.00	0.00	0.00	0.00	0.00	0.00	0.00	0.00	0.00	0.00
Mg	0.25	0.37	0.18	0.53	0.51	0.44	0.00	0.38	0.30	0.31	0.67	0.30	0.00	0.67	0.35	0.17
Cr#	0.74	0.39	0.73	0.51	0.39	0.62	0.47	0.74	0.54	0.732	0.2	0.58	0.20	0.74	0.55	0.17
Mg#	0.24	0.35	0.18	0.52	0.5	0.43	0	0.39	0.30	0.29	0.71	0.35	0.00	0.71	0.35	0.18
Fe ³⁺ #	0	0.06	0.06	0	0.03	0.04	0	0	0	0.009	0	0	0.00	0.06	0.02	0.02

$$\text{Cr\#}=\text{Cr}/(\text{Cr}+\text{Al}); \text{Mg\#}=\text{Mg}/(\text{Mg}+\text{Fe}^{2+}); \text{Fe}^{3+}=\text{Fe}^{3+}/(\text{Fe}^{3+}+\text{Cr}+\text{Al})$$

4.3.3. Detrital Garnet and Ilmenite

A trace of garnet grains was observed in one sample of the Tukai Formation (Spessartine and Almandine varieties). Spessartine garnet with MnO – 34.2 wt.%; Al₂O₃ – 21.7 wt.%; FeO – wt.7.6% and Almandine with FeO – 29.3 wt.%; Al₂O₃ – 24.9 wt.%; MnO – 9.8 wt.% is presented in **Table 4.5**. Only one sample yielded ilmenite mineral (n=8), which is enriched in SiO₂ and TiO₂ with 42.72 wt.% and 33.76 wt.% respectively. Meanwhile, the ilmenites from the Tukai Formation is enriched in Al₂O₃ but depleted in FeO with 15.37% and 6.11 wt % respectively, as shown in **Table 4.5**. Na₂O content is low and is recorded at 2.05 wt.% and ilmenites present which is classified as leucozene.

Table 4.5 Representative composition of detrital ilmenite and garnets from sediment of the Tukau Formation

Sample Number	S07	S14A	S14B
Oxides	Ilmenite	Garnet	Garnet
SiO ₂	42.72	30.93	34.64
TiO ₂	33.76	1.07	0.00
Al ₂ O ₃	15.37	21.67	24.89
Cr ₂ O ₃	0.00	0.00	0.00
FeO	6.11	5.31	29.17
Fe ₂ O ₃	--	2.49	0.18
MnO	0.00	34.24	0.00
MgO	0.00	0.00	9.80
NaO	2.04	0.00	0.00
CaO	0.00	4.54	1.34
ZnO	0.00	0.00	0.00
NiO	0.00	0.00	0.00
Sum	100.00	100.25	100.02

4.4 Geochemistry Results

The minimum, maximum, average and standard deviation of major oxides, trace elements and rare earth element (REE) concentrations of clastic sediments of the Tukau Formation are summarized in **Table 4.6**.

4.4.1. Geochemical Classification of Sandstone

The modified classification of Pettijohn et al. (1972) by Herron (1988) was used to classify the clastic sediments of the Tukau Formation into different lithotypes based on their geochemical characters. The plot works better since it avoids alkali problems while this scheme also measures the mineral stability. Based on Herron's (1988) plot, the clastic sediments of the Tukau Formation are classified as shale (n=3), wackes (n=32); arkoses (n=6; grouped arkoses and subarkoses together for easy discussion and less number of samples in the individual fields); litharenites (n=16; grouped litharenites and sublitharenites together) and quartz arenites (n=6) as shown in **Figure 4.9**. These major names stated above are referred as shales, wackes, arkoses, litharenites and quartz arenites throughout the discussion part here onwards in this thesis.

Table 4.6. Statistical summary of the geochemical data of the sedimentary rocks from the Tukai Formation

Sample No	Wacke (n=32 for major; n=24 for trace & REE)				Shale (n=3 for major; n=2 for trace & REE)			
	Min	Max	Avg	St.Dev	Min	Max	Avg	St.Dev
SiO ₂ %	66.25	75.16	70.84	2.55	62.57	66.43	64.03	2.10
SiO ₂ (adj)	73.01	78.61	75.56	1.76	68.30	72.33	69.96	2.10
TiO ₂ %	0.72	0.95	0.84	0.07	0.75	0.77	0.76	0.01
Al ₂ O ₃ %	13.20	18.61	16.44	1.44	15.38	17.61	16.73	1.19
Fe ₂ O _{3t} %	1.11	4.26	2.29	0.79	5.52	6.29	5.87	0.39
MnO %	0.00	0.02	0.01	0.00	0.02	0.09	0.05	0.04
MgO %	0.41	1.12	0.63	0.13	1.12	1.50	1.25	0.22
CaO %	0.06	0.10	0.07	0.01	0.07	0.25	0.13	0.10
Na ₂ O %	0.00	0.19	0.09	0.05	0.05	0.13	0.08	0.04
K ₂ O %	1.86	2.83	2.48	0.25	2.42	2.65	2.56	0.12
P ₂ O ₅ %	0.03	0.06	0.04	0.01	0.05	0.07	0.06	0.01
LoI %	4.06	9.71	6.48	1.60	8.21	9.57	8.72	0.74
Total	99.35	101.10	100.21	0.44	99.91	100.58	100.24	0.34
V	35.00	119.00	93.96	18.18	96.00	108.00	102.00	8.49
Cr	40.00	230.00	84.58	33.10	80.00	80.00	80.00	0.00
Co	1.00	28.00	8.17	6.88	15.00	16.00	15.50	0.71
Ni	20.00	40.00	31.67	9.37	30.00	40.00	35.00	7.07
Cu	10.00	50.00	27.50	13.33	20.00	20.00	20.00	0.00
Zn	30.00	110.00	50.00	24.90	50.00	100.00	75.00	35.36
Ga	6.00	21.00	16.92	3.17	16.00	18.00	17.00	1.41
Ge	1.00	2.00	1.36	0.49	1.00	1.00	1.00	0.00
As	5.00	11.00	7.40	1.80	6.00	7.00	6.50	0.71
Rb	32.00	142.00	114.71	23.55	114.00	122.00	118.00	5.66
Sr	23.00	89.00	63.46	13.79	74.00	75.00	74.50	0.71
Y	9.00	44.00	25.04	5.78	24.00	32.00	28.00	5.66
Zr	126.00	369.00	246.83	59.59	205.00	205.00	205.00	0.00
Nb	4.00	10.00	7.75	1.67	5.00	11.00	8.00	4.24
Sn	2.00	6.00	2.52	0.95	1.00	2.00	1.50	0.71
Cs	2.60	11.40	8.98	2.01	8.40	9.00	8.70	0.42
Ba	77.00	293.00	240.00	44.75	243.00	262.00	252.50	13.44
Hf	2.90	8.40	5.70	1.33	4.50	5.00	4.75	0.35
Ta	0.40	1.20	0.96	0.15	0.80	0.90	0.85	0.07
W	1.00	11.00	2.25	1.98	1.00	1.00	1.00	0.00
Tl	0.30	0.50	0.43	0.08	0.30	0.40	0.35	0.07
Pb	9.00	60.00	20.21	9.97	13.00	14.00	13.50	0.71
Th	4.50	16.50	12.60	2.42	11.80	13.80	12.80	1.41
U	1.10	4.00	3.21	0.55	3.40	3.60	3.50	0.14
La	12.70	42.50	35.39	6.01	31.20	35.20	33.20	2.83
Ce	24.60	90.00	69.99	12.48	61.90	70.70	66.30	6.22
Pr	2.79	10.80	7.85	1.49	6.96	8.14	7.55	0.83
Nd	10.70	42.70	28.87	5.82	25.70	30.70	28.20	3.54
Sm	2.00	10.50	5.45	1.47	4.90	6.40	5.65	1.06
Eu	0.39	2.51	1.14	0.37	1.08	1.40	1.24	0.23
Gd	1.70	10.60	4.55	1.56	4.30	5.90	5.10	1.13
Tb	0.30	1.60	0.73	0.23	0.70	0.90	0.80	0.14
Dy	1.50	9.00	4.42	1.25	4.10	5.50	4.80	0.99
Ho	0.30	1.60	0.88	0.22	0.80	1.10	0.95	0.21
Er	1.00	4.40	2.70	0.56	2.50	3.10	2.80	0.42
Tm	0.15	0.62	0.41	0.08	0.39	0.45	0.42	0.04
Yb	1.00	4.00	2.80	0.51	2.70	2.90	2.80	0.14
Lu	0.16	0.59	0.45	0.08	0.40	0.48	0.44	0.06

Table 4.6 (Contd.). Statistical summary of the geochemical data of the sedimentary rocks from the Tukai Formation

Sample No	Litharenites (n=16 for major; n=15 for trace & REE)				Arkoses (n=6 for major; n=3 for trace & REE)			
	Min	Max	Avg	St.Dev	Min	Max	Avg	St.Dev
SiO ₂ %	80.20	96.19	89.33	5.34	74.13	89.06	78.50	5.55
SiO ₂ (adj)	82.72	96.59	90.68	4.39	77.14	89.71	81.44	4.42
TiO ₂ %	0.11	0.68	0.36	0.16	0.50	1.19	0.80	0.22
Al ₂ O ₃ %	2.22	12.02	6.12	2.94	7.54	15.97	13.23	3.01
Fe ₂ O _{3t} %	0.62	3.06	1.47	0.74	0.80	1.37	1.12	0.22
MnO %	0.00	0.01	0.00	0.00	0.00	0.01	0.01	0.00
MgO %	0.05	0.41	0.19	0.11	0.16	0.59	0.47	0.16
CaO %	0.06	0.09	0.07	0.01	0.06	0.07	0.07	0.00
Na ₂ O %	0.00	0.08	0.03	0.03	0.00	0.10	0.04	0.04
K ₂ O %	0.25	1.65	0.86	0.44	1.12	3.01	2.05	0.62
P ₂ O ₅ %	0.01	0.04	0.02	0.01	0.03	0.06	0.04	0.01
LoI %	0.04	4.06	1.90	1.30	1.09	5.76	3.79	1.51
Total	98.96	100.96	100.36	0.52	99.72	100.75	100.12	0.41
V	19.00	83.00	44.60	21.14	67.00	90.00	82.33	13.28
Cr	20.00	80.00	53.85	19.81	80.00	90.00	86.67	5.77
Co	1.00	7.00	2.43	2.15	1.00	3.00	2.00	1.00
Ni	-	-	--	-	-	-	-	-
Cu	10.00	260.00	63.33	80.49	10.00	20.00	15.00	7.07
Zn	40.00	100.00	57.50	28.72	0.00	0.00	-	-
Ga	3.00	15.00	8.27	3.92	13.00	17.00	15.33	2.08
Ge	1.00	2.00	1.20	0.41	1.00	1.00	1.00	0.00
As	5.00	16.00	8.70	3.65	5.00	6.00	5.50	0.71
Rb	13.00	84.00	48.60	24.83	77.00	111.00	98.33	18.58
Sr	14.00	70.00	41.00	18.15	42.00	54.00	48.67	6.11
Y	6.00	25.00	14.33	6.09	19.00	27.00	24.00	4.36
Zr	60.00	749.00	250.00	212.58	244.00	439.00	342.00	97.50
Nb	2.00	8.00	4.20	2.01	4.00	6.00	5.33	1.15
Sn	1.00	3.00	1.89	0.60	1.00	2.00	1.67	0.58
Cs	0.90	6.70	3.59	2.06	6.00	9.30	7.70	1.65
Ba	40.00	204.00	118.27	51.78	180.00	230.00	213.00	28.58
Hf	1.60	16.90	5.75	4.73	5.60	9.70	7.57	2.06
Ta	0.20	0.90	0.55	0.22	0.70	1.00	0.90	0.17
W	1.00	2.00	1.14	0.38	2.00	2.00	2.00	0.00
Tl	0.10	0.30	0.20	0.06	0.20	0.40	0.33	0.12
Pb	6.00	21.00	11.57	3.94	12.00	29.00	21.33	8.62
Th	3.50	13.10	7.63	3.23	11.60	13.10	12.43	0.76
U	0.80	3.40	2.09	0.86	2.90	3.80	3.37	0.45
La	9.60	31.60	20.33	7.62	28.50	39.20	34.43	5.44
Ce	17.50	63.00	39.26	15.31	55.30	80.20	68.43	12.51
Pr	1.97	6.97	4.41	1.72	6.07	8.98	7.64	1.47
Nd	7.10	25.60	16.03	6.38	21.80	33.80	28.13	6.03
Sm	1.20	4.50	2.91	1.13	4.10	6.30	5.20	1.10
Eu	0.20	0.90	0.55	0.21	0.73	1.21	0.96	0.24
Gd	1.00	3.50	2.32	0.89	2.70	5.00	3.97	1.17
Tb	0.20	0.60	0.39	0.16	0.50	0.80	0.67	0.15
Dy	1.00	3.80	2.35	0.96	3.20	4.60	4.07	0.76
Ho	0.20	0.80	0.49	0.21	0.70	0.90	0.83	0.12
Er	0.60	2.60	1.53	0.67	2.00	2.90	2.57	0.49
Tm	0.10	0.42	0.24	0.11	0.32	0.48	0.41	0.08
Yb	0.60	3.00	1.68	0.74	2.30	3.30	2.87	0.51
Lu	0.09	0.49	0.27	0.12	0.39	0.53	0.47	0.07

Table 4.6(Contind.). Statistical summary of the geochemical data of the sedimentary rocks from the Tukau Formation

Sample Type	Arenites (n=6)			
	Min	Max	Avg	St.Dev
SiO ₂ %	96.89	98.45	97.75	0.62
SiO ₂ (adj)	97.28	98.67	97.75	0.53
TiO ₂ %	0.06	0.16	0.09	0.04
Al ₂ O ₃ %	0.60	1.96	1.23	0.58
Fe ₂ O _{3t} %	0.32	1.57	0.70	0.48
MnO %	0.00	0.01	0.00	0.00
MgO %	0.00	0.04	0.01	0.02
CaO %	0.05	0.07	0.06	0.01
Na ₂ O %	0.00	0.09	0.01	0.04
K ₂ O %	0.07	0.23	0.14	0.06
P ₂ O ₅ %	0.01	0.02	0.01	0.01
LoI %	0.33	0.65	0.49	0.13
Total	99.98	100.93	100.49	0.36
V	5.00	22.00	13.20	7.09
Cr	40.00	40.00	40.00	
Co	-	-	-	-
Ni	-	-	-	-
Cu	20.00	170.00	95.00	106.07
Zn	160.00	160.00	160.00	-
Ga	2.00	4.00	2.60	0.89
Ge	1.00	1.00	1.00	0.00
As	19.00	19.00	19.00	-
Rb	4.00	19.00	9.33	5.47
Sr	9.00	31.00	16.17	8.01
Y	3.00	8.00	5.33	1.75
Zr	37.00	209.00	79.00	65.25
Nb	1.00	3.00	1.75	0.96
Sn	1.00	1.00	1.00	0.00
Cs	0.50	1.20	0.78	0.30
Ba	24.00	62.00	35.83	14.41
Hf	0.90	5.00	2.00	1.51
Ta	0.10	0.30	0.17	0.08
W	-	-	-	-
Tl	-	-	-	-
Pb	5.00	11.00	7.50	2.65
Th	1.30	4.60	2.33	1.19
U	0.50	1.20	0.70	0.26
La	4.90	25.00	9.85	7.66
Ce	8.60	37.30	16.48	10.69
Pr	0.96	3.11	1.65	0.79
Nd	3.60	11.40	6.00	2.83
Sm	0.60	2.00	1.02	0.51
Eu	0.12	0.40	0.21	0.10
Gd	0.50	1.40	0.83	0.31
Tb	0.10	0.30	0.14	0.09
Dy	0.60	1.40	0.87	0.29
Ho	0.10	0.30	0.18	0.08
Er	0.40	0.90	0.57	0.19
Tm	0.05	0.14	0.09	0.03
Yb	0.40	1.00	0.60	0.23
Lu	0.06	0.18	0.10	0.05

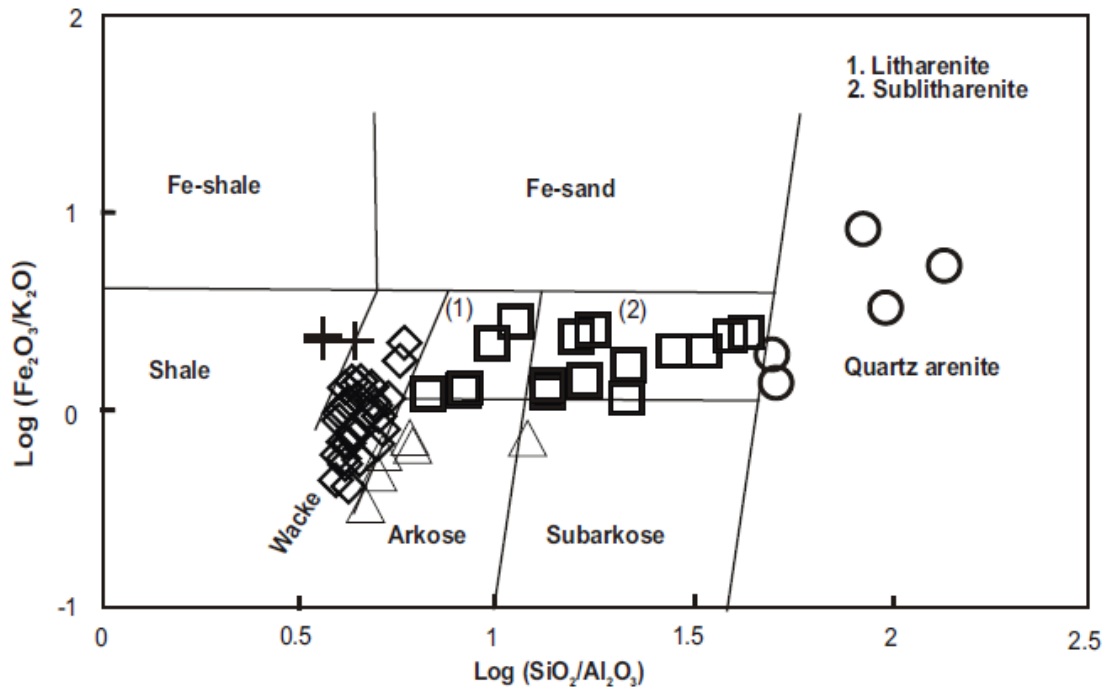


Figure 4.9. Geochemical classification of clastic sediments of the Tukau Formation (after Herron, 1988) (Refer this plot for the symbol description)

4.4.2. Major Oxides

The samples show a large degree of variation specifically with regards to their SiO_2 , P_2O_5 , Al_2O_3 , CaO and Fe_2O_3 contents amongst the types of shales and sandstone being studied. SiO_2 is the most dominant oxide in all the studied samples and is recorded with 97.75 wt%; 89.33 wt%; 78.50 wt%; 70.84 wt% and 64.03 wt% in quartz arenites, litharenites, arkoses, wackes and shales respectively. The Al_2O_3 content is recorded to be higher in shales and wackes (15.38-17.61 wt%; avg. 16.73 wt%; 13.20-18.61 wt%; avg. 16.44 wt%) compared to other sandstone types (Al_2O_3 =2.22-12.02 wt% for litharenites; 7.54-15.97 wt% for Arkoses and 0.60-1.96 wt % for quartz arenites respectively). Shales have a higher proportion of K_2O and are depleted in Na_2O , which reflects the greater proportion of clay minerals (especially illite and I-S) in the finer deposits. CaO and Na_2O content has a lower record (<0.15 wt% and <0.1 wt% respectively) in all the studied samples of Tukau Formation. All the major oxides studied are recorded to be lower than the UCC except SiO_2 , TiO_2 in sandstones and shales respectively as shown in **Figure. 4.10**.

4.4.3. Trace Elements

The trace elements are classified into four groups according to their geochemical behavior. Trace elements groups are transitional trace elements (TTE: Sc, V, Cr, Mn, Co, Ni, Cu, Zn); large ion lithophile elements (LILE; Rb, Cs, Ba, Sr), high field strength elements (HFSE; Zr, Hf, Nb, Ta, Y, Th, U, Ta and W) and rare earth elements (REE: La-Lu).

4.4.3.1. Transitional trace elements (TTE: Sc, V, Cr, Mn, Co, Ni, Cu, Zn)

Transitional elements are distributed widely between the samples and are enriched in shales and wackes compared to other sandstone types except for Cr, Cu and Zn. Their range are recorded as 96-108 ppm and 35-119 ppm for V; 6.88-15.00 ppm and 1-28 ppm for Co; 30.00-40.00 ppm and 20.00-40.00 ppm for Ni in shales and wackes respectively. Higher content of Cu and Zn in arenites (avg.95 ppm; 160 ppm) and Cr in arkoses (avg.86.67ppm) are related to the presence of heavy mineral phase and micro pyrite concretions in these sandstone types.

4.4.3.2. Large ion lithophile element (LILE; Rb, Cs, Ba, Sr, Be)

LILE also shows a significant variation among the shale and sandstone types and their range are recorded in shales as follows: 114-122 ppm; 32-142 ppm for Rb; 8.40-9.00 ppm; 2.60-11.40 ppm for Cs, 243-262 ppm; 77-293 ppm for Ba; and 74-75 ppm; 23-89 ppm for Sr respectively. Rb shows moderate to high positive correlation with K_2O , TiO_2 , Al_2O_3 , Ba, Ga and Cs which confirms its association with clay minerals.

4.4.3.3. High field strength elements (HFSE; Zr, Hf, Nb, Ta, Y, Th, U, and W)

The high field strength elements have distinct characters as they have small ionic radius with higher charge and possess higher resistance from the weathering processes. Thus, these elements are able to survive longer in sediments although the sediments undergo multiple cycles of deposition (recycling). Zr content is higher (i.e. >210ppm) in arkoses (342 ppm), litharenites (250 ppm) and wacke (247 ppm), thus, indicating the effects the recycling and sorting effect. Hf also

shows similar distribution as Zr in the studied shale and sandstone types. Th and U content is higher in shale followed by wacke, arkoses, litharenites and arenites.

Meanwhile, trace element concentration that is normalized against UCC shows a wider distribution of their content between the samples (**Figure 4.10**). However, a similar trend is observed among the samples except quartz arenites. Quartz arenites and litharenites are mostly depleted in all the trace element content except in Cu, Zn As. An opposite trend is observed in shales and wackes which are enriched in all the trace elements contents except Co and Ni. Overall, Ba, Sr, Ni, Ge, Nb and Sn contents are recorded to be lower than the UCC whilst As content is higher than UCC in all the studied samples (**Figure 4.10**), indicating that the provenance is mainly controlling these elements, particularly As which is mainly associated with pyrite concretions. In these sediments, Zr and Hf are mainly controlled by zircon which is enriched in many samples (**Figure 4.10**) due to the sorting and recycling effect. Zr and Hf show significant negative correlation with HREE excluding the contribution of REE from zircon minerals.

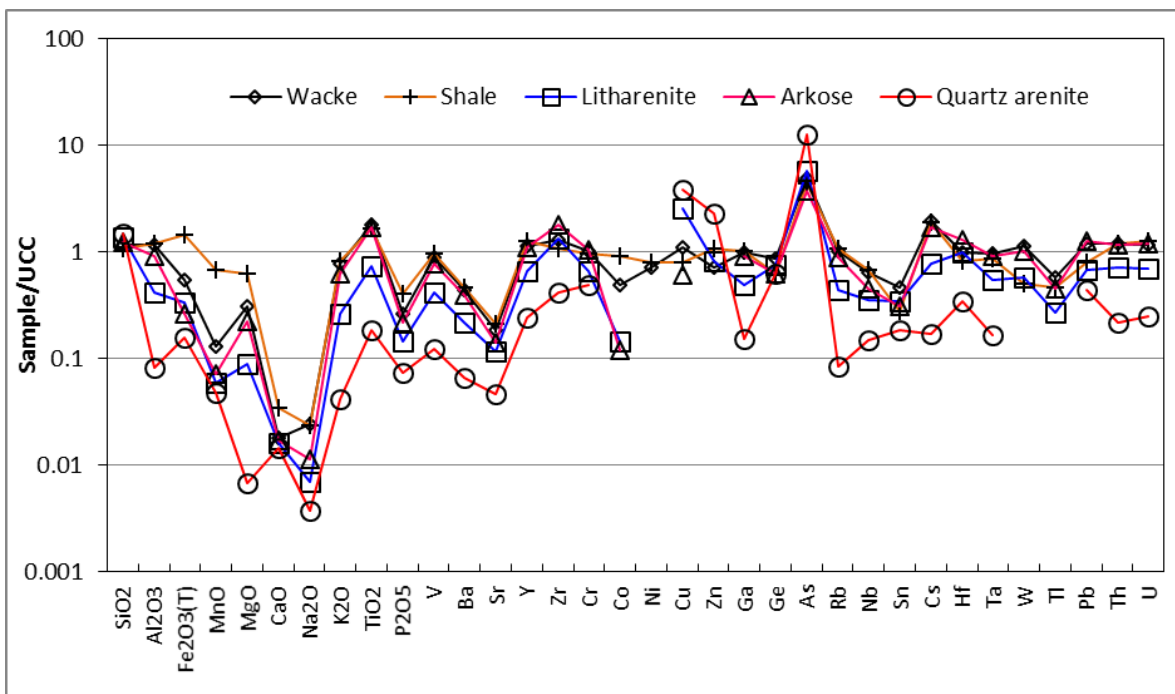


Figure 4.10 UCC normalized major oxides and trace elements recorded in Tukai sediments

4.4.3.4. Rare Earth Elements

Σ REE content varies significantly between the lithotypes as the highest concentrations are found in wackes (166 ppm), arkoses (161 ppm) and shales (160 ppm) compared to litharenites (93 ppm) and quartz arenites (39 ppm). This indicates that their association is mostly with fine grained particles and is mainly controlled by clay minerals in wackes, arkoses and shales compared to litharenites and quartz arenites. Chondrite normalized REE pattern shows a LREE enriched/fractionated ($\text{La/Yb}_{\text{CN}} = 7.18-9.27; 2.29-8.83; 7.81-8.20; 5.81-10.81$ and $7.21-16.89$ for wackes, arkoses, shales, litharenites and quartz arenites respectively). Meanwhile, HREE depleted/parallel to subparallel REE patterns ($\text{Gd/Yb}_{\text{CN}} = 1.00-2.15; 0.95-1.35; 1.29-1.65; 0.89-1.35$ and $1.01-1.30$ for wackes, arkoses, shales, litharenite and quartz arenites respectively) with significant negative Eu/Eu^* anomalies ($0.65-0.73; 0.62-0.67; 0.70-0.72; 0.55-0.72$ and $0.64-0.75$ for wackes, arkoses, shales, litharenites and quartz arenites respectively) indicates their felsic nature. All the lithotypes show a consistent and uniformed negative Eu anomalies between 0.65 and 0.71. The average wackes, shales and arkoses of the present is comparable with PAAS and UCC while litharenites and quartz arenites are recorded to have lower REE content compared to the PAAS and UCC (**Figure 4.11 and 4.12**).

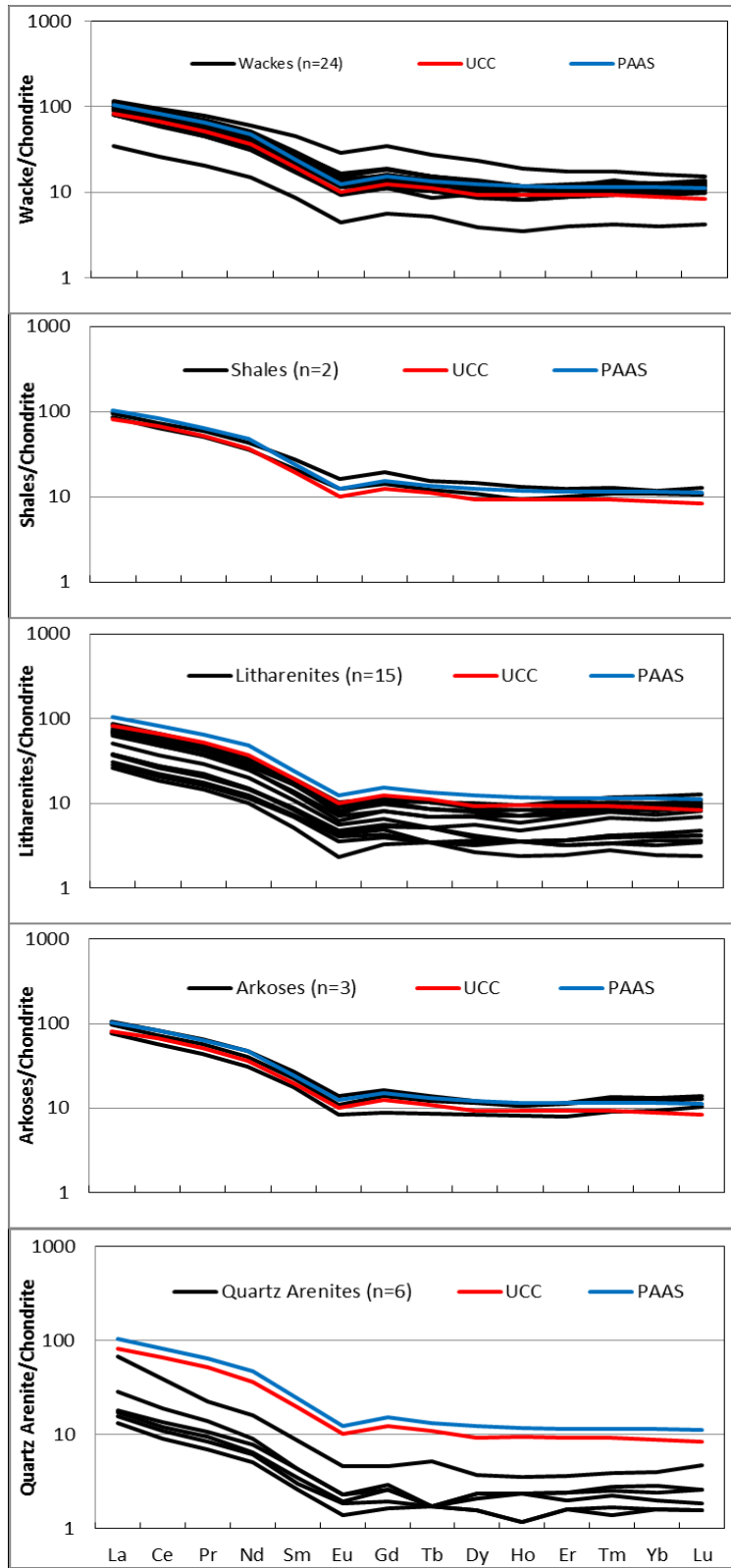


Figure 4.11. Chondrite normalized REE pattern for Clastic Sediments of Tukai Formation

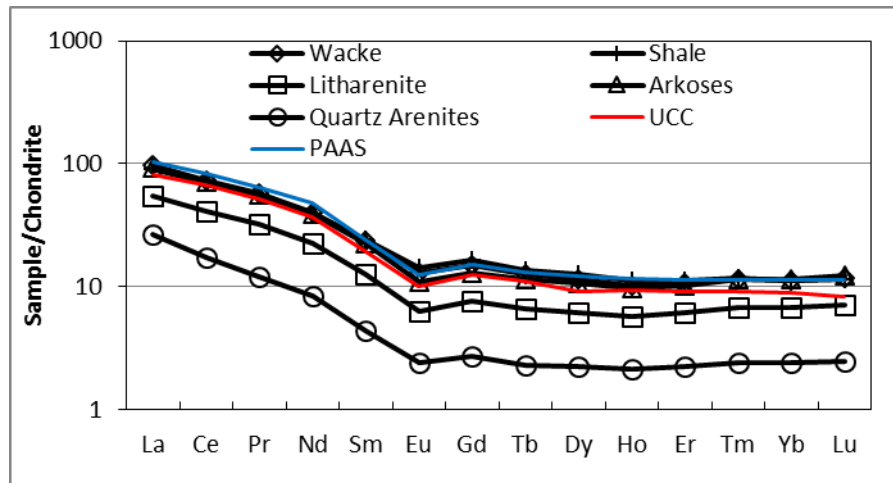


Figure 4.12. Chondrite normalized REE pattern for the average Sandstone and shales of Tukau Formation.

4.4.4 Geochemistry of zircon grains

The studied zircons were mostly detrital and showed very loose clusters. Amongst the U-Pb dating data, the best three age clusters were extracted and discussed in this section. Based on the $^{206}\text{Pb}/^{238}\text{U}$ age of <10% discordant data, the youngest group was 117-130 Ma with dominant peaks in 114-119 Ma age range (Lower Cretaceous). Another age group was of 220-240 Ma with a peak in 225 Ma (Upper Triassic). The older zircons were of 1300-2440 Ma (Meso-Paleo Proterozoic) in age (**Fig. 4.13 and 4.14**). The older ages of zircons were also recently reported in other studies (Ramkumar et al., 2018). The conventional U-Pb concordia plots for whole zircon analysis and younger age zircon analysis are presented in Figure 8a. Similarly, the relative frequency plots of youngest zircon ages are shown in Figure 8b. Meanwhile, Uranium and Th concentrations in the studied zircons range from 45 - 2300 ppm (avg. 458 ppm) and 25 - 771 ppm (avg. 179 ppm) respectively. U/Th ratio varies between 0.76 and 21.4 with an average of 3.2.

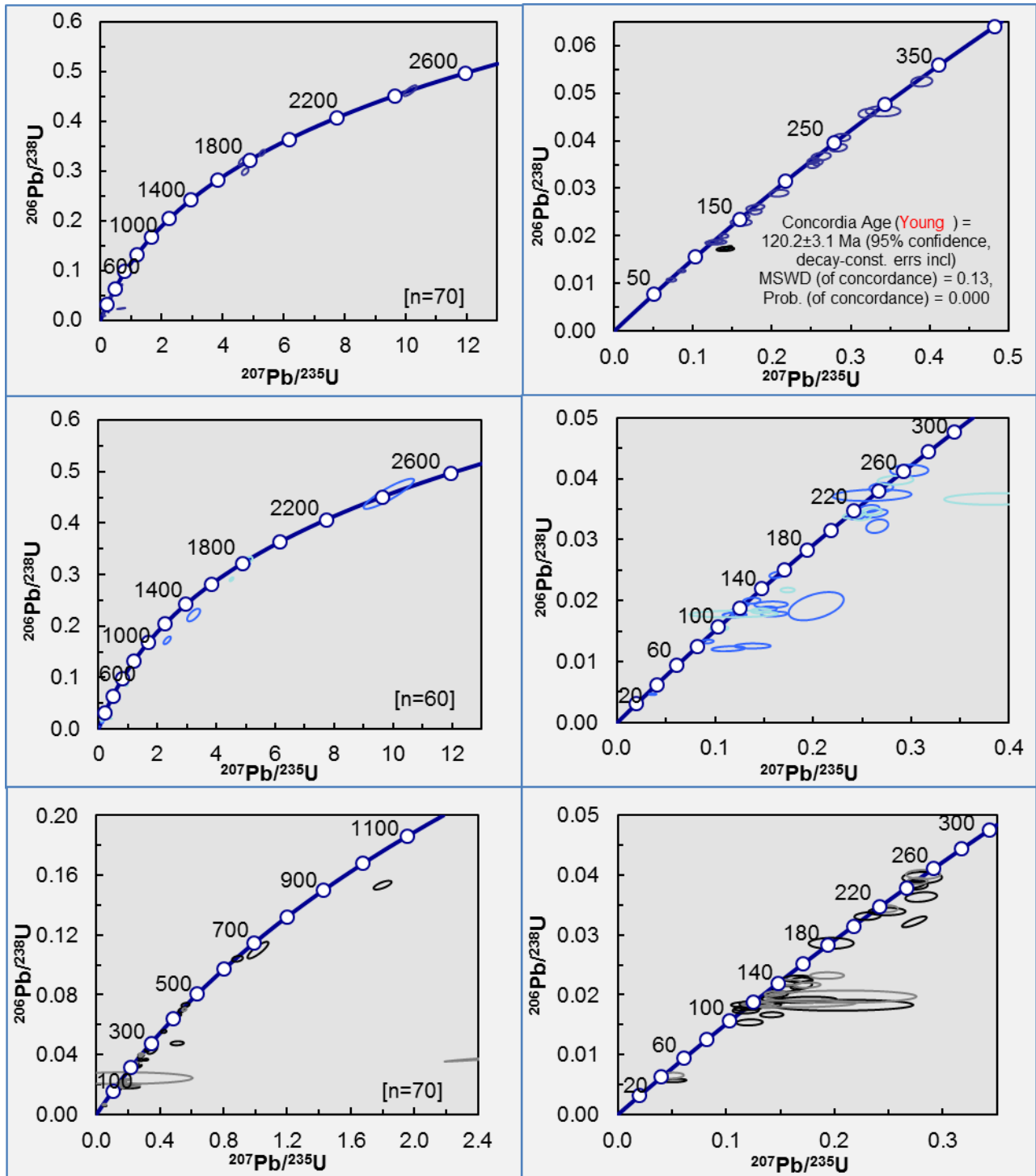


Figure 4.13 U-Pb Concordia plots for all age populations and younger age populations for the zircons extracted from the sandstones of the Tuku Formation

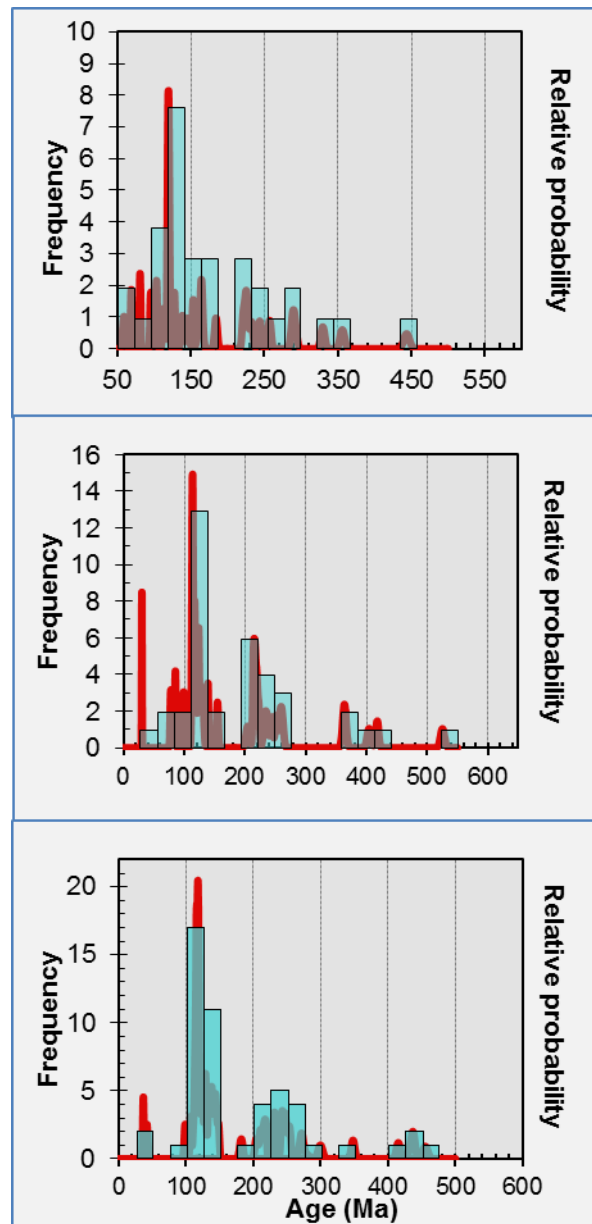


Figure 4.14 Relative frequency zircon age plots for the zircons extracted from sandstones of the Tukau Formation

4.5. Discussion

4.5.1. Paleoweathering

Weathering of sediment indicates the degree of alteration that a rock or sediment experience at a certain point in time after the exposure to weathering agents. Weathering intensity can be measured from any ancient sediment or recent sediments from different environment by using different indexes based on their major oxide concentrations, in particular, Al_2O_3 vs alkali and alkali earth elements (Nesbitt and Young, 1982). CIA (**C**hemical **I**ndex of **A**lteration; Nesbitt and Young, 1982), and PIA (**P**lagioclase **I**ndex of **A**lteration; Fedo et al. 1995) are used to assess the intensity of weathering. Based on the CIA values, the rock's weathering intensity can be categorized into i) no weathering (fresh parent rock: $\text{CIA} < 50$), ii) weak weathering ($\text{CIA} = 50-70$), iii) moderate weathering ($\text{CIA} = 70-80$) and iv) intense weathering ($\text{CIA} > 80$). In general, removal of easily displaced cations (K^+ , Na^+ , and Ca^{2+}) are relatively more stable elements/residual constituents (Al^{3+} and Ti^{4+}) through conversion of feldspar to clay minerals (Nesbitt and Young, 1982). Thus, fresh igneous rocks show CIA values from 45 to 55 while highly intensified weathered sediments (kaolinite, gibbsite, chlorite and bohemite) show CIA values that go up to ~ 100 . Moderate weathering is shown by smectite and illite group of clays with $\text{CIA} = \sim 60-80$. PIA values are also calculated in addition to CIA to support the interpretation, which mainly describes Ca rich end member of feldspar (plagioclase) hydrolyses since this mineral is most abundant in silicate rocks.

The CIA values are uniformly distributed throughout the stratigraphic horizon except one quartz arenite sample which shows low CIA values of 65. In the present study, the average CIA values recorded are 79 for quartz arenites; ($\text{CIA} = 82$ when one sample is discarded which shows lowest value 65), 84 for shales and 85 for wackes, litharenites and arkoses respectively, indicating intensive weathering which is well supported by the high PIA values from 93 to 98 and the absence of plagioclase feldspar in modal composition (minor amount of Ca poor feldspar is recorded).

Other than PIA and CIA indexes, weathering history of the Tukai sediments was estimated by plotting A-CN-K ternary diagram where in molecular ratio, A stands for Al_2O_3 , CN represents $\text{CaO}^* + \text{Na}_2\text{O}$ and K indicates K_2O (Nesbitt and Young 1984; Nesbitt 2003). The A-CN-K ternary plot (**Figure 4.15**) shows initial weathering trends which specify the alternation of igneous rocks that comes directly from the pristine rocks. As time goes by, the rock is weathered further causing

the plagioclase to be broken down and the process synchronously removes Na₂O and CaO from the bulk composition, moving the plots nearer towards A–K boundary. The highest level of weathering within the trend occurs when potassium and K-feldspar are removed in relative to Aluminium. The progress can be seen when the plots are distributed along the predicted weathering trend line in the A–CN–K plot.

The sandstones and shales of Tukai Formation are plotted above the feldspar join and an average shale indicates the moderate to intensive nature of weathering in the source region. Also, the studied samples are clustered together except some quartz arenites near illitic composition, indicating the dominance of illitic clay minerals in the studied samples except quartz arenites which are compositionally highly matured and are dominated by quartz. The intensive weathering is further evidenced by the abundant illite content over feldspar in the XRD and QEMSCAN analyses. Weathering trend in the A-CN-K plot indicates that the Tukai sediments are derived from felsic dominated cratons. Mineralogically these samples are enriched in illite and smectite than kaolinite as this can be clearly seen from the plot and is also confirmed by the XRD analysis where Illite and Illite-smectite are the dominant clay phases (avg. 20.43 wt %). Illite is the dominating clay in all the sediments of Tukai Formation except two samples, which are dominated by Kaolinite. Illite and chlorite are considered to be formed by weak hydrolysis and/or strong physical erosion of parent rocks under relatively dry climatic conditions (Galan and Ferrel, 2013; Hu et al., 2014). Presence of illite and association with quartz and feldspars can be related to the detrital origin and deposited in an arid climate (Adate and Keller, 1998). It is one of the early products of weathering of feldspathic and micaceous rocks and this clay is stable under temperate climate condition (Chaudhri and Kalitha, 1985). In general, illite is derived from parent rocks alteration and is poorly developed in soils (Diester-Haass et al. 1993). Illites are developed from moderate weathering of acidic rocks in the source area under temperate climate and are particularly common at middle latitudes (Krissek, 1989). The results from this study showed that illite has a grain size greater than 2 μ m; often an indication of the presence of detrital and/or mica. Hydrolysis of mica and feldspar in the parent rock may yield illite and kaolinite. They also can be derived from the weathering of low to moderate grade of metamorphic rocks (schists and slates; Sáez et al., 2003), which are common in the source region. Also, the illite content of the samples may include some muscovites. The muscovite rich low grade metamorphic rocks may be yielded more illite illite-smectite clays as the detrital minerals. Illites in the present studied samples are mainly

derived as detrital illites from the low grade metamorphic rocks from the source region rather than formed by diagenesis or metamorphism after the deposition. The kaolinite rich samples only indicates hydrolysis. Detrital mineral illite originated from muscovite or diagenetic –metamorphic illitic material can be indicated by their existence in coarse clay fraction (Velde & Meunier, 2008). Weaver (1956) stated that muscovite is the most significant sources for 2M illites and therefore indicating detrital in origin. Erosional processes also contributes to the formation of clay minerals. Therefore, the abundance of illite is representing the source material and the type of weathering rather than environmental diagenesis. Also, the adsorption of water into the interlayer of illite and muscovite resembles the diagenesis process but it does not modified the lattice structures (Weaver,1956).

However, formation of kaolinite is favoured under intense weathering and tropical conditions (Biscaye, 1965; Wan and Chen, 1988). The ‘crystallinity’, a measure of the lattice ordering (the full width at half maximum height (FWHM) of the illite 10 Å peak). Poorly crystalline illites are formed due to intense hydrolysis in the hinterland source area under warm humid climatic conditions (Das et al., 2013). Lower values of illite crystallinity indicates good crystallinity and higher value of illite crystallinity represent poor crystallinity indicate weak and strong hydrolysis respectively under arid and cold (humid and warm) climatic conditions in continental sources (Chanley,1989; Krumm and Buggisch, 1991; Ehrmann, 1998; Liu et al., 2008a; Liu et al., 2008b). During weathering, illite chemistry index and crystallinity responding to the hydrolysis and the climate (Liu et al., 2007). The studied samples from the Tukai Formation have low to moderate illite crystallinity, indicating that they have experienced less post-depositional thermal alteration (Krissek and Horner, 1991). Moderately crystalline illites indicates that physical weathering has dominated the source area as it was not degraded further and lacks neoformation (Gaucher, 1981). Meanwhile, moderate crystallinity indicates a mixture of illite and muscovites from different continental sources. Poor crystallinity which have higher crystallinity index are Al-rich illites (muscovites) and are formed by strong hydrolysis in the source area under warm humid climatic conditions. Active tectonic setting of the northern Borneo favoured stronger physical erosion of parent rocks during the Oligocene-Miocene, (Rangin et al., 1990; Hutchison, 2005). The intense seasonal precipitation also supported the physical erosion and deposition of illite and chloite dominated clay minerals (i.e., Liu et al., 2012). In addition, the moderate chemical

weathering of recycled sediments increased the abundance of kaolinite in some arkose samples (S01 and S08). Meanwhile, feldspar is not as abundant across all samples. The minor amount of feldspar could be due to the dissolution of the grains as they are easily degraded when subjected to weathering processes (e.g. moderate to intensive weathering).

The presence of kaolinite indicates intense weathering under possible tropical conditions (Biscaye, 1965) where high rainfall favours ionic transfer and pedogenic development (Wong and Chen, 1988; Islam et al., 2002; Xie et al., 2015). With presence of meteoric water, kaolinite formed in sediments from feldspar and mica particularly in region with tropical and subtropical climate (Bjorlykke, 1998). Heine and Völkel (2010) also mentioned that secondary clay minerals can be derived from the weathering of the parent rocks via physical and chemical disaggregation. Feldspar weathering will create void which later will be filled up by kaolinite as the secondary minerals which is well-supported in the present study that the kaolinite mainly occurred as book masses and fill the pores (Modenesi-Gauttieri et al., 2011). Low salinity water favours kaolinite settling, thus, non-marine successions are normally enriched with kaolinite. The high content of kaolinite in two studied samples may be the end product of rock disintegration in the hinterland and in situ weathering profiles. Samples S01 and S08 show higher content of kaolinite (49% and 50%; less than 2µm) indicating intensive hydrolysis under warm and humid climate in which kaolinite is generally formed by monosialitization of parent rocks, enriched in alkali and alkaline elements (granite, granodiorite and intermediate-acid volcanic rocks). According to Wilson (1999) hydrolysis is common in warm humid tropics; usually obvious in dry subtropics and warm temperate. Oxidation of biotite (Mica group) could also explain the direct formation of kaolinite through the exfoliation (Ojanuga, 1973). Throughout Cenozoic, Borneo was experiencing a humid tropical climate (van Hattum et al., 2013). Therefore, kaolinite is mainly formed during sedimentation and thus represents extreme chemical weathering (hydrolysis) under sub-tropical conditions prevailed during Miocene.

Smectite is recorded significantly on S04, which can be either detrital or formed in situ through authigenic processes (early diagenesis, alteration of volcanic glasses and hydrothermalism) (Ehrmann et al. 2005). Kaolinite corresponds to diagenetic origin, indicating warm, semi-humid to humid climatic conditions (precipitation >700mm/y), extensive meteoric

water flushing and formation of kaolinite (Weaver, 1989). Illite is the primary mineral with chlorite absent which is formed through weak hydrolysis and/or strong physical erosion of parent rocks. According to lithotype analysis the illite clay is finely intermixed with calcite mud and Fe bearing illite clays. The poorly crystalline illites are formed due to intense hydrolysis in the hinterland source area under warm humid climatic conditions. A lower content of smectite in the studied samples and higher ratios of illite, quartz and feldspar indicate that a moderately weathered continental (acidic) terrane. These types of continental source terranes contain acidic igneous and/or metamorphic lithologies and pre-existing sedimentary rocks, which are common throughout NW Borneo.

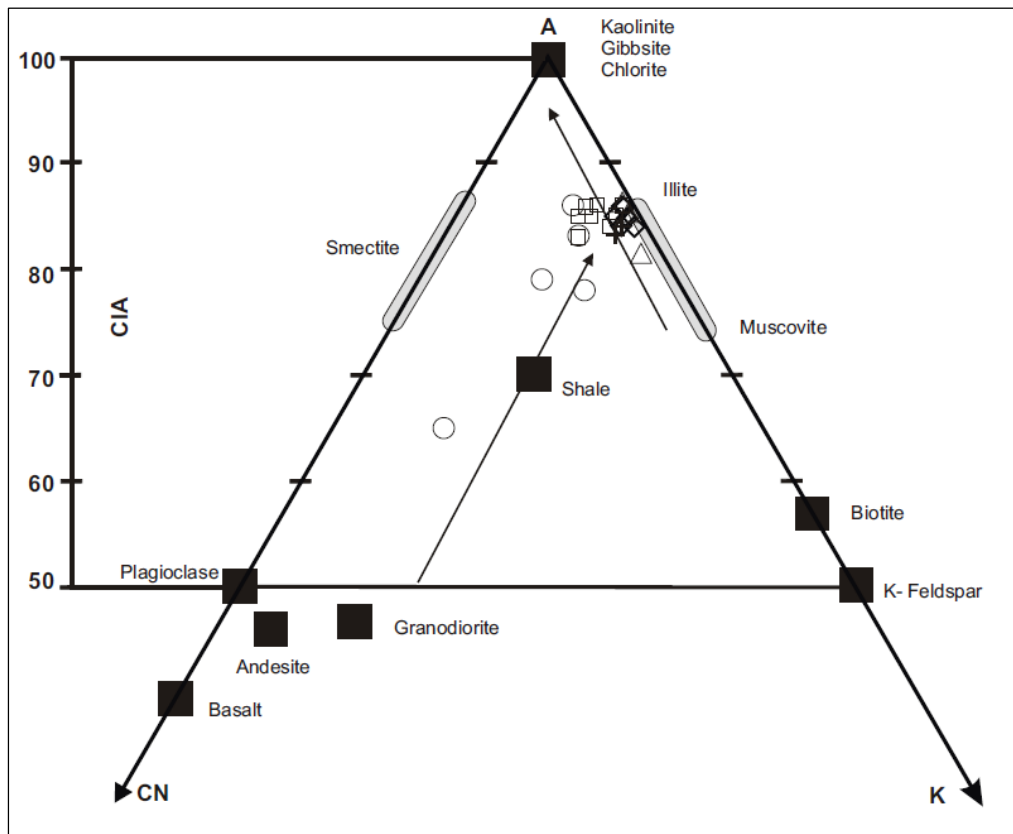


Figure 4.15. $\text{Al}_2\text{O}_3 - (\text{CaO}^* + \text{Na}_2\text{O}) - \text{K}_2\text{O}$ (A-CN-K, in molecular proportion; Nesbitt and Young, 1982) ternary diagram shows the intensity of weathering for the Sediments of Tukau Formation

4.5.2 *Maturity*

Maturity of sandstone is measured based on mineralogy and texture. Sediments maturity is caused by weathering processes, long transportation with unstable minerals almost disappearing or non-existent in the composition and presence of rounded grains. Different researchers refer to maturity in different terms, for example, Selley (1981) defined maturity based on physical and chemical aspects, Plumley (1948) considered well sorted and mineralogically mature as matured sandstone while Folk (1951) defined maturity based on the absent of interstitial clay, well sorting and rounded. To sum up, maturity relies on fine grained materials, sorting and roundness of the grains. As observed from the samples, most of them have approximately 5 – 10 % clay matrix and with most grains sub-angular to sub-rounded. Therefore, it can be summarized that the samples fall into the “texturally immature” category based on Folk (1951).

The maturity of sandstone can be linked to the depositional environment. Some researchers also claimed that the maturity can be linked to the intensity of tectonic activity in the region. Intense tectonic activity will generate immature sediments, mild tectonic activity generates sub mature sediments and inactive tectonic activity will produce mature sediments. Texturally immature samples may indicate that the depositional areas have had intense tectonic activity. In terms of mineralogical maturity, majority of the samples are considered as mature due to the abundance of quartz grains compared to feldspars and rock fragments.

The mineralogical "maturity" of the heavy mineral assemblages of sandstones is quantitatively defined by a proposed zircon-tourmaline-rutile (ZTR) index (Hubert, 1962). The ZTR index is the percentage of the combined zircon, tourmaline, and rutile grains among the transparent, non-micaceous, detrital heavy minerals. The ZTR index is commonly high in beach or littoral zone depositional environment due to the long transport distances from the source and the high energy of the environment. These minerals are found in abundance in sediments due to their high specific gravity and resistance to weathering. The ZTR index in the sediments of Tukai and sediments are recorded higher values of >95 indicate that these sediments are highly texturally matured.

Al₂O₃-TiO₂- Zr Ternary plot may illustrate the presence of sorting related to fractionations thus eliminating the weathering effects (Garcia et al., 1991). In this plot the

Tukau sediments plot towards Zr are characterized by changes in the $\text{Al}_2\text{O}_3/\text{Zr}$ ratio, which is due to a recycling effect (**Figure. 4.16**). Sediment maturity can be estimated based on $\text{SiO}_2/\text{Al}_2\text{O}_3$ ratio, which increases via the increase in quartz at the expense of primary clay sized material and decrease in trace element concentration (McLennan et al. 1993). Accordingly, quartz arenites and litharenites show higher maturity compared to arkoses, wackes and shales. This is further affirmed by higher values of clay/ feldspar ratio in the Tukau sediments.

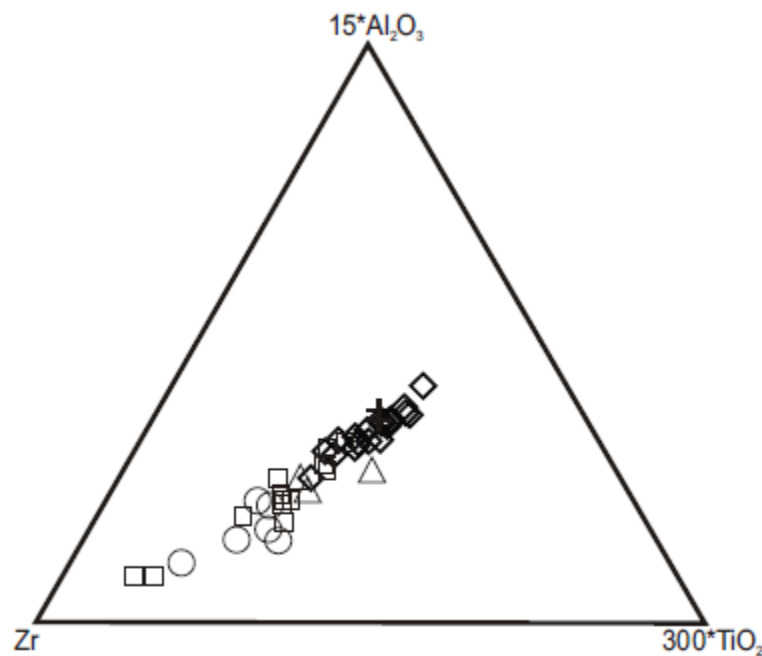


Figure 4.16 Al_2O_3 -Zr- TiO_2 plot showing the sorting trend for the clastic sediments of the Tukau Formations (after Garcia et al., 1991)

4.5.3. Provenance

Mineralogy and geochemistry data were used in order to reconstruct the provenance information of the Tukau Formation which will be compared with petrographic data later. Mineralogically the Tukau sediments are enriched in quartz and illitic clay minerals suggesting that the source are contains more felsic origins. The Tukau sediments commonly contain abundant rutile/anatase and

zircon and minor amount of chromite. Heavy minerals such as zircon, rutile/anatase and chromites are common in these sediments where zircon is mainly associated with felsic igneous rocks, and rutile mostly associated with high grade metamorphic rocks. The range of shapes in zircons may suggest that they might be mixed with fresh sediments which is clearly shown by the fractions of strongly rounded grains occur with idiomorphic or hipidiomorphic ones. Overall, the mixture of euhedral and well-rounded grains of heavy minerals suggests a mixture of metamorphic/metasedimentary and granitic source areas. A significant variation in the calculated provenance sensitive heavy mineral ratio such as garnet:zircon (GZi) and rutile:zircon (RuZi) indicates a provenance source from metasedimentary source and/or an acid igneous rocks including allanite bearing granitoid. High and low values of GZi and RuZi are an indication of a metasedimentary and an acid igneous source respectively (Ratcliffe et al 2007). The variation in RuZi (38.6-87.2) and low to moderate content CZi (5.5-24.7) indicates that mixture of rutile bearing (metapelitic and/or metamafic rocks) and rutile poor lithologies (acid igneous sediment) in the source area.

Major elements based on discrimination diagram (Roser and Korsch, 1988) and trace element based plot (Hf vs La/Th; Floyd and Leveridge 1987) were used in order to elucidate the provenance of the Tukai sediments. The studied shales and sandstones falls in quartzose sedimentary provenance field in the provenance discriminant plot of Roser Korsch (1988) except two shale samples plot on the igneous provenance indicating the felsic nature of source rocks with significant amount of recycled material from the source region in addition to minor contribution from mafic-ultramafic region (**Figure 4.17**). Similarly, shales that are enriched with mafic minerals fall into the mafic igneous source area. The felsic and recycled nature of sediments is again reaffirmed by the Hf vs La/Th plot (**Figure 4.18**) where an increasing trend of Hf indicates the recycled/old sedimentary passive margin source or progressive dissection of an arc. Wackes are mostly plotted in acidic arc field and are comparable to UCC and PAAS. One quartz arenite sample plot in mixed felsic and mafic sources indicates a certain contribution from the mafic to ultramafic sources. Sediment recycling and weathering increase the Rb/Sr values in the sediments (McLennan et al., 1993). The higher average values of Rb/Sr in the present study with 1.84 for wackes; 1.58 for shales; 1.18 for litharenites; 2.01 for arkoses and 0.56 for quartz arenites indicate a strong recycling history in the Tukai Formation. The felsic dominated source rocks from the source region is also confirmed by the incompatible trace elements such as REEs nature: LREE enriched, HREE depleted, negative Eu/Eu* anomaly and high LREE/HREE values (**Figure 4.11**,

4.12). The obvious negative Eu anomalies in the studied shales and sandstones reflect their derivation from materials that had experienced fractionation of feldspar, thus suggesting a granitoid dominated provenance for the first cycle of sedimentation. The Eu/Eu* values of litharenites and arkoses are comparable with PAAS (Eu/Eu*=0.66), whilst the ratio that is increased in wackes, shales and quartz arenites may be due to recycling effect since more feldspar is destroyed in a second cycle of weathering (e.g. Hassan et al., 1999; Mongelli et al., 2006). According to Mongelli et al. (2006) the Eu released during the feldspar dissolution should be retained by clay minerals and thus reducing the effect of recycling induced increase of Eu anomaly. Also the recorded Eu/Eu* values of different lithotypes of the Tukai Formation are comparable with the range of Eu/Eu* values reported for recycled sedimentary rocks (Eu/Eu* = 0.6 – 0.7; McLennan et al., 1993). Recycling of the sediments is also addressed by the low K₂O/Al₂O₃ ratio (<0.3; present study <0.2), enrichment of LREE/HREE values (8 and above), enrichment of less soluble elements such as Th and Y and depletion of highly soluble elements such as U and Sr (Cox and Lowe, 1995; Cox et al., 1995). Heavy minerals such as zircon, rutile/anatase and chromites are common in these sediments where zircon is mainly associated with felsic igneous rocks, while rutile is mostly associated with high grade metamorphic rocks and chromites are mostly associated with ultramafic/mafic rocks as the primary minerals as a result of magmatic differentiation and occurs as veins or embedded mass in peridotite rocks and the serpentinites. The relative contribution of mafic-ultramafic rocks from the source region can be evaluated by the concentration of Cr, V, Ni, Sc (Cullers, 2000) and the ratios of Y/Ni and Cr/V (Hiscott, 1984). High content of Cr and Ni with a value of >150 ppm and >100 ppm are the distinct characters of ultramafic sources (Garver et al. 1996). The Cr content in the studied sediments is 85, 80, 54, 87, and 40 ppm in wacke, shale, litharenites, arkoses, and quartz arenites respectively which indicate less or no significant input from ultramafic source rocks. However, one of the wacke samples shows high content of Cr (230ppm in 12D) which indicates that it has received significant input from mafic-ultramafic rocks and/or presence of chromian spinels. Nickel (Ni) composition is mostly recorded between BDL to maximum 40ppm. A small amount of mafic-ultramafic rocks input is also confirmed from the heavy mineral analysis where chromites to chrome spinels are commonly found in selected samples as subhedral and broken grains. Chromites are mostly associated with ultramafic/mafic rocks as the resulting primary minerals of magmatic differentiation and occur as veins, or embedded mass in peridotite rocks and the serpentinites.

Mineralogically the Tukai sediments are enriched in quartz and illitic clay minerals accompanied by fractionated heavy minerals such as zircon, rutile/anatase and chromites which suggests a felsic dominated source.

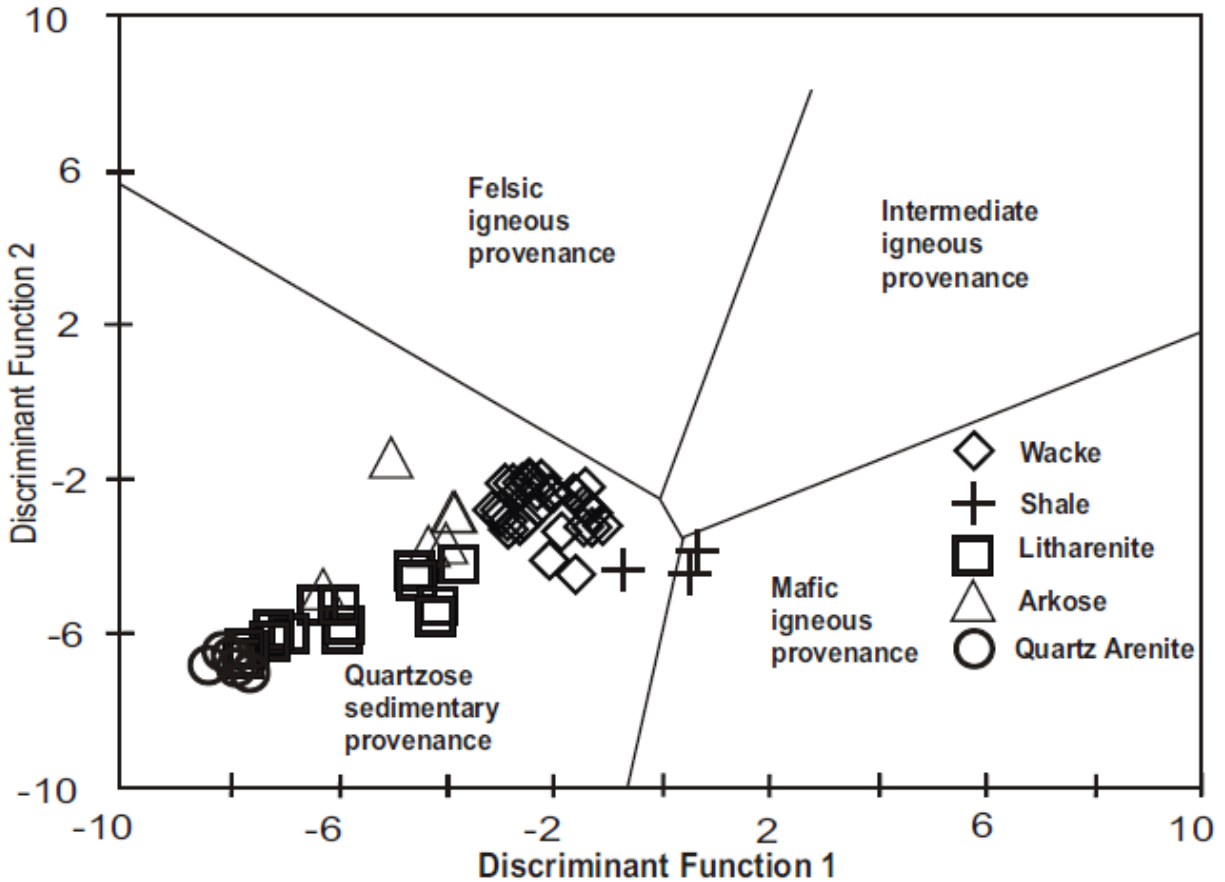


Figure 4.17 Major oxide based provenance discrimination plot shows the possible provenance for the Tukai sediments (after Roser and Korsch, 1988)

In addition to mineralogy and bulk rock geochemistry, mineral chemistry of tourmaline and chromian spinels was also used to reconstruct the provenance of the Tukai clastic sediments. Two powerful provenance discrimination diagrams ($Al-Al_{50}Mg_{50}-Al_{50}-Fe_{(tot)_{50}}$ and $Ca-Fe_{total}-Mg$ ternary diagrams; Henry and Guidotti, 1985), based on the chemistry of detrital tourmaline were used to trace the provenance since these diagrams clearly evaluate the similarities and differences between the detrital tourmaline populations besides giving a clear picture on the nature of their source areas, where tourmaline is stable in both weathering and diagenetic environments (Morton and Hallsworth, 2007). The tourmaline compositions are plotted on the provenance-discrimination ternary diagram ($Al-Al_{50}Mg_{50}-Al_{50}-Fe_{(tot)_{50}}$) (Henry and Guidotti, 1985) based on the relative

abundances of Al, Fe, and Mg. Most of the tourmalines from the Tukai sediments fall in Field B and D according to Henry and Guidotti (1985) (**Figure 4.19b**) indicating that the tourmalines are predominantly derived from metasedimentary rocks (metapelites, metapsammities; aluminous) with subordinate input from Li poor granitoids, pegmatites and aplites.

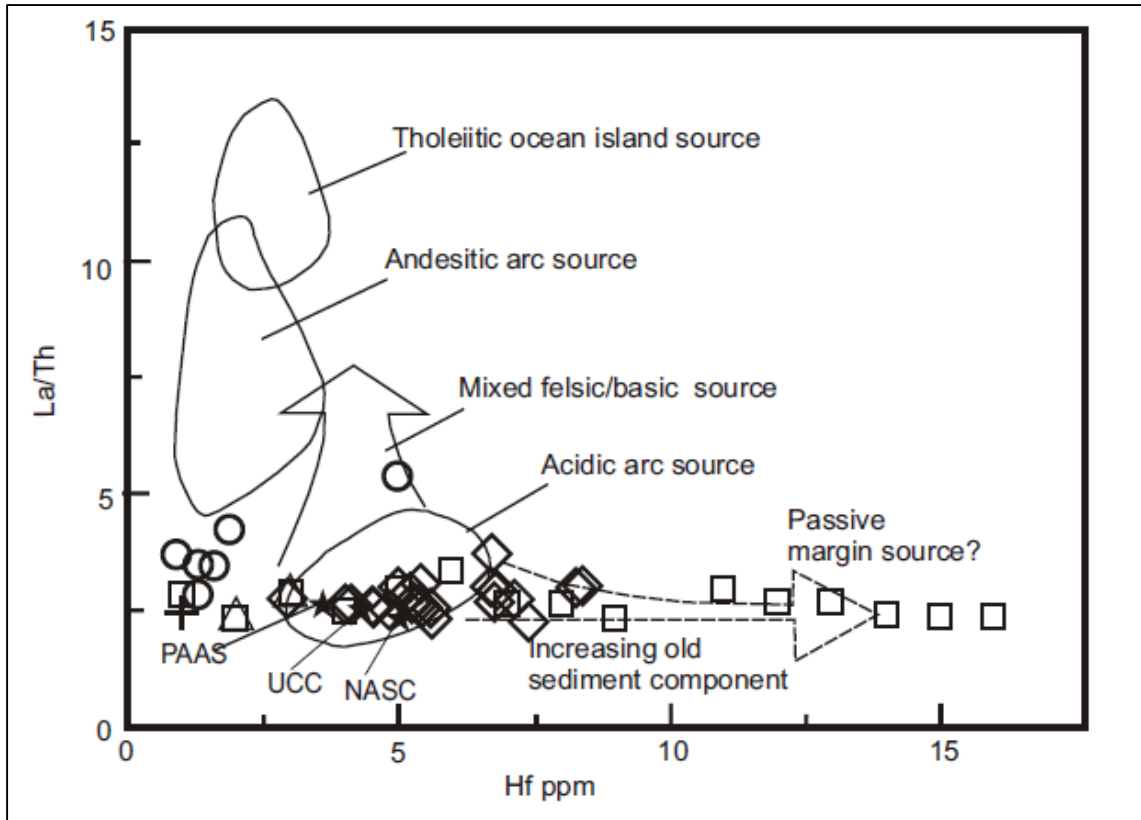


Figure 4.18 Hf Vs. La/Th bi-plot shows the provenance fields for the Tukai sediments (after Floyd and Leveridge, 1987).

The same results shown by Ca-Fe_{total}-Mg ternary diagram (Henry and Guidotti, 1985) where the Tukai samples plot in the fields 2 and 4 (**Figure 4.19a**). This result is also confirmed by Mg/(Mg+Fe_{total}) vs Al/(Al+Fe_{total}+Mg) plot by Henry and Guidotti (1985) where majority of the tourmalines fall in fields B and D indicating that these tourmalines are derived from aluminous metapelites and metapsammities with minor contribution from Li-poor granitoids, pegmatites and aplites (**Figure 4.20**). The same results were observed based on garnets. The garnet types were plotted on a ternary plot (plot not shown due to low number of samples) with known

provenance fields and inferred that the garnets mainly derived from granulite grade metasediments and acidic igneous rocks.

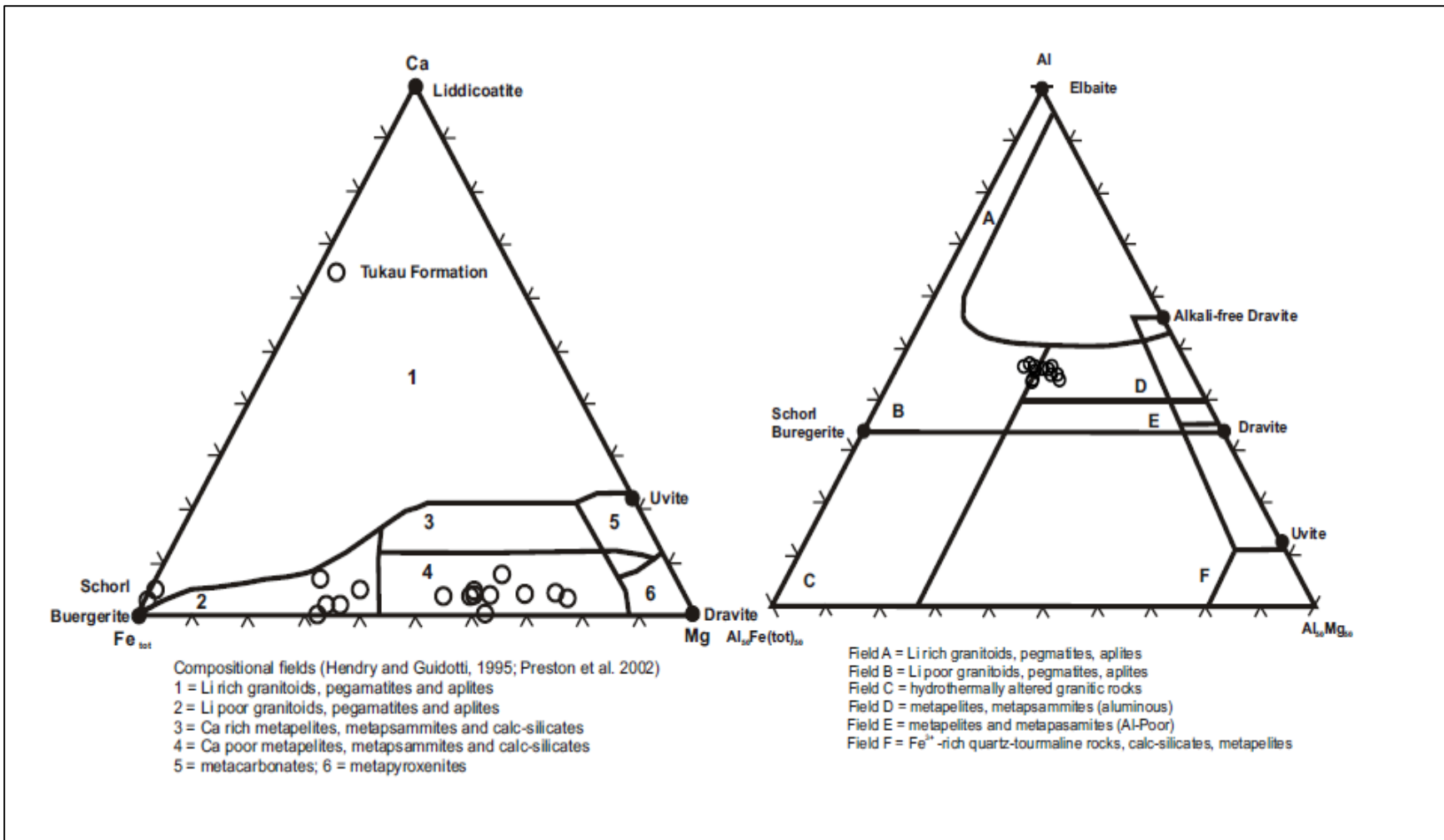


Figure 4.19a. Detrital Tourmalines, plotted on the provenance discriminant Ca-Fe_{total}-Mg ternary diagram of Hendry and Guidotti (1985) adopted from Mange et al. (2007); b. Detrital Tourmalines, plotted on the provenance discriminant Al-Fe_{total}-Mg ternary diagram of Hendry and Guidotti (1985)

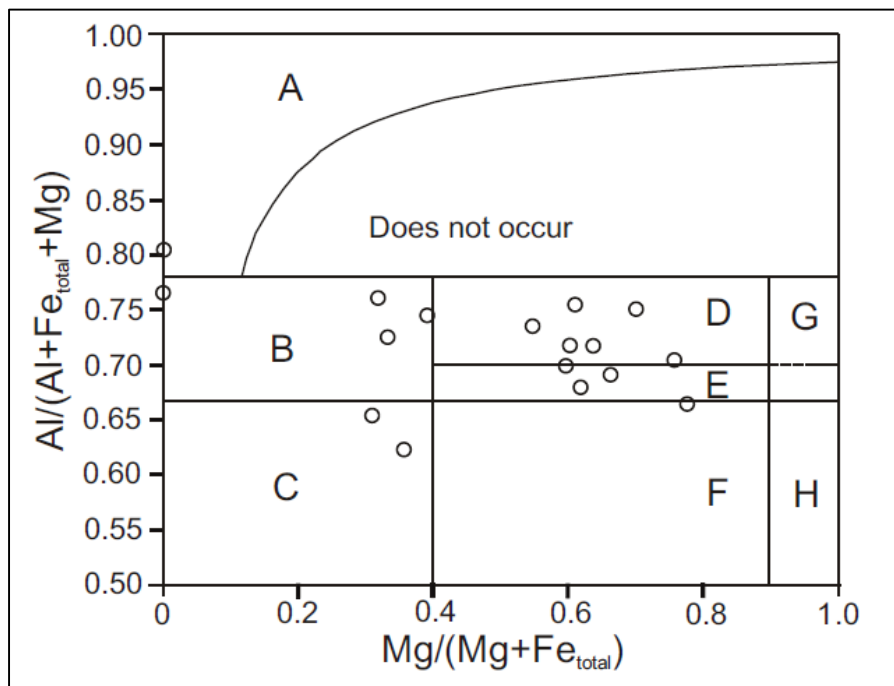


Figure 4.20. Al-Fe-Mg diagram (in molecular proportions) for detrital tourmaline from Tukai Formation. Zone A-Li-rich granitoids, pegmatites and aplites, zone B-Li-poor granitoids, pegmatites and aplites, Zone C-hydrothermally altered granitic rocks, Zone D-Aluminous metapelites and metapsammites, Zone E-Al-poor metapelites and metapsammites, Zone F-Fe³⁺-rich quartz-tourmaline rocks, calc-silicates and metapelites, Zone G-Low Ca ultramafics, Zone H-metacarbonates and metapyroxenites (after Hendry and Guidotti, 1985).

The detrital chromian spinels of the Tukai sediments are chromite and spinel types and are characterized by the Cr# and Mg# >0.5 and <0.5 and <0.5 and >0.5 respectively. The Cr# of the chromites corresponds to both Al rich chromite composition (< 0.6) and Cr-rich chromites composition (> 0.6) (Proenza, et al. 2008). According to Lee (1999) spinels with Cr# <5 are derived from lherzolitic bodies, such as abyssal peridotites of slow spreading ridges and also from back arc basins (Cookenboo et al. 1997). Al₂O₃ content was plotted against Cr₂O₃ and it was noted that many samples are plotted on podiform field (**Figure 4.21b**) and in the transition between stratiform and podiform fields. This suggests that these chromian spinels are mainly derived from Alpine type ophiolite and is well supported by the Cr³⁺, Al³⁺ and Fe³⁺ triangular plot (**Figure 4.21a**), where almost all the samples are plotted on Alpine type peridotite field. The studied chromites have primitive chromite compositions within the range of ophiolitic chromites. The chemical and mineralogical data revealed the Alpine type

peridotite source for the studied chromian spinels. The Alpine type peridotites are similar to podiform type and are rich in Al where Cr^{3+} increases with Fe^{3+} , however, Fe^{3+} remains quite low (Lee, 1999). Omang (1995) studied on chromites from Darvel Bay and the results showed that the X_{Mg} values range between 0.59 and 0.62 while X_{Cr} range between 0.38 and 0.39. This range is typically Alpine type chromites. Meanwhile, Omang (1995) deduced a mantle temperature (1030-1100° C) and Pressure of 11-16 kbar based on the chemistry of chromite phase, in which this P-T combination reflects exactly the Island-Arc geotherm which is comparable with the chromites of the present study and its tectonic environment. According to Hutchison (2005), chromite concentration in the peridotite and serpentinized peridotite in Northern Borneo is too small since the chromite layers are thin and podiform which is also comparable with the present study chromites. According to the Cr# vs Mg# plot, it suggests that the studied chromites are relatively derived from Lherzolites rather than Harzbergites and fall away from compared Greek ophiolites (**Figure. 4.21**). The serpentinized peridotites of Northern Borneo is comparable to Alpine type peridotites and this supports that the Alpine type serpentinized peridotites are the source rocks for the studied chromian spinels.

The sandstones are all quartz-dominated, with lithic fragments ranked second in abundance and a minor amount of feldspar and micas. In these samples, more than 80% of the compositions are monocrystalline quartz. According to Dabbagh and Rogers (1983), sandstones with higher proportions of monocrystalline quartz than polycrystalline quartz indicate the presence of higher energy during the time of deposition or it could be related to long distance transportation. The presence of both monocrystalline quartz and polycrystalline quartz also suggests a possibility of sources derived from igneous and metamorphic rocks (Tortosa et al., 1991). The undulose extinction found in quartz suggests sources from plutonic rocks (granitic), meanwhile, monocrystalline quartz is linked to the metamorphic sources (Basu et al., 1975). Generally, feldspar is the common grain that can be found in sandstones. However, their population is not that abundant across the samples. The minor amount of feldspar could be due to the dissolution of the grains as they are easily degraded when subjected to weathering processes (e.g. moderate weathering). In these samples, it was observed that alkali feldspar was more than plagioclase feldspar. This indicates that the source rocks came from granitic sources. Presence of sedimentary to metasedimentary lithic fragments in most of the samples could also suggest that older sedimentary rocks are the major source rocks for the Tukai Formation sedimentary rocks. Lower percentage of lithic fragments in some of the samples could result from transportation processes that weakened lithic grains, causing them

to break into smaller pieces. The processes' intensity is further aided by the humid tropical environment (Suttner et al., 1981; Johnsson et al., 1988; Smyth et al., 2008; van Hattum et al., 2013).

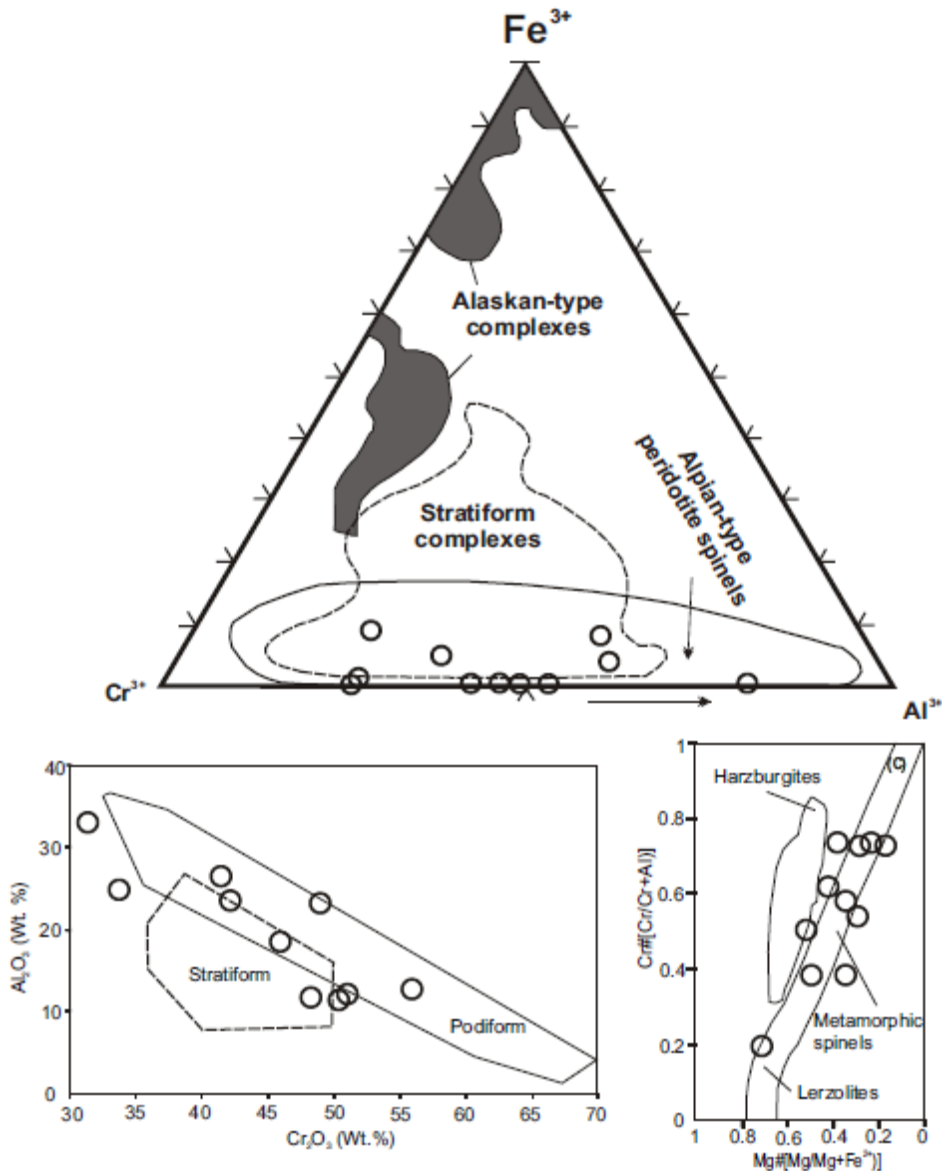


Figure 4.21. Chemical composition of chromites to discriminate their protoliths. a) Trivalent major cation plot ($Fe^{3+}-Al^{3+}-Cr^{3+}$), discriminating between different types of ultramafic complexes (after Cookenboo et al. 1997) b. Al_2O_3 versus Cr_2O_3 plot for the accessory fresh chrome spinels (after Bonavia et al., 1993). c. Variation of $Mg/(Mg+Fe^{2+})$ against $Cr/(Cr+Al)$ of detrital chrome spinels from the sediments of the Tukau Formation (Fields of spinels from harzburgites and lherzolites after Pober and Faupl, (1988) and field of Greek ophiolites after Gartzos et al. (1990)

4.5.4 The possible provenance area

Three zircon age clusters recorded in this study are comparable to age clusters reported by Van Hattum et al. (2013) where the Crocker and Rajang Group of sediments are considered to be the source area for the present study sediments. The two major zircon age clusters belongs to Cretaceous and Triassic. The Cretaceous age cluster can be related to the Schwaner pluton (e.g. Hanning et al., 2017; Breitfeld et al., 2017) whereas the Triassic age cluster can be related to the granitic plutons of Peninsular Malaysia. The older zircons might have been sourced from a more distal source (e.g., Indo-Australian plate) and possibly have undergone several recycling phases (van Hattum et al. 2006). The Schwaner plutons have been considered as a major source rock for the Borneo Orogenic Belt in the prior studies based on U-Pb geochronology of zircons. Ages of these plutons range from 130 ± 2.8 Ma to 77.4 ± 1.7 Ma (Williams et al., 1988; Van Hattum et al., 2006; Witts et al., 2012; Davies et al., 2014; Li et al., 2015). According to White et al. (2016), samples collected within Borneo yielded dominant age populations between 75 and 110 Ma. Similarly, Hanning et al. 2017 have reported zircon ages for the samples granitoids and diorites from NW Schwaner Montains as 100 and 81Ma (I-type granites) and 118Ma (S-type granitoids). Comparable ages suggested that the Schwaner Mountains were the principal source rocks for the Rajang Group of rocks and were subsequently recycled further north and northwest of Borneo during the Neogene.

In addition to the Schwaner Mountains, granitoids of the Peninsular Malaysia is another possible source area. The Bentong-Raub suture (consisting of serpentinites, deeps sea radiolarian cherts and Middle Devonian to Late Permian sedimentary rocks) divides granitoids of the Peninsular Malaysia into Main Range and Eastern provinces (Ng et al., 2015 and references provided there in). Eastern province granitoids have U-Pb zircon ages of 289-220 Ma with some younger ages (~80 Ma). The Main Range province magmatism was constrained between 219 and 198 Ma (Searle et al., 2012; Ng et al., 2015). According to the same authors, a progressive westward younging trend was apparent across the Eastern province and it was less obvious in the Main Range province. The Main Range granites of the Peninsular Malaysia consists of tin-bearing S-type granites of Triassic age (Bignell and Snelling, 1977; Liew and Page, 1985) and the Eastern provinces are dominated by I-type granite of Permian-Triassic age (Searle et al. 2012 and references provided there in). Similarly, the southwestern Thailand-Myanmar province granites are mixture of tin bearing S-type and I-type plutons of the Cretaceous age. Zircon age of the Tukai Formation is comparable to the Main Range granites rather than the southwestern Thailand-Myanmar province. In different studies, detrital

cassiterites (tin bearing mineral) were found in the Crocker range sediments (Van Hattum et al., 2013) as well as the Neogene sediments of northwestern Borneo (Nagarajan et al., 2015). It supports that the tin bearing granitoids were one of the major possible sources for the sediments of Crocker-Rajang accretionary complex. Identification of the Schwaner Mountains and peninsular Main Range as source rocks for the sedimentary rocks of central Borneo and their subsequent recycling for the Neogene deposits of northern Borneo is in agreement with the previous studies by Van Hattum et al. (2003, 2013) and White et al. (2016).

4.5.5. Tectonic setting

The tectonic settings of the Tukai Formation sediments were identified using Dickinson and Suczek (1979) trilinear plot (QFL). On the QFL triangular diagram (**Figure 4.22**), majority of the samples fall into recycled orogenic with some samples slightly shifting towards craton interior region. According to Dickinson and Suczek (1979), Dickinson et al. (1983) and Dickinson (1985, 1988), there are three main types of tectonic provenances which are continental blocks, magmatic arcs and recycled orogens. Sources from recycled orogens are associated to the folding and faulting events of sedimentary or metasedimentary terranes. The events caused the rocks detritus to be recycled into associated basins. The interpretations of the diagram are supported by the majority of sandstones belonging to medium to fine-grained sandstones with a few exceptions. It is further supported by the low feldspar contents. Thus, it also reflects a region of passive margin basins. Based on the composition of the samples observed, there is a high likelihood of them being collision orogens product. Intermediate quartz contents, lithics fragments consist of sedimentary-metasedimentary, while cherts are among the composition's characteristics of rocks from collision orogens (Dickinson and Suczek, 1979). This also could indicate of a moderate to minimal influence of climate and transportation during the deposition of sediments. Plus, the presents of quartz grains and chert fragments from the observation also revealed that continental sources are involved.

Generally, feldspar is the common grains that can be found in sandstones. However, its population is not that abundant across all samples. The minor amount of feldspar could be due to the dissolution of the grains as they are easily degraded when subjected to weathering processes (e.g. moderate to high intensity of weathering). In these samples, it was observed that alkali feldspar was more than plagioclase feldspar. This indicates that the source rocks come from granitic sources.

Presence of sedimentary to metasedimentary lithic fragments could also suggest older sedimentary rocks as one of the source rocks for the samples. Majority of the observed samples show the presence of sedimentary to meta-sedimentary rock fragments (meta-sandstone, meta-mudstone, chert) and schists. Lower percentage of lithic fragments in some samples could be resulted from transportation processes that weakens the lithic grains, causing them to break into smaller pieces. The processes is further intensified as it is aided by humid tropical environment (Suttner et al., 1981; Johnsson et al., 1988; Smyth et al., 2008; van Hattum et al., 2013).

Optimum discriminations of the tectonic settings of sedimentary basins can be achieved on the basis of major, trace and rare earth element geochemistry which have been proposed and used by many authors (Bhatia and Crook, 1986; Roser and Korsch, 1986; Girty et al., 1993; McLennan, et al. 1993; Verma and Armstrong-Altrin, 2013, 2016). NW Borneo basins are forland basins and show complex tectonic history. Different tectonic setting discrimination plots are used in order to reconstruct the possible tectonic setting for the Tukai Formation. The Tukai samples are mainly plotted (recalculated to 100% volatile free) in the passive margin field in the K_2O/Na_2O-SiO_2 discrimination diagram (after Roser and Korsch, 1986) which is consistent with the provenance characters where the Tukai sediments are mostly recycled from sedimentary to metasedimentary that dominated the source region (**Figure 4.23**). Similarly, in the discrimination diagram (after Verma and Armstrong-Altrin, 2013), the Tukai samples are clustered mostly in collisional field and some samples (wacke and litharenites) plot in rift field, (**Figure 4.24**) which is consistent with the regional tectonic setting of NW Borneo during the deposition of the Tukai sediments.

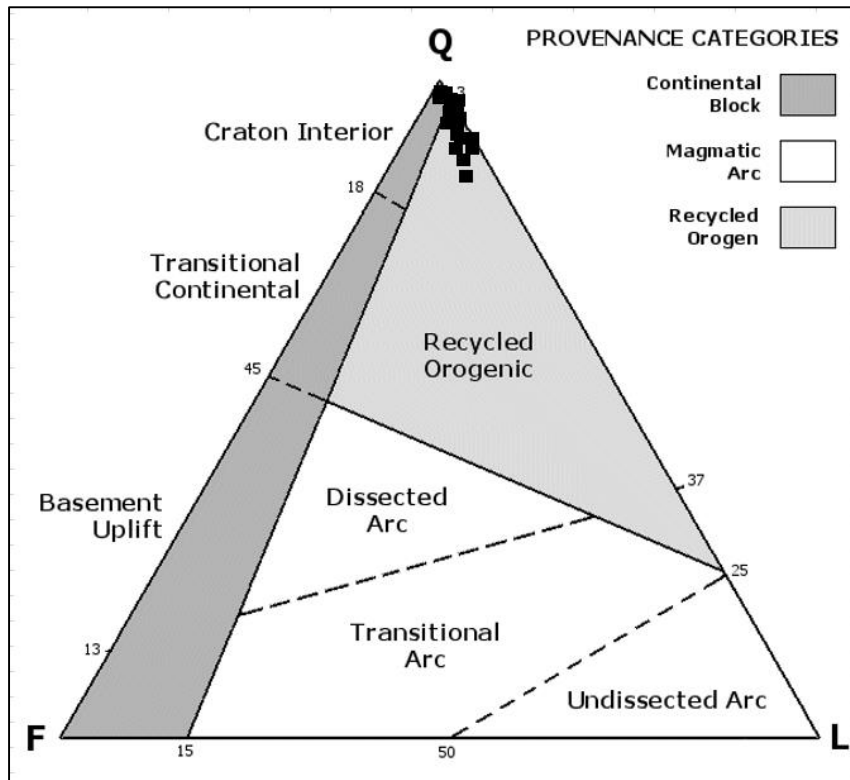


Figure 4.22 QFL Diagram after Dickinson (1970) for determination of tectonic settings. Majority sample fall into recycled orogenic. 8 samples fall into craton interior provenance type.

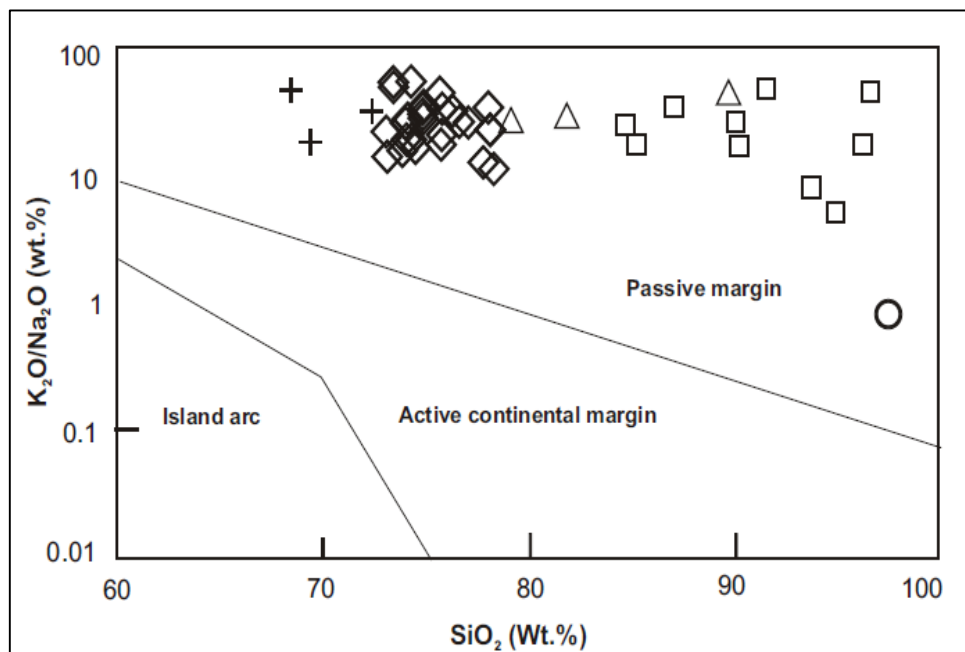


Figure 4.23. K_2O/Na_2O vs. SiO_2 tectonic discrimination diagram (Roser and Korsch 1986) for clastic sediments of the Tuaku Formation (some quartz arenites are not included due to absence of Na_2O content).

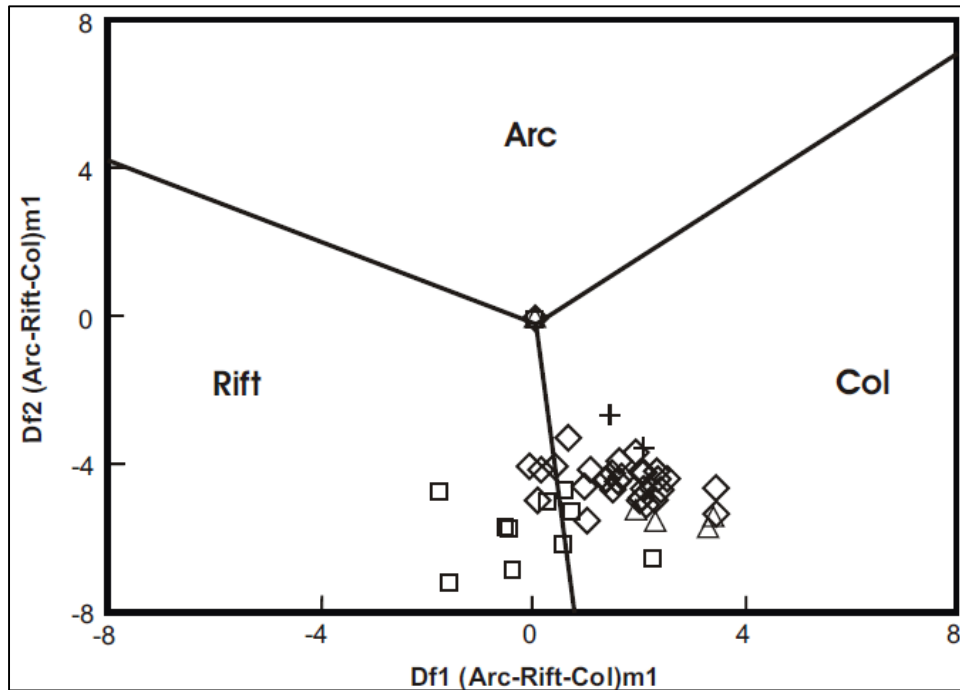


Figure 4.24 Discriminant-function multi-dimensional diagram (after Verma and Armstrong-Altrin, 2013) showing the tectonic setting for the high-silica clastic sediments from the Tukai Formations. The subscript m1 in DF1 and DF2 represents the high silica diagram based on loge-ratios of major elements. The discrimination function equation are $DF1(\text{Arc-Rift-Col})m1 = (-0.263 \times \ln(\text{TiO}_2/\text{SiO}_2)_{\text{adj}}) + (0.604 \times \ln(\text{Al}_2\text{O}_3/\text{SiO}_2)_{\text{adj}}) + (-1.725 \times \ln(\text{Fe}_2\text{O}_3/\text{SiO}_2)_{\text{adj}}) + (0.660 \times \ln(\text{MnO}/\text{SiO}_2)_{\text{adj}}) + (2.191 \times \ln(\text{MgO}/\text{SiO}_2)_{\text{adj}}) + (0.144 \times \ln(\text{CaO}/\text{SiO}_2)_{\text{adj}}) + (-1.304 \times \ln(\text{Na}_2\text{O}/\text{SiO}_2)_{\text{adj}}) + (0.054 \times \ln(\text{K}_2\text{O}/\text{SiO}_2)_{\text{adj}}) + (-0.330 \times \ln(\text{P}_2\text{O}_5/\text{SiO}_2)_{\text{adj}}) + 1.588$. $DF2(\text{Arc-Rift-Col})m1 = (-1.196 \times \ln(\text{TiO}_2/\text{SiO}_2)_{\text{adj}}) + (1.604 \times \ln(\text{Al}_2\text{O}_3/\text{SiO}_2)_{\text{adj}}) + (-0.303 \times \ln(\text{Fe}_2\text{O}_3/\text{SiO}_2)_{\text{adj}}) + (0.436 \times \ln(\text{MnO}/\text{SiO}_2)_{\text{adj}}) + (0.838 \times \ln(\text{MgO}/\text{SiO}_2)_{\text{adj}}) + (-0.407 \times \ln(\text{CaO}/\text{SiO}_2)_{\text{adj}}) + (1.021 \times \ln(\text{Na}_2\text{O}/\text{SiO}_2)_{\text{adj}}) + (-1.706 \times \ln(\text{K}_2\text{O}/\text{SiO}_2)_{\text{adj}}) + (-0.126 \times \ln(\text{P}_2\text{O}_5/\text{SiO}_2)_{\text{adj}}) - 1.068$.

In addition, the new discrimination diagrams proposed by Verma and Armstrong-Altrin (2016) are also used to discriminate the tectonic setting for the Neogene Tukai Formation from NW Borneo. It is consistent with the mineralogical, petrological and geochemical observation suggesting that these rocks were recycled from sedimentary to metasedimentary dominated source regions. All samples fall in the passive margin setting of the plot based on major oxides alone whilst in the major - trace element based discriminant plot, some of the samples are plotted on the transition field between passive and active tectonic setting boundary (**Figure 4.25**).

Sarawak Orogeny (Hutchison, 2007) had a big impact on change in sedimentation as a transition from flysch to molasses in the NW Borneo which took place during Late Eocene (Hutchison, 2007) where major Rajang Group Turbidite flysch was folded, thrust and uplifted. Later, the Early Miocene rifting took place in the South China Sea. During this period, rifting and subduction were slow down and resulted further in the uplift of the Borneo landmass. According to Kessler and Jong (2015), the transition from muddy Mid-Miocene shelf (Setap Shale and Sibuti Formation) to an unusual sandy formation can be attributed to the rise of the Borneo part of Sundaland in the Middle to Late Miocene due to tectonic compression. This regional tectonism in addition to climate enhanced the erosion of Rajang/Croker Formations and deposited sandy rich formations in the NW Borneo. The northern Borneo possibly had collisional tectonic setting and the passive rifts might have developed along faulted margins in the zones of continental collision (e.g. Ingersoll, 1988). Rifts are also common along the collisional boundaries due to irregularities of continental margins and by normal faulting due to nonperpendicular collision (e.g., Condie, 2011).

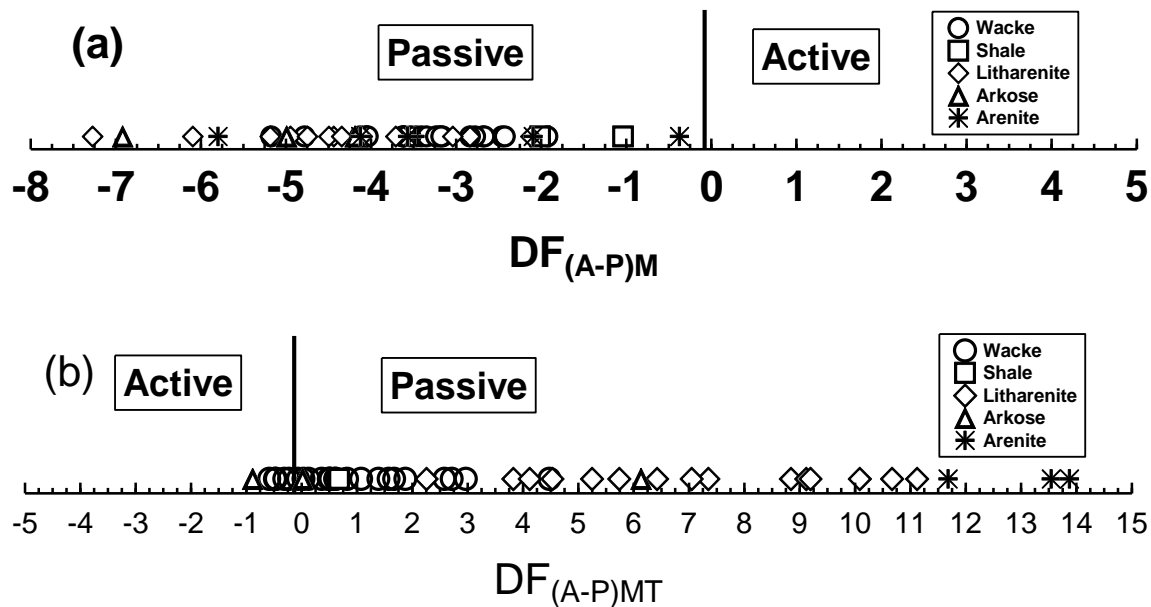


Figure 4.25 (a) Discrimination diagrams based on major element (oxides) and (b) based on major and trace elements (after Verma and Armstrong-Altrin (2016))

CHAPTER 5

CONCLUSIONS AND FUTURE RECOMMENDATIONS

5.1 Introduction

As introduced in the literature review, with the complex geological history of Borneo Island, the deposition of the Tukai Formation created question marks on its' past geological history that has yet to be fully studied. In this chapter, research questions are revisited and explained in accordance to the research objectives. This chapter also will discuss on the possible future works that can be expanded and conducted on the Tukai Formation.

5.2 Conclusions

For the first time, an integrated method has been applied in assessing the Tukai Formation to overcome the limitations encountered when relying on a single method. For example, petrography method is only suitable for medium to coarse grained rocks. However, several information that is useful for deciphering provenance can also be found in fine-grained rocks. Sediments from the Tukai Formation generally range from coarse-grained to fine-grained sizes. Therefore, by integrating geochemical and mineralogical method, all of the information from various grain sizes is now possible to be retrieved. In this research, by adopting both of these methods, a clear agreement can be established between the results obtained from both methods and narrowing down the scope in term of provenance and tectonic setting.

The first research objective is to study the mineralogical and petrographic characteristics of the sandstones. Based on the observation on petrography, the sandstones were classified into sublitharenites and quartz arenites using QFL diagram. This result matched the results gained from the geochemical analysis which identifies that the Tukai Formation mainly consists of sandstones and are classified geochemically as wacke, litharenites and quartz arenites and have a lesser extent compared to shale. The result also achieving the second research objective which is to study the chemical composition of sandstones and mudstones. The higher percentage of silica (SiO_2) in geochemical results are being reflected in the abundance amount of quartz grains observed under petrographic observation. Meanwhile, lower percentage of CaO and Na_2O could be explained by the lower number of feldspar grains found in the sample.

Integrating both results that are gathered through petrographic and geochemical analysis allows inferences to be made concerning the paleo-weathering, provenance and tectonic setting of clastic sediments of the Tukai Formation. Using the A-CN-K diagram, the chemical weathering of the Tukai Formation is identified as moderate to intensive weathering due to the effects of tropical climate during the period of deposition. The results are concordance with the previous research that Borneo experienced tropical climate that may contributed to a higher rate of erosion during Miocene.

Based on the results, provenance of these sedimentary rocks was felsic and recycled mainly from meta-sedimentary rocks (Rajang group of rocks as major source) and with minor input from granitoids and mafic-ultramafic rocks which are clearly confirmed by the bulk rock geochemistry, tourmaline and chrome-spinel chemistry. A similar observation has also been made from petrographic analysis with several samples containing sedimentary and metamorphic lithic fragments. Based on the U-Pb geochronology results, three random age clusters were identified from the detrital zircons extracted from the Tukai sandstones which are Precambrian, Cretaceous and Triassic ages. In which, the Cretaceous age cluster can be related to the Schwaner pluton (Southern Borneo) and the Triassic age cluster can be related to the granitic plutons of Peninsular Malaysia (outside Borneo). The older zircons might be derived from more distal source (e.g., Indo-Australian plate; outside Borneo) and possibly undergone several recycling phases. These interpretations are also consistent with the recent studies that used zircon geochronology from the various parts of the Borneo. Overall, the comparable ages suggested that the Schwaner Mountains were the principal source rocks for the Rajang Group of rocks and were subsequently recycled further north and northwest of Borneo during the Neogene. Also, the morphology of heavy minerals especially zircons are derived from various sources and many of them have been recycled more than a sedimentary cycle.

Tectonically, these sediments show mainly passive margin characters with some deviation towards active margin boundary. In addition to tectonic setting, climate has played a major role in the chemistry of these sediments. The findings are somehow similar with studies conducted by Galin et al. (2017) which showed that the tectonic setting was a non-active region.

5.3 Future Recommendations

Though the present study integrated many results to elucidate the provenance, weathering and tectonic settings, there are still plenty of research aspects that can be considered in near future

in order to unravel the formation's geological history which is located in a region with complex tectonic history.

Studies on detailed sedimentary facies analysis such as sedimentary structures, micro-facies analysis will indicate the variations in the paleo-depositional, paleoenvironmental condition and their tectonic settings.

As certain environment possesses different characteristics, trace fossils could be useful in identifying depth range (Tucker, 2001). Individuals and communities will be influenced by the changes in environment and thus, trace fossils are reliable tools for in situ records (Bromley, 1996). Hutchison (2005) stated that fossils are limited in the Tukai formation and only contains brackish-water fauna. However, with more lands being cleared with the construction of various infrastructures such as roads, we are expecting more exposed outcrops to be found where trace fossils studies can be intensified. Although it might not contribute that much in identifying the stratigraphical age as mentioned by Wilford (1961), the findings will help in narrowing down the depositional environment of the Tukai Formation.

Due to the Rajang Unconformity, the depositional environment of Sarawak region changes drastically in the Late Middle Miocene from deep marine to terrestrial sedimentation. The changes also caused the current coastal area to be built up in shallow marine shelf. Therefore, Galin et al. (2017) suggested further studies to be done to the Neogene rocks in terms of upliftment history. This is also an indication that the structural aspects of the Tukai Formation are not fully studied. Further field studies can be planned in near future, probably using seismic survey. Adding in seismic survey allows identification of buried rock boundaries thus enables in determining its' layers continuity or to confirm any existence of fault.

The study of paleomagnetism in Borneo Island remains controversial despite the availability of great number of result data, which are either gleaned from the island itself or from the surrounding regions. In fact, there have been various theories that are presented (ie: Lee and Lawver, 1993, 1995; Rangin et al., 1990; Haile et al., 1977; Hall, 1996; Hamilton, 1979; Schmidtke et al., 1990; Briaies et al., 1993).

Permeability, porosity, and evolution of the geometry of the pore are also one of the interesting study topics that can be conducted in this formation. It is not included in this research study as most of the rock samples are partly unconsolidated. The study itself can be expanded and contributed to a detailed geological and hydrological understanding of the

region. Okazaki et al. (2014) had conducted a similar study on the Neogene rocks in Northern Hokkaido, Japan by drilling 11 boreholes of 1km depth each. The results that they yielded from the compaction studies were extracted to understand the diagenesis, hydraulic properties and microstructures characteristics. This method is slightly different from current approach as most of the studies done related to the Tukai formation use surface samples.

Through all the suggested recommendations, it may help us to advance our understanding on the Tukai Formation. In the future, similar research (comprehensive studies) should be conducted for other rock formations in Sarawak to elucidate their source to sink relationships.

REFERENCES

- Abd. Rahman, A. H., Menier, D., & Mansor, M. Y. (2014).** Sequence stratigraphic modelling and reservoir architecture of the shallow marine successions of Baram field, West Baram Delta, offshore Sarawak, East Malaysia. *Marine and Petroleum Geology*, 58, Part B(0), 687-703. doi:http://dx.doi.org/10.1016/j.marpetgeo.2014.03 .010
- Abieda, H.S., Abd. Rahman, A. H., & Harith, Z.Z.T. (2005).** Facies, Depositional Framework and Sequence Stratigraphy of the Miri Formation (Middle Miocene), Miri, Sarawak. PGCE 2005. *Geological Society of Malaysia*
- Abieda H.S., Harith, Z.Z.T., & Abd. Rahman, A. H. (2005).** Depositional controls on petrophysical properties and reservoir characteristics of Middle Miocene Miri Formation sandstones, Sarawak. *Warta Geologi*, 31(3)
- Aitchison, J., & J. Egozcue, J. (2005).** Compositional Data Analysis: Where Are We and Where Should We Be Heading?. *Mathematical Geology*, 37(7),829-850. doi: 10. 1007 /s11004-005-7383 -7
- Al-Harbi, O. A., & Khan, M. M. (2008).** Provenance, diagenesis, tectonic setting and geochemistry of Tawil Sandstone (Lower Devonian) in Central Saudi Arabia. *Journal of Asian Earth Sciences*, 33(3-4), 278-287. doi:http://dx.doi.org/10.1016/j.jseaes.2008.01.004
- Alekseevskiy, N. I., Berkovich, K. M., & Chalov, R. S. (2008).** Erosion, sediment transportation and accumulation in rivers. *International Journal of Sediment Research*, 23(2), 93-105. doi: https://doi.org/10.1016/S1001-6279(08)60009-8
- Ali, A. M., & Padmanabhan, E. (2014).** Quartz surface morphology of Tertiary rocks from North East Sarawak, Malaysia: Implications for paleo-depositional environment and reservoir rock quality predictions. *Petroleum Exploration and Development*, 41(6), 761-770. doi:10.1016/S1876-3804(14)60090-2
- Andò, S., Garzanti, E., Padoan, M., & Limonta, M. (2012).** Corrosion of heavy minerals during weathering and diagenesis: A catalog for optical analysis. *Sedimentary Geology*, 280, 165-178. doi:http://dx.doi.org/10.1016/j.sedgeo.2012.03.023
- Arai, S. (1992).** Chemistry of chromian spinel in volcanic rocks as a potential guide to magma chemistry. *Minerogical Magazine*, 56, 173-184.

- Armstrong-Altrin, J.S., R.Nagarajan, V.Balaram, O.Natalhy-Pineda (2015).** Petrography and geochemistry of sands from the Chachalacas and Veracruz beach area, Western Gulf of Mexico, Mexico: Constraints on provenance and tectonic setting. *South American Journal of Earth Sciences*. 64 (1): 199-216. doi:10.1016/j.j.sames. 2015. 10. 012.
- Armstrong-Altrin J.S., Nagarajan R, Lee Yong Il, Kasper-Zubillaga Juan J., Córdoba-Saldaña Leslie P., (2014).** Geochemistry of sands along the San Nicolás and San Carlos beaches, Gulf of California, Mexico: implication for provenance. *Turkish Journal of Earth Sciences*. 23: 533-558. doi: 10.3906/yer-1309-21
- Armstrong-Altrin, J. S., Nagarajan, R., Madhavaraju, J., Rosalez-Hoz, L., Lee, Y. I., Balaram, V., Cruz-Martinez, A., Avila-Ramírez, G. (2013).** Geochemistry of the Jurassic and Upper Cretaceous shales from the Molango Region, Hidalgo, eastern Mexico: Implications for source-area weathering, provenance, and tectonic setting. *Comptes Rendus Geoscience*, 345(4), 185-202. doi:http://dx.doi.org/10.1016/j.crte.2013.03.004
- Armstrong-Altrin, J. S., & Verma, S. P. (2005).** Critical evaluation of six tectonic setting discrimination diagrams using geochemical data of Neogene sediments from known tectonic settings. *Sedimentary Geology*, 177(1–2), 115-129. doi: http://dx.doi.org/10.1016/j.sedgeo.2005.02.004
- Asiedu, D.K., Suzuki, S. and Shibata , T. (2000).** Provenance of sandstones from the Wakino Subgroup of the Lower Cretaceous Kanmon Group, northern Kyusyu Japan. *Island Arc*, 9, 128-144. doi: https://doi.org/10.1046/j.1440-1738.2000.00266.x
- Atkinson, C.D., Goesten,M.J.B.G., Speksnuder. A. & van der Vlugt, W. (1986).** Storm-Generated Sandstone in the Miocene Miri Formation, Seria Field, Brunei (N.W. Borneo). *American Association of Petroleum Geologists (AAPG)*, 11, 213-240
- Bailey, J.C.(1981).** Geochemical criteria for a refined tectonic discrimination of orogenic andesites. *Chemical Geology*,32(1),139-154. doi: https://doi.org/10.1016/0009-2541(81) 90135-2
- Bassis, A., Hinderer, M., & Meinhold, G. (2016).** Petrography and geochemistry of Palaeozoic quartz-rich sandstones from Saudi Arabia: implications for provenance and

chemostratigraphy. *Arabian Journal of Geosciences*, 9(5), 1-26. doi:10.1007/s12517-016-2412-z

Basu, A., Bickford, M.E., Deasy, R., (2016). Inferring tectonic provenance of siliciclastic rocks from their chemical compositions: A dissent. *Sedimentary Geology* 336, 26–35.

Basu, A. (2017). Chapter 2 - Evolution of Siliciclastic Provenance Inquiries: A Critical Appraisal. In Mazumder, R (Eds), *Sediment Provenance: Influences on Compositional Change from Source to Sink* (pp. 5-23). Elsevier. doi: <https://doi.org/10.1016/B978-0-12-803386-9.00002-2>

Bauluz, B., Mayayo, M. J., Fernandez-Nieto, C., & Gonzalez Lopez, J. M. (2000). Geochemistry of Precambrian and Paleozoic siliciclastic rocks from the Iberian Range (NE Spain): implications for source-area weathering, sorting, provenance, and tectonic setting. *Chemical Geology*, 168(1–2), 135-150. doi: [http://dx.doi.org/10.1016/S0009-2541\(00\)00192-3](http://dx.doi.org/10.1016/S0009-2541(00)00192-3)

Beddoes Jr, L. R. (1981). Hydrocarbon plays in Tertiary basins of Southeast Asia. *Energy*, 6(11), 1141-1163. doi: [http://dx.doi.org/10.1016/0360-5442\(81\)90030-X](http://dx.doi.org/10.1016/0360-5442(81)90030-X)

Belousova, E. A., Griffin, W. L., O'Reilly, S. Y., & Fisher, N. I. (2002). Apatite as an indicator mineral for mineral exploration: trace-element compositions and their relationship to host rock type. *Journal of Geochemical Exploration*, 76(1), 45-69. doi: [http://dx.doi.org/10.1016/S0375-6742\(02\)00204-2](http://dx.doi.org/10.1016/S0375-6742(02)00204-2)

Ben-Awuah, J., & Eswaran, P. (2015). Effect of bioturbation on reservoir rock quality of sandstones: A case from the Baram Delta, offshore Sarawak, Malaysia. *Petroleum Exploration and Development*, 42(2), 223-231. doi :[http://dx.doi.org/10.1016/S1876-3804\(15\)30009-4](http://dx.doi.org/10.1016/S1876-3804(15)30009-4)

Ben-Awuah, J., Padmanabhan, E., & Sokkalingam, R. (2017). Geochemistry of Miocene sedimentary rocks from offshore West Baram Delta, Sarawak Basin, Malaysia, South China Sea: implications for weathering, provenance, tectonic setting, paleoclimate and paleoenvironment of deposition. *Geosciences Journal*, 21(2), 167-185. doi: 10. 100 7 / s12303-016-0056-3

- Bergstroem, S. M., Huff, W. D., & Kolata, D. R. (1998).** The Lower Silurian Osmundsberg K-bentonite. Part I: stratigraphic position, distribution, and palaeogeographic significance. *Geological Magazine*, 135(01), 1-13
- Bhatia, M. R. (1983).** Plate Tectonics and Geochemical Composition of Sandstones. *The Journal of Geology*, 91(6), 611-627. doi:10.2307/30064711
- Bhatia, M. R., & Crook, K. A. W. (1986).** Trace element characteristics of graywackes and tectonic setting discrimination of sedimentary basins. *Contributions to Mineralogy and Petrology*, 92(2), 181-193. doi:10.1007/BF00375292
- Biscaye, P. E. (1965).** Mineralogy and sedimentation of recent deep-sea clays in the Atlantic Ocean and adjacent seas and oceans. *Bull. Geol. Soc*(76), 803.
- Bjørlykke, K. (1998).** Clay Mineral Diagenesis in Sedimentary Basins — A Key to the Prediction of Rock Properties. Examples from the North Sea Basin. *Clay Minerals*, 33(1), pp.15-34.
- Blatt, H., Middleton, G., & Murray, R. (1972).** *Origin of Sedimentary Rocks: Englewood Cliffs*. New Jersey, Prentice-Hall, 634 p.
- Blatt, H. (1967).** Provenance determinations and recycling of sediments. *Journal of Sedimentary Research*, 37(4), 1031-1044. doi:10.1306/74d71825-2b21-11d7- 86 48 00 0102c1865d
- Boggs, J. S., (2009).** *Petrology of Sedimentary Rocks*. Cambridge University Press.
- Boggs, S. (1968).** Experimental study of rock fragments. *Journal of Sedimentary Research*, 38(4), 1326-1339. doi:10.1306/74d71b72-2b21-11d7-8648000102c1865d
- Bojar, A.-V., Bojar, H.-P., Ottner, F., & Grigorescu, D. (2010).** Heavy mineral distributions of Maastrichtian deposits from the Hațeg basin, South Carpathians: Tectonic and palaeogeographic implications. *Palaeogeography, Palaeoclimatology, Palaeoecology*, 293(3), 319-328. doi:http://dx.doi.org/10.1016/j.palaeo.2009.10.002
- Borges, J. B., Huh, Y., Moon, S., & Noh, H. (2008).** Provenance and weathering control on river bed sediments of the eastern Tibetan Plateau and the Russian Far East. *Chemical Geology*, 254(1), 52-72. doi:https://doi.org/10.1016/j.chemgeo.2008.06.002

- Bortnikov, N. S., Gorelikova, N. V., Korostelev, P. G., & Gonevchuk, V. G. (2008).** Rare earth elements in tourmaline and chlorite from tin-bearing assemblages: Factors controlling fractionation of REE in hydrothermal systems. *Geology of Ore Deposits*, 50(6), 445-461. doi:10.1134/s1075701508060032
- Breitfeld, H., Hennig, J., BouDagher-Fadel, M., & Hall, R. (2017).** The Rajang Unconformity: Major provenance change between the Eocene and Miocene sequences in NW Borneo. *American Geophysical Union, Fall Meeting 2017*. Retrieved from <http://discovery.ucl.ac.uk/id/eprint/1568304>
- Bruguier, O., Lancelot, J. R., & Malavieille, J. (1997).** U–Pb dating on single detrital zircon grains from the Triassic Songpan–Ganze flysch (Central China): provenance and tectonic correlations. *Earth and Planetary Science Letters*, 152(1–4), 217-231. doi: [http://dx.doi.org/10.1016/S0012-821X\(97\)00138-6](http://dx.doi.org/10.1016/S0012-821X(97)00138-6)
- Butcher, A. R., & Botha, P. W. S. K. (2010).** Automated mineralogy derives key characteristics directly from reservoir rock. *The American Oil & Gas Reporter*, 4.
- Caja, M.A., Marfil, R., Lago, M., Salas, R., Ramseyer, K., 2007.** "Provenance discrimination of Lower Cretaceous synrift sandstones (Eastern Iberian Chain, Spain): Constraints from detrital modes, heavy minerals, and geochemistry", In: José Arribas, Mark J. Johnsson, Salvatore Critelli (Eds). *Sedimentary Provenance and Petrogenesis: Perspectives from Petrography and Geochemistry*. Geological Society of America, 420: doi: <https://doi.org/10.1130/SPE420>
- Camuti, K. S., & McGuire, P. T. (1999).** Preparation of polished thin sections from poorly consolidated regolith and sediment materials. *Sedimentary Geology*, 128(1–2), 171-178. doi:[http://dx.doi.org/10.1016/S0037-0738\(99\)00073-1](http://dx.doi.org/10.1016/S0037-0738(99)00073-1)
- Carter, A., & Bristow, C. S. (2003).** Linking hinterland evolution and continental basin sedimentation by using detrital zircon thermochronology: a study of the Khorat Plateau Basin, eastern Thailand. *Basin Research*, 15(2), 271-285. doi:10.1046/j.1365-2117.2003.00201.x
- Castillo, P., Lacassie, J. P., Augustsson, C., & Herve, F. (2015).** Petrography and geochemistry of the Carboniferous–Triassic Trinity Peninsula Group, West Antarctica: implications for provenance and tectonic setting. *Geological Magazine*, 152(4), 575-588. doi:10.1017/s0016756814000454

- Cawood, P. A. (1983).** Modal composition and detrital pyroxene geochemistry of lithic sandstones from the New England fold belt (east Australia), a Paleozoic forearc terrane: *Geol. Soc. America Bull.*, v. 94, p. 1199–1214.
- Chayes, F. (1949).** A simple point-counter for thin section analysis. *American Mineralogist*, 34, 1-11.
- Chayes, F. (1956).** *Petrographic modal analysis*. New York: Wiley and Sons.
- Condie, K. C. (1991).** Another look at rare earth elements in shales. *Geochimica et Cosmochimica Acta*, 55(9), 2527-2531. doi:[http://dx.doi.org/10.1016/0016-7037\(91\)90370-K](http://dx.doi.org/10.1016/0016-7037(91)90370-K)
- Condie, K. C. (1993).** Chemical composition and evolution of the upper continental crust: Contrasting results from surface samples and shales. *Chemical Geology*, 104(1), 1-37. doi:[https://doi.org/10.1016/0009-2541\(93\)90140-E](https://doi.org/10.1016/0009-2541(93)90140-E)
- Condie, K. C., & Wronkiewicz, D. J. (1990).** A new look at the Archean-Proterozoic boundary: Sediments and the tectonic setting constraint. In: S.M. Naqvi (Editor), *Precambrian Continental Crust and Its Economic Resources*. Elsevier, Amsterdam, 61-84.
- Cox, R., & Lowe, D. R. (1996).** Quantification of the effects of secondary matrix on the analysis of sandstone composition, and a petrographic-chemical technique for retrieving original framework grain modes of altered sandstones. *Journal Sediment Research*, 66(3), 548-558.
- Cox, R., Lowe, D. R., & Cullers, R. L. (1995).** The influence of sediment recycling and basement composition on evolution of mudrock chemistry in the southwestern United States. *Geochimica et Cosmochimica Acta*, 59(14), 2919-2940. doi:[https://doi.org/10.1016/0016-7037\(95\)00185-9](https://doi.org/10.1016/0016-7037(95)00185-9)
- Cozzens, A. B. (1931).** Rates of Wear of Common Minerals. *Washington University Studies, Science and Technology*, no. 5, 71-80.
- Crook, K. A. W. (1974).** Lithogenesis and geotectonics: the significance of compositional variation in flysch arenites (graywackes). In: Dott Jr., R.H., Shaver, R.H. (Eds.), *Modern and Ancient Geosynclinal Sedimentation*. *SEPM Special Publications*, 19, 304-310.

- Cullen, A. B. (2010).** Transverse segmentation of the Baram-Balabac Basin, NW Borneo: refining the model of Borneo's tectonic evolution. *Petroleum Geoscience*, 16(1), 3-29. doi:10.1144/1354-079309-828
- Cullers, R. L. (2000).** The geochemistry of shales, siltstones and sandstones of Pennsylvanian–Permian age, Colorado, USA: implications for provenance and metamorphic studies. *Lithos*, 51(3), 181-203. doi:http://dx.doi.org/10.1016/S0024-4937(99)00063-8
- Cullers, R. L., Basu, A., & Suttner, L. J. (1988).** Geochemical signature of provenance in sand-size material in soils and stream sediments near the Tobacco Root batholith, Montana, U.S.A. *Chemical Geology*, 70(4), 335-348. doi:https://doi.org/10.1016/0009-2541(88)90123-4
- Curiale, J., Lin, R., & Decker, J. (2005).** Isotopic and molecular characteristics of Miocene-reservoired oils of the Kutei Basin, Indonesia. *Organic Geochemistry*, 36(3), 405-424. doi:https://doi.org/10.1016/j.orggeochem.2004.09.007
- Dabbagh, M. E., & Rogers, J. J. W. (1983).** Depositional environments and tectonic significance of the Wajid Sandstone of southern Saudi Arabia. *Journal of African Earth Sciences (1983)*, 1(1), 47-57. doi:https://doi.org/10.1016/0899-5362(83)90031-3
- Dickinson, W. (1985).** Interpreting Provenance Relations from Detrital Modes of Sandstones. In G. G. Zuffa (Ed.), *Provenance of arenites*, 148, 333-361: Springer Netherlands. doi: 10.1007/978-94-017-2809-6_15
- Dickinson, W. R. (1970).** Interpreting detrital modes of graywacke and arkose. *Journal of Sedimentary Research*, 40(2).
- Dickinson, W. R., Beard, L. S., Brakenridge, G. R., Erjavec, J. L., Ferguson, R. C., Inman, Kerry, F., Knepp, R.A., Lindberg, F.A., Ryberg, P. T. (1983).** Provenance of North American Phanerozoic sandstones in relation to tectonic setting. *Geological Society of America Bulletin*, 94(2), p. 222-235. doi:10.1130/0016-7606(1983)94 <222:PONAPS> 2.0.CO;2
- Dickinson, W. R., D. W. Harbaugh, A. H. Saller, P. L. Heller, and W. S. Snyder (1983b).** Detrital modes of upper Paleozoic sandstones derived from Antler orogen in Nevada: implications for nature of Antler orogeny. *American Journal of Science*, 283 (6), 481–509. doi: 10.2475/ajs.283.6.481

- Dickinson, W. R., & Suczek, C. A. (1979).** Plate tectonics and sandstone compositions. *AAPG Bulletin*, 63(12), p. 2164-2182.
- Diester-Haass, L., Robert, C., Chamley, H. (1993).** Paleooceanographic and paleoclimatic evolution in the Weddell Sea (Antarctica) during the Middle Eocene–Late Oligocene, from a coarse sediment fraction and clay mineral data (ODP Site 689). *Marine Geology*, 114(3-4), 233-250. doi: [https://doi.org/10.1016/0025-3227\(93\)90030-Y](https://doi.org/10.1016/0025-3227(93)90030-Y)
- Diskin, S., Evans, J., Fowler, M. B., & Guion, P. D. (2011).** Recognising different sediment provenances within a passive margin setting: Towards characterising a sediment source to the west of the British late Carboniferous sedimentary basins. *Chemical Geology*, 283(3–4), 143-160. doi: <http://dx.doi.org/10.1016/j.chemgeo.2010.10.007>
- Dou, Y., Yang, S., Liu, Z., Clift, P. D., Shi, X., Yu, H., & Berne, S. (2010).** Provenance discrimination of siliciclastic sediments in the middle Okinawa Trough since 30ka: Constraints from rare earth element compositions. *Marine Geology*, 275(1), p.212-220. doi: <http://dx.doi.org/10.1016/j.margeo.2010.06.002>
- Dunkle, I., Frisch, W., Kuhlemann, J. & Brügel, A. (1998).** Pebble-population-dating: a new method for provenance analysis. *Terra Nostra*, 98, 45. Retrieved from <http://www.sediment.uni-goettingen.de/staff/dunkl/zips/Dunkl-et-al-2009.pdf>
- Egozcue, J. J., Pawlowsky-Glahn, V., Mateu-Figueras, G., & Barceló-Vidal, C. (2003).** Isometric Logratio Transformations for Compositional Data Analysis. *Mathematical Geology*, 35(3), 279-300. doi:10.1023/a:1023818214614
- Ehlmann, A.J. (1968).** Clay Mineralogy of Weathered Products and of River Sediments, Puerto Rico. *SEPM Journal of Sedimentary Research*, Vol. 38.
- Ehrmann, W. (1998).** Implications of late Eocene to early Miocene clay mineral assemblages in McMurdo Sound (Ross Sea, Antarctica) on paleoclimate and ice dynamics. *Palaeogeography, Palaeoclimatology, Palaeoecology*, 139(3-4), 213-231. doi: 10.1016/s0031-0182(97)00138-7
- Ehrmann, W., Setti, M., & Marinoni, L. (2005).** Clay minerals in Cenozoic sediments off Cape Roberts (McMurdo Sound, Antarctica) reveal paleoclimatic history. *Palaeogeography, Palaeoclimatology, Palaeoecology*, 229(3), 187-211. doi: <https://doi.org/10.1016/j.palaeo.2005.06.022>

- Ershova, V. B., Prokopiev, A. V., & Khudoley, A. K. (2015).** Integrated provenance analysis of Carboniferous deposits from Northeastern Siberia: Implication for the late Paleozoic history of the Arctic. *Journal of Asian Earth Sciences*, *109* (0), 38-49. doi:<http://dx.doi.org/10.1016/j.jseaes.2015.04.046>
- Federico, L., Capponi, G., Crispini, L., & Scambelluri, M. (2004).** Exhumation of alpine high-pressure rocks: insights from petrology of eclogite clasts in the Tertiary Piedmontese basin (Ligurian Alps, Italy). *Lithos*, *74*(1–2), 21-40. doi:<http://dx.doi.org/10.1016/j.lithos.2003.12.001>
- Floyd, P., & Leveridge, B. (1987).** Tectonic environment of the Devonian Gramscatho basin, south Cornwall: framework mode and geochemical evidence from turbiditic sandstones. *Journal of the Geological Society*, *144*(4), 531-542.
- Floyd, P. A., Leveridge, B. E., Franke, W., Shail, R., & Dörr, W. (1990).** Provenance and depositional environment of Rhenohercynian synorogenic greywackes from the Giessen Nappe, Germany. *Geologische Rundschau*, *79*(3), 611-626. doi:10.1007/BF01879205
- Folk, R. L. (1974).** *Petrology of Sedimentary Rocks*. Hemphills Publishing.
- Force, E. R. (1980).** The provenance of rutile. *Journal of Sedimentary Research*, *50*(2), 485-488. doi:10.1306/212f7a31-2b24-11d7-8648000102c1865d
- Friese, F. W. (1931).** Untersuchung von Mineralen auf abnutzbarkeit bei Verfrachtung in Wasser. *Zeitschrift für Kristallographie, Mineralogie und Petrographie*, *41*(1), 1-6.
- Fuller, M., Ali, J. R., Moss, S. J., Frost, G. M., Richter, B., & Mahfi, A. (1999).** Paleomagnetism of Borneo. *Journal of Asian Earth Sciences*, *17*(1), 3-24. doi:[https://doi.org/10.1016/S0743-9547\(98\)00057-9](https://doi.org/10.1016/S0743-9547(98)00057-9)
- Fyffe, L. R., & Pickerill, R. K. (1993).** Geochemistry of Upper Cambrian-Lower Ordovician black shale along a Northeastern Appalachian transect. *Geological Society of America Bulletin*, *105*(7), 897-910.
- Gaillardet, J., Dupré, B., & Allègre, C. J. (1999).** Geochemistry of large river suspended sediments: silicate weathering or recycling tracer?. *Geochimica et Cosmochimica Acta*, *63*(23), 4037-4051. doi:[https://doi.org/10.1016/S0016-7037\(99\)00307-5](https://doi.org/10.1016/S0016-7037(99)00307-5)

- Galehouse, J. S. (1971).** Sedimentation Analysis, in Carver, R.E.(ed.),*Procedures in Sedimentary Petrology*. John Wiley and Sons, New York, pp. 69-64.
- Galin, T., Breitfeld, H. T., Hall, R., & Sevastjanova, I. (2017).** Provenance of the Cretaceous–Eocene Rajang Group submarine fan, Sarawak, Malaysia from light and heavy mineral assemblages and U-Pb zircon geochronology. *Gondwana Research*, 51(Supplement C), 209-233. doi:<https://doi.org/10.1016/j.gr.2017.07.016>
- Gartzos, E., Migiros, G., & Parcharidis, I. (1990).** Chromites from ultramafic rocks of northern Evia (Greece) and their geotectonic significance. *Schweizerische Mineralogische und Petrographische Mitteilungen*, 70, 301-307.
- Garver, J.I., Royce, P.R., & A, S. T. (1996).** Chromium and Nickel in Shale of the Taconic Foreland: A Case Study for the Provenance of Fine-Grained Sediments with an Ultramafic Source. *Journal of Sedimentary Research, Section A: Sedimentary Petrology and Processes*, 66(1), 100-106.
- Garzanti, E., Andò, S., & Vezzoli, G. (2009).** Grain-size dependence of sediment composition and environmental bias in provenance studies. *Earth and Planetary Science Letters*, 277(3), 422-432.
- Garzanti, E., Limonta, M., Resentini, A., Bandopadhyay, P. C., Najman, Y., Andò, S., & Vezzoli, G. (2013).** Sediment recycling at convergent plate margins (Indo-Burman Ranges and Andaman–Nicobar Ridge). *Earth-Science Reviews*, 123, 113-132. doi:<http://dx.doi.org/10.1016/j.earscirev.2013.04.008>
- Garzanti E, Padoan M, Andò S, Resentini A, Vezzoli G, Lustrino M .(2013).** Weathering at the equator: petrology and geochemistry of East African Rift sands. *The Journal of Geology*, 121(6):547–580. doi: <https://doi.org/10.1086/673259>
- Garzanti, E. (2016).** From static to dynamic provenance analysis Sedimentary petrology upgraded. *Sedimentary Geology*, 336, 3-13.
- Garzanti, E., & Resentini, A. (2016).** Provenance control on chemical indices of weathering (Taiwan river sands). *Sedimentary Geology*, 336(Supplement C), 81-95. doi:<https://doi.org/10.1016/j.sedgeo.2015.06.013>

- Garzanti, E., Wang, J.G, Vezzolia, G., Limonta, M. (2016).** Tracing provenance and sediment fluxes in the Irrawaddy River basin (Myanmar). *Chemical Geology*, 440, 73-90. doi: <https://doi.org/10.1016/j.chemgeo.2016.06.010>
- Getaneh, W. (2002).** Geochemistry provenance and depositional tectonic setting of the Adigrat Sandstone northern Ethiopia. *Journal of African Earth Sciences*, 35(2), 185-198. doi:[https://doi.org/10.1016/S0899-5362\(02\)00126-4](https://doi.org/10.1016/S0899-5362(02)00126-4)
- Gingele, F., Müller, P., & Schneider, R. (1998).** Orbital forcing of freshwater input in the Zaire Fan area—clay mineral evidence from the last 200 kyr. *Palaeogeography, Palaeoclimatology, Palaeoecology*, 138(1-4), 17-26. doi: 10.1016/s0031-0182(97)00121-1
- Gottlieb, P., Wilkie, G., Sutherland, D., Ho-Tun, E., Suthers, S., Perera, K., Jenkins, B., Spencer, S., Butcher, A., & Rayner, J. (2000).** Using quantitative electron microscopy for process mineralogy applications. *Journals of The Minerals, Metals & Materials Society (JOM)*, 52(4), 24-25. doi:10.1007/s11837-000-0126-9
- Götze, J. (1998).** Geochemistry and provenance of the Altendorf feldspathic sandstone in the Middle Bunter of the Thuringian basin (Germany). *Chemical Geology*, 150(1), 43-61. doi:[https://doi.org/10.1016/S0009-2541\(98\)00052-7](https://doi.org/10.1016/S0009-2541(98)00052-7)
- Gower, R. J. W. (1990).** Early Tertiary plate reconstructions for the South China Sea region: constraints from northwest Borneo. *Journal of Southeast Asian Earth Sciences*, 4(1), 29-35. doi:[http://dx.doi.org/10.1016/0743-9547\(90\)90022-6](http://dx.doi.org/10.1016/0743-9547(90)90022-6)
- Hall, R. (1996).** Reconstructing Cenozoic SE Asia. *Geological Society, London, Special Publications*, 106(1), 153-184. doi:10.1144/gsl.sp.1996.106.01.11
- Hall, R. (2013).** Contraction and extension in northern Borneo driven by subduction rollback. *Journal of Asian Earth Sciences*, 76 (Supplement C), 399-411. doi:<https://doi.org/10.1016/j.jseaes.2013.04.010>
- Hall, R., & Nichols, G. (2002).** Cenozoic sedimentation and tectonics in Borneo: Climatic influences on orogenesis. In Jones and Frostick (Eds.), *Sediment Flux to Basins: Causes, Controls and Consequences Vol. 5, Issue 191* (pp. 5-22). London, England: Geological Society of London.

- Handler, R., Dallmeyer, R.D. & Neubauer, F. (1997).** $^{40}\text{Ar}/^{39}\text{Ar}$ ages of detrital white mica from Upper Austroalpine units in the Eastern Alps, Austria: Evidence for Cadomian and contrasting Variscan sources. *Geologische Rundschau*, 86(1), 69-80. doi: <https://doi.org/10.1007/s005310050122>
- Harnois, L. (1988).** The CIW index: A new chemical index of weathering. *Sedimentary Geology*, 55(3-4), 319-322. doi:[http://dx.doi.org/10.1016/0037-0738\(88\)90137-6](http://dx.doi.org/10.1016/0037-0738(88)90137-6)
- Hassan, S., Ishiga, H., Roser, B. P., Dozen, K., & Naka, T. (1999).** Geochemistry of Permian–Triassic shales in the Salt Range, Pakistan: implications for provenance and tectonism at the Gondwana margin. *Chemical Geology*, 158(3-4), 293-314. doi:[http://dx.doi.org/10.1016/S0009-2541\(99\)00057-1](http://dx.doi.org/10.1016/S0009-2541(99)00057-1)
- Haughton, P. D. W., Todd, S. P., & Morton, A. C. (1991).** Sedimentary provenance studies. *Geological Society, London, Special Publications*, 57(1), 1-11. Retrieved from <http://sp.lyellcollection.org/content/57/1/1.short>
- Hawkesworth, C., Cawood, P., Kemp, T., Storey, C., & Dhuime, B. (2009).** A Matter of Preservation. *Science*, 323(5910), 49-50. doi:10.1126/science.1168549
- Heine, K., & Volkel, J. (2010).** Soil Clay Minerals in Namibia and their Significance for the Terrestrial and Marine Past Global Change Research. *African study monographs. Supplementary issue*, 40, 31-50. Retrieved from <http://dx.doi.org/10.14989/96299>
- Heller, P. L. & Frost, C.D. (1988).** Isotopic provenance of clastic deposits—application of geochemistry to sedimentary provenance studies. In: *New Perspectives in Basin Analysis* (Ed. by K. Kleinspehn & C. Paola), *Springer-Verlag, New York*, 27-42.
- Henry, D. J. & Guidotti, C. V. (1985).** Tourmaline as a petrogenetic indicator mineral: an example from the staurolite-grade metapelites of NW Maine. *American Mineralogist*, 70, 1-15.
- Henry, D. J. & Dutrow, B.L. (1992).** Tourmaline in a low grade clastic metasedimentary rock; an example of the petrogenetic potential of tourmaline. *Contributions to Mineralogy and Petrology*, 112(2-3), 203-218.
- Hernández-Hinojosa, V., Montiel-García, P.C., Armstrong-Altrin, J.S., Nagarajan, R., Kasper-Zubillaga J.J., (2018)** Textural and geochemical characteristics of beach

sands along the western Gulf of Mexico, Mexico. *Carpathian Journal of Earth and Environmental Sciences*, 13(1): 161-174.

Herron, M. M. (1988). Geochemical classification of terrigenous sands and shales from core or log data. *Journal of Sedimentary Research*, 58(5), 820-829. doi:10.1306/212f8e77-2b24-11d7-8648000102c1865d

Hinz, K., Fritsch, J., Kempter, E. H. K., Mohammad, A. M., Meyer, J., Mohamed, D., Vosberg, H., Weber, J., & Benavidez, J. (1989). Thrust tectonics along the north-western continental margin of Sabah/Borneo. *Geologische Rundschau*, 78(3), 705-730. doi:10.1007/BF01829317

Hirsch, D. M. (2012). How to make a thin section. Retrieved from <https://davehirsch.com/other/thinsections/>

Hiscott, R. N. (1984). Ophiolitic source rocks for Taconic-age flysch: trace element evidence. *Bulletin of the Geological Society of America*, 95, 1251-1267.

Hiscott, R. N. (2001). Depositional sequences controlled by high rates of sediment supply, sea-level variations, and growth faulting: the Quaternary Baram Delta of northwestern Borneo. *Marine Geology*, 175(1-4), 67-102. doi:http://dx.doi.org/10.1016/S0025-3227(01)00118-9

Hossain, H. M. Z., Kawahata, H., Roser, B. P., Sampei, Y., Manaka, T., & Otani, S. (2017). Geochemical characteristics of modern river sediments in Myanmar and Thailand: Implications for provenance and weathering. *Chemie der Erde - Geochemistry*, 77(3), 443-458. doi:https://doi.org/10.1016/j.chemer.2017.07.005

Hossain, H. M. Z., Roser, B. P., & Kimura, J. I. (2010). Petrography and whole-rock geochemistry of the Tertiary Sylhet succession, Northeastern Bengal Basin, Bangladesh: Provenance and source area weathering. *Sedimentary Geology*, 228(3-4), 171-183. doi:http://dx.doi.org/10.1016/j.sedgeo.2010.04.009

Hubert, J. F. (1962). A zircon-tourmaline-rutile maturity index and independence of composition of heavy mineral assemblages with gross composition and texture of sandstone. *Journal of Sedimentary Petrology*, 32, 440-450.

Huntsman-Mapila, P., Kampunzu, A. B., Vink, B., & Ringrose, S. (2005). Cryptic indicators of provenance from the geochemistry of the Okavango Delta sediments,

- Botswana. *Sedimentary Geology*, 174(1),123-148. doi:<https://doi.org/10.1016/j.sedgeo.2004.11.001>
- Hutchison, C. S. (1989).** *Geological evolution of South-east Asia* (Vol. 13): Oxford University Press, USA.
- Hutchison, C. S. (1996).** The 'Rajang accretionary prism' and 'Lupar Line' problem of Borneo. *Geological Society, London, Special Publications*, 106(1), 247-261. doi:10.1144/gsl.sp.1996.106.01.16
- Hutchison, C. S. (2004).** Marginal basin evolution: the southern South China Sea. *Marine and Petroleum Geology*, 21(9), 1129-1148. doi:<http://dx.doi.org/10.1016/j.marpetgeo.2004.07.002>
- Hutchison, C. S. (2005).** *Chapter VI - Miri Zone Geology of North-West Borneo* (pp. 77-134). Amsterdam: Elsevier.
- Ibbeken, H., & Schleyer, R. (1991).** *Source and sediment. A case Study of Provenance and Mass Balance at an Active Plate Margin (Calabria, Southern Italy)*. Berlin, Germany :Springer-Verlag. doi: 10.1007/978-3-642-76165-2
- Ingersoll, R. V., Fullard, T. F., Ford, R. L., Grimm, J. P., Pickle, J. D., & Sares, S. W. (1984).** The effect of grain size on detrital modes; a test of the Gazzi-Dickinson point-counting method. *Journal of Sedimentary Research*, 54(1), 103-116.
- Ingram, G. M., Chisholm, T. J., Grant, C. J., Hedlund, C. A., Stuart-Smith, P., & Teasdale, J. (2004).** Deepwater North West Borneo: hydrocarbon accumulation in an active fold and thrust belt. *Marine and Petroleum Geology*, 21(7), 879-887. doi:<http://dx.doi.org/10.1016/j.marpetgeo.2003.12.007>
- Ingram, R. L. (1971).** Sieve Analysis. In: Carver, R.E., Ed., *Procedures in Sedimentary Petrology*. Wiley Interscience, New York, 46-49.
- Islam, M., Stuart, R., Risto, A. and Vesa, P. (2002).** Mineralogical changes during intense chemical weathering of sedimentary rocks in Bangladesh. *Journal of Asian Earth Sciences*, 20(8), pp.889-901.

- Isphording, W. C. (2007).** Chapter 38 Forensic Use of Heavy Minerals in Civil and Criminal Investigations. In A. M. Maria & T. W. David (Eds.), *Developments in Sedimentology* (58, pp. 963-982): Elsevier.
- Jacobsen, Y., Münker, C., & Mezger, K. (2003).** Hf isotope compositions in detrital zircons as a new tool for provenance studies, presented at the EGS-AGU-EUG Joint Assembly, Nice, 2003.
- Jalal P., and Ghosh S.K (2012).** Provenance of the Late Neogene Siwalik sandstone, Kumaun Himalayan Foreland Basin: Constraints from the metamorphic rank and index of detrital rock fragments. *Journal of Earth Science*. 121 (3), 781–792
- Jia, T. Y., & Rahman, A. H. A. (2009).** Comparative analysis of faciès and reservoir characteristics of Miri Formation (Miri) and Nyalau Formation (Bintulu), Sarawak. *Bulletin of the Geological Society of Malaysia* (55), 39-45. Retrieved from <http://www.gsm.org.my/products/702001-100463-PDF.pdf>
- Johnsson, M. J., Stallard, R. F., & Meade, R. H. (1988).** First-Cycle Quartz Arenites in the Orinoco River Basin, Venezuela and Colombia. *The Journal of Geology*, 96(3), 263-277.
- Kamenetsky, V. S., Crawford, A. J., & Meffre, S. (2001).** Factors controlling chemistry of magmatic spinel: An empirical study of associated olivine, Cr-spinel and melt inclusions from primitive rocks. *Journal of Petrology*, 42(4), 655-671.
- Kemp, A. I. S., Hawkesworth, C. J., Paterson, B. A., & Kinny, P. D. (2006).** Episodic growth of the Gondwana supercontinent from hafnium and oxygen isotopes in zircon. *Nature*, 439(7076), 580-583. doi: 10.1038/nature04505
- Kessler, F. L. (2010).** Observations on sediments and deformation characteristics of the Sarawak Foreland, Borneo Island. *Warta.Geologi*, 35, 1-10.
- Kettanah, Y. A., & Ismail, S. A. (2016).** Heavy mineral concentrations in the sandstones of Amij Formation with particular emphasis on the mineral chemistry and petrographic characteristics of monazite, western desert of Iraq. *Journal of African Earth Sciences*, 123, 350-369. doi:<http://dx.doi.org/10.1016/j.jafrearsci.2016.06.017>

- Kimberley, M. M., & Grandstaff, D. E. (1986).** Profiles of elemental concentrations in Precambrian paleosols on basaltic and granitic parent materials. *Precambrian Research*, 32(2–3), 133-154. doi:[http://dx.doi.org/10.1016/0301-9268\(86\)90004-5](http://dx.doi.org/10.1016/0301-9268(86)90004-5)
- Kosler, J., & Sylvester, P. J. (2003).** Present Trends and the Future of Zircon in Geochronology: Laser Ablation ICPMS. *Reviews in Mineralogy and Geochemistry*, 53(1), 243-275. doi: <https://doi.org/10.2113/0530243>
- Krippner, A., Meinhold, G., Morton, A. C., Russell, E., & von Eynatten, H. (2015).** Grain-size dependence of garnet composition revealed by provenance signatures of modern stream sediments from the western Hohe Tauern (Austria). *Sedimentary Geology*, 321, 25-38. doi: <https://doi.org/10.1016/j.sedgeo.2015.03.002>
- Krippner, A., Meinhold, G., Morton, A. C., Schönig, J., & von Eynatten, H. (2016).** Heavy minerals and garnet geochemistry of stream sediments and bedrocks from the Almklovdalen area, Western Gneiss Region, SW Norway: Implications for provenance analysis. *Sedimentary Geology*, 336, 96-105. doi:<http://dx.doi.org/10.1016/j.sedgeo.2015.09.009>
- Kroonenberg, S. B. (1994).** Effects of provenance, sorting and weathering on the geochemistry of fluvial sands from different tectonic and climatic environments. *Proceedings of the 29th International Geological Congress, Part A*, 69-81.
- Krumm, S., & Buggisch, W. (1991).** Sample preparation effects on illite crystallinity measurement: grain-size gradation and particle orientation. *Journal of Metamorphic Geology*, 9(6), 671-677. doi: 10.1111/j.1525-1314.1991.tb00557.x
- Krynine, P. D. (1940).** Petrology and Genesis of the Third Bradford Sand. *Pennsylvania State College Mineral Industries Experimental Station, Bulletin 27*.
- Krynine, P. D. (1946).** The tourmaline group in sediments. *The Journal of Geology* (54), 65-87. URL: <http://www.jstor.org/stable/30060476>
- Kurniawan, A., Wan Ismail, W.Y., Almanna, L.L., Nurhajeerah, M.H. (2017).** Characteristics of Pore Pressure and Effective Stress Changes in Sandstone Reservoir Through Velocity Analysis Approach Due to Hydrocarbon Production. *Proceedings of the International Conference on Integrated Petroleum Engineering and Geosciences (ICIPEG2016)*, 385-402. Springer.

- Kutterolf, S., Diener, R., Schacht, U., & Krawinkel, H. (2008).** Provenance of the Carboniferous Hochwipfel Formation (Karawanken Mountains, Austria/Slovenia) — Geochemistry versus petrography. *Sedimentary Geology*, 203(3–4), 246-266. doi:http://dx.doi.org/10.1016/j.sedgeo.2007.12.004
- Kyaw Linn, O., Khin, Z., Meffre, S., Myitta, Day Wa, A., & Lai, C. K. (2015).** Provenance of the Eocene sandstones in the southern Chindwin Basin, Myanmar: Implications for the unroofing history of the Cretaceous–Eocene magmatic arc. *Journal of Asian Earth Sciences*, 107(0), 172-194. doi:http://dx.doi.org/10.1016/j.jseaes.2015.04.029
- Lambiase, J. J., Abdul Rahim, A. A., & Peng, C. Y. (2002).** Facies distribution and sedimentary processes on the modern Baram Delta: implications for the reservoir sandstones of NW Borneo. *Marine and Petroleum Geology*, 19(1), 69-78. doi:http://dx.doi.org/10.1016/S0264-8172(01)00048-4
- Lambiase, J. J., & Cullen, A. B. (2013).** Sediment supply systems of the Champion “Delta” of NW Borneo: Implications for deepwater reservoir sandstones. *Journal of Asian Earth Sciences*, 76(0), 356-371. doi:http://dx.doi.org/10.1016/j.jseaes.2012.12.004
- Lee, Y. I., & Sheen, D. H. (1998).** Detrital modes of the Pyeongan Supergroup (Late Carboniferous–Early Triassic) sandstones in the Samcheog coalfield, Korea: implications for provenance and tectonic setting. *Sedimentary Geology*, 119(3–4), 219-238. doi:http://dx.doi.org/10.1016/S0037-0738(98)00053-0
- Lelong, F., Tardy, Y., Grandin, G., Trescases, J., & Boulange, B. (1976).** Pedogenesis, Chemical Weathering and Processes of Formation of Some Supergene Ore Deposits. *Supergene and Surficial Ore Deposits*, 93-173. doi:10.1016/b978-0-444-41403-8.50007-8
- Lev, S. M., McLennan, S. M., Meyers, W. J., & Hanson, G. N. (1998).** A petrographic approach for evaluating trace-element mobility in a black shale. *Journal of Sedimentary Research*, 68(5), 970-980. Retrieved from <GotoISI>://WOS:00007623 3600025
- Li, B., Zhuang X., Liu X., Wu, C., Zhou J., Ma, X. (2016)** .Mineralogical and geochemical composition of Middle Permian Lucaogou Formation in the southern Junggar Basin, China: implications for paleoenvironment, provenance, and tectonic setting. *Arabian Journal of Geosciences* 9:3.

- Liu, Z., Colin, C., Huang, W., Chen, Z., Trentesaux, A., & Chen, J. (2007).** Clay minerals in surface sediments of the Pearl River drainage basin and their contribution to the South China Sea. *Chinese Science Bulletin*, 52(8), 1101-1111. doi:10.1007/s11434-007-0161-9
- Liu, Z., Tuo, S., Colin, C., Liu, J., Huang, C., & Selvaraj, K., Chen, C.A., Zhao, Y., Siringan, F.P., Boulay, S. & Chen, Z. (2008a).** Detrital fine-grained sediment contribution from Taiwan to the northern South China Sea and its relation to regional ocean circulation. *Marine Geology*, 255(3-4), 149-155. doi: 10.1016/j.margeo.2008.08.003
- Liu, Z., Tuo, S., Colin, C., Liu, J., Huang, C., & Selvaraj, K., Chen, C.A., Zhao, Y., Siringan, F.P., Boulay, S. & Chen, Z. (2008b).** Detrital fine-grained sediment contribution from Taiwan to the northern South China Sea and its relation to regional ocean circulation. *Marine Geology*, 255(3-4), 149-155. doi: 10.1016/j.margeo.2008.08.003
- Lotter, N. O., Kormos, L. J., Oliveira, J., Fragomeni, D., & Whiteman, E. (2011).** Modern Process Mineralogy: Two case studies. *Minerals Engineering*, 24(7), 638-650. doi:http://dx.doi.org/10.1016/j.mineng.2011.02.017
- Lozano, R., & J.P.Bernal. (2005).** Characterization of a new set of eight geochemical reference materials for XRF major and trace elements analysis. *Revista Mexicana de Ciencias Geológicas*, 22(3), 329-344.
- Lupker, M., France-Lanord, C., Galy, V., Lavé, J., Gaillardet, J., Gajurel, A. P., Guilmette, C., Rahman, M., Singh, S.K., & Sinha, R. (2012).** Predominant floodplain over mountain weathering of Himalayan sediments (Ganga basin). *Geochimica et Cosmochimica Acta*, 84(Supplement C), 410-432. doi:https://doi.org/10.1016/j.gca.2012.02.001
- Mackie, W. (1897).** The sands and sandstones of Eastern Moray. *Transactions of the Edinburgh Geological Society*, 7(3), 148-172. doi:10.1144/transed.7.3.148
- Madhavaraju, J., Pacheco-Olivas, S. A., González-León, C. M., Espinoza-Maldonado, I. G., Sanchez-Medrano, P. A., Villanueva-Amadoz, U., Monreal, R., Pi-Piug, T., Ramirez-Montoya, E., Grijalva-Noriega, F. J. (2017).** Mineralogy and geochemistry of the Lower Cretaceous siliciclastic rocks of the Morita Formation, Sierra San José

section, Sonora, Mexico. *Journal of South American Earth Sciences*, 76(Supplement C), 397-411. doi: <https://doi.org/10.1016/j.jsames.2017.04.001>

Malaza, N., Liu, K., & Zhao, B. (2016). Petrology and geochemistry of clastic sedimentary rocks as evidences for provenance of the Late Palaeozoic Madzaringwe Formation, Tshipise-Pafuri Basin, South Africa. *Science China Earth Sciences*, 59(12), 2411-2426. doi:10.1007/s11430-016-5274-z

Mange, M. A., and Morton, A.C. (2007). Geochemistry of heavy minerals, In Mange, M., and Wright, D.T. (Eds.), *Heavy Minerals in Use: Developments in Sedimentology* (pp. 345-391). Amsterdam: Elsevier

Mat-Zin, I. C., & Swarbrick, R. E. (1997). The tectonic evolution and associated sedimentation history of Sarawak Basin, eastern Malaysia: a guide for future hydrocarbon exploration. *Geological Society, London, Special Publications*, 126(1), 237-245. Retrieved from <http://sp.lyellcollection.org/content/126/1/237.abstractN2>

Mat-Zin, I. C., & Tucker, M. E. (1999). An alternative stratigraphic scheme for the Sarawak Basin. *Journal of Asian Earth Sciences*, 17(1), 215-232. doi:[http://dx.doi.org/10.1016/S0743-9547\(98\)00042-7](http://dx.doi.org/10.1016/S0743-9547(98)00042-7)

Mathew, M.J., Menier, F., Siddiqui, N., Kumar, S.G., Authemayou, C. (2016). Active tectonic deformation along rejuvenated faults in tropical Borneo: Inferences obtained from tectono-geomorphic evaluation. *Geomorphology*, 267 (Supplement C), 1-15. doi: <https://doi.org/10.1016/j.geomorph.2016.05.016>

Maravelis, A. and Zeligidis, A. (2010). Petrography and geochemistry of the late Eocene–early Oligocene submarine fans and shelf deposits on Lemnos Island, NE Greece. Implications for provenance and tectonic setting. *Geological Journal*, 45 (4), 412–433. doi:10.1002/gj.1183

Maynard, J. B. (1984). Composition of plagioclase feldspar in modern deep-sea sands: relationship to tectonic setting. *Sedimentology*, 31(4), 493-501. doi:10.1111/j.1365-3091.1984.tb01815.x

Maynard, J. B., Valloni, R., & Yu, H. S. (1982). Composition of modern deep-sea sands from arc-related basins. *Geological Society, London, Special Publications*, 10(1), 551-561.

- McLennan, S. (1989).** Rare earth elements in sedimentary rocks; influence of provenance and sedimentary processes. *Reviews in Mineralogy and Geochemistry*, 21(1), 169-200.
- McLennan, S. M., Hemming, S. R., McDaniel, D. K., & Hanson, G. N. (1993).** Geochemical approaches to sedimentation, provenance, and tectonics. *Geological Society of America Special Papers*, 284, 21-40.
- McLennan, S. M., Nance, W. B., & Taylor, S. R. (1979).** Rare earth element-thorium correlations in sedimentary rocks, and the composition of the continental crust. *Geochimica et Cosmochimica Acta*, 44(11), 1833-1839. doi:[http://dx.doi.org/10.1016/0016-7037\(80\)90232-X](http://dx.doi.org/10.1016/0016-7037(80)90232-X)
- McLennan, S. M., & Taylor, S. R. (1991).** Sedimentary Rocks and Crustal Evolution: Tectonic Setting and Secular Trends. *The Journal of Geology*, 99(1), 1-21. Retrieved from <http://www.jstor.org/stable/30068762>
- McLennan, S. M., Taylor, S. R., McCulloch, M. T., & Maynard, J. B. (1990).** Geochemical and Nd/ Sr isotopic composition of deep-sea turbidites: crustal evolution and plate tectonic associations. *Geochimica et Cosmochimica Acta*, 54(7), 2015-2050.
- Merodio, J. C., Spalletti, L. A., & Bertone, L. M. (1992).** A Fortran Program for the calculation of Normative Composition of Clay-Minerals and Pelitic Rocks. *Computers & Geosciences*, 18(1), 47-61. doi:10.1016/0098-3004(92)90057-x
- Metcalfe, I. (1996).** Pre-Cretaceous evolution of SE Asian terranes. *Geological Society, London, Special Publications*, 106(1), 97-122. Retrieved from <http://sp.lyellcollection.org/content/106/1/97.abstractN2>
- Métivier, F., Gaudemer, Y., Tapponnier, P., & Klein, M. (1999).** Mass accumulation rates in Asia during the Cenozoic. *Geophysical Journal International*, 137(2), 280-318. doi:10.1046/j.1365-246X.1999.00802.x
- Modenesi-Gauttieri, M., de Toledo, M., Hiruma, S., Taioli, F. and Shimada, H. (2011).** Deep weathering and landscape evolution in a tropical plateau. *CATENA*, 85(3), pp.221-230.

- Morley, C. K., Tingay, M., Hillis, R., & King, R. (2008).** Relationship between structural style, overpressures, and modern stress, Baram Delta Province, northwest Borneo. *Journal of Geophysical Research: Solid Earth*, 113(B9).
- Morton, A. C. (1991).** Geochemical Studies of Detrital Heavy Minerals and Their Application to Provenance Studies. In: Morton A.C., Todd S.P., and Haughton P.D.W. (Eds.). *Developments in Sedimentary Provenance Studies. Special Publications Geological Society of London*, 57, 31-45.
- Morton, A. C., & Hallsworth, C. (1994).** Identifying provenance-specific features of detrital heavy mineral assemblages in sandstones. *Sedimentary Geology*, 90(3), 241-256. doi:http://dx.doi.org/10.1016/0037-0738(94)90041-8
- Morton, A. C., & Hallsworth, C. R. (1999).** Processes controlling the composition of heavy mineral assemblages in sandstones. *Sedimentary Geology*, 124(1-4), 3-29. doi:http://dx.doi.org/10.1016/S0037-0738(98)00118-3
- Morton, A. C., Whitham, A. G., & Fanning, C. M. (2005).** Provenance of Late Cretaceous to Paleocene submarine fan sandstones in the Norwegian Sea: Integration of heavy mineral, mineral chemical and zircon age data. *Sedimentary Geology*, 182(1), 3-28. doi:http://dx.doi.org/10.1016/j.sedgeo.2005.08.007
- Morton, A. C. H., C.R. (2007).** Stability of detrital heavy minerals during burial diagenesis. In: Mange, M. and Wright, D.K. (Eds), *Heavy Minerals In Use* (pp. 215-245). Amsterdam: Elsevier
- Mounteney, I., Burton, A. K., Farrant, A. R., Watts, M. J., Kemp, S. J., & Cook, J. M. (2018).** Heavy mineral analysis by ICP-AES a tool to aid sediment provenancing. *Journal of Geochemical Exploration*, 184(Part A), 1-10. doi:https://doi.org/10.1016/j.gexplo.2017.10.007
- Munksgaard, N. C., Lim, K., & Parry, D. L. (2003).** Rare earth elements as provenance indicators in North Australian estuarine and coastal marine sediments. *Estuarine, Coastal and Shelf Science*, 57(3), 399-409. doi:10.1016/S0272-7714(02)00368-2
- Nagarajan, R., Madhavaraju, J., Armstrong-Altrin, J. S., Nagendra, R. & J. Moutte (2007a)** Geochemistry of Neoproterozoic shales of Rabanpalli Formation, Bhima basin,

northern Karnataka, southern India: Implications for provenance and paleoredox conditions, *Revista Mexicana de Ciencias Geológicas*, 24(2):20-30.

Nagarajan, R. Armstrong-Altrin, J. S. Nagendra, R. Madhavaraju, J. and Moutte J. (2007b) Petrography and Geochemistry of Terrigenous Sedimentary Rocks in the Neoproterozoic Rabanpalli Formation, Bhima Basin, Southern India: Implications for Paleoweathering Conditions, Provenance and Source Rock Composition. *Journal of the Geological Society of India*, 70 (2): 297-312.

Nagarajan, R., Roy, P. D., Jonathan, M. P., Lozano, R., Kessler, F. L., & Prasanna, M. V. (2014). Geochemistry of Neogene sedimentary rocks from Borneo Basin, East Malaysia: Paleo-weathering, provenance and tectonic setting. *Chemie der Erde - Geochemistry*, 74(1), 139-146. doi:<http://dx.doi.org/10.1016/j.chemer.2013.04.003>

Nagarajan, R. Armstrong-Altrin, J.S. Kessler, F. L. Hidalgo-Moral, E. L. Dodge-Wan, D., & Taib N. I. (2015b) Provenance and tectonic setting of Miocene siliciclastic sediments, Sibuti Formation, Northwestern Borneo. *Arabian Journal of Geosciences*. 8(10), pp.8549-8565. doi: 10.1007/s12517-015-1833-4.

Nagarajan, R., Armstrong-Altrin, J. S., Kessler, F. L., & Jong, J. (2017a). Petrological and Geochemical Constraints on Provenance, Paleoweathering, and Tectonic Setting of Clastic Sediments from the Neogene Lambir and Sibuti Formations, Northwest Borneo. In R. Mazumder (Ed.), *Sediment Provenance* (pp. 123-153). Amsterdam: Elsevier.

Nagarajan, R., Jong, J., Kessler, F.L., (2017b). Provenance of the Neogene sedimentary rocks from the Tukai and Belait Formations, Northeastern Borneo by mineralogy and geochemistry. *Warta Geologi*, 43 (2), 10-16.

Nesbitt, H. W., & Young, G. M. (1982). Early Proterozoic climates and plate motions inferred from major element chemistry of lutites. *Nature*, 299(5885),715-717. doi:10.1038/299715a0

Nesbitt, H. W., & Young, G. M. (1984). Prediction of some weathering trends of plutonic and volcanic rocks based on thermodynamic and kinetic considerations. *Geochimica et Cosmochimica Acta*, 48(7), 1523-1534. doi:[http://dx.doi.org/10.1016/0016-7037\(84\)90408-3](http://dx.doi.org/10.1016/0016-7037(84)90408-3)

- Nesbitt, H. W., Young, G. M., McLennan, S. M., & Keays, R. R. (1996).** Effects of Chemical Weathering and Sorting on the Petrogenesis of Siliciclastic Sediments, with Implications for Provenance Studies. *The Journal of Geology*, *104*(5), 525-542. doi:10.2307/30065140
- Nie, J., Horton, B. K., Saylor, J. E., Mora, A., Mange, M., Garziona, C. N., Basu, A., Moreno, C.J., Caballero, V., Parra, M. (2012).** Integrated provenance analysis of a convergent retroarc foreland system: U-Pb ages, heavy minerals, Nd isotopes, and sandstone compositions of the Middle Magdalena Valley basin, northern Andes, Colombia. *Earth-Science Reviews*, *110*(1-4),111-126. doi:10.1016/j.earscirev.2011.11.002
- Nowrouzi, Z., Moussavi-Harami, R., Mahboubi, A., Mahmudy Gharaie, M. H., & Ghaemi, F. (2014).** Petrography and geochemistry of Silurian Niur sandstones, Derenjal Mountains, East Central Iran: implications for tectonic setting, provenance and weathering. *Arabian Journal of Geosciences*, *7*(7), 2793-2813. doi:10.1007/s12517-013-0912-7
- Ohta, T. (2004).** Geochemistry of Jurassic to earliest Cretaceous deposits in the Nagato Basin, SW Japan: implication of factor analysis to sorting effects and provenance signatures. *Sedimentary Geology*, *171*(1), 159-180. doi:https://doi.org/10.1016/j.sed geo.2004.05.014
- Ojanuga A.G. (1973).** Weathering of biotite in soils of a humid tropical climate. *Soil Science Society of America Proceedings*, *37*, 644 - 646.
- Olivarius, M., Rasmussen, E. S., Siersma, V., Knudsen, C., Kokfelt, T. F., & Keulen, N. (2014).** Provenance signal variations caused by facies and tectonics: Zircon age and heavy mineral evidence from Miocene sand in the north-eastern North Sea Basin. *Marine and Petroleum Geology*, *49*, 1-14. doi:https://doi.org/10.1016/j.marpetgeo.2013.09.010
- Omang, S., A.K. (1995).** Petrology and geochemistry of the mantle sequence peridotite of the Darvel Bay Ophiolite, Sabah, Malaysia. *Geological Society of Malaysia Bulletin*, *38*, 31-48.

- Oni, S. O., Olatunji, A. S., & Ehinola, O. A. (2014).** Determination of Provenance and Tectonic Settings of Niger Delta Clastic Facies Using Well-Y, Onshore Delta State, Nigeria. *Journal of Geochemistry*, 2014, 13. doi:10.1155/2014/960139
- Osae, S., Asiedu, D. K., Banoeng-Yakubo, B., Koeberl, C., & Dampare, S. B. (2006).** Provenance and tectonic setting of Late Proterozoic Buem sandstones of southeastern Ghana: Evidence from geochemistry and detrital modes. *Journal of African Earth Sciences*, 44(1), 85-96. doi:http://dx.doi.org/10.1016/j.jafrearsci.2005.11.009
- Pacle, N. A. D., Dimalanta, C. B., Ramos, N. T., Payot, B. D., Faustino-Eslava, D. V., Queaño, K. L., & Yumul, G. P. (2017).** Petrography and geochemistry of Cenozoic sedimentary sequences of the southern Samar Island, Philippines: Clues to the unroofing history of an ancient subduction zone. *Journal of Asian Earth Sciences*, 142(Supplement C), 3-19. doi:https://doi.org/10.1016/j.jseaes.2016.07.030
- Palenik, S. (2007).** Chapter 37 Heavy Minerals in Forensic Science. In A. M. Maria & T. W. David (Eds.), *Developments in Sedimentology*, 58, 937-961, Elsevier.
- Pantopoulos, G., & Zelilidis, A. (2012).** Petrographic and geochemical characteristics of Paleogene turbidite deposits in the southern Aegean (Karpathos Island, SE Greece): Implications for provenance and tectonic setting. *Chemie der Erde - Geochemistry*, 72(2), 153-166. doi:http://dx.doi.org/10.1016/j.chemer.2011.05.001
- Pe-Piper, G., Triantafyllidis, S., & Piper, D. J. W. (2008).** Geochemical Identification of Clastic Sediment Provenance from Known Sources of Similar Geology: The Cretaceous Scotian Basin, Canada. *Journal of Sedimentary Research*, 78(9), 595-607. doi:10.2110/jsr.2008.067
- Pe-Piper, G., Piper, D. J. W., Wang, Y., Zhang, Y., Trottier, C., Ge, C., & Yin, Y. (2016).** Quaternary evolution of the rivers of northeast Hainan Island, China: Tracking the history of avulsion from mineralogy and geochemistry of river and delta sands. *Sedimentary Geology*, 333 (Supplement C), 84-99. doi:https://doi.org/10.1016/j.sedgeo.2015.12.008
- Pearce, J. A., & Cann, J. R. (1973).** Tectonic setting of basic volcanic rocks determined using trace element analyses. *Earth and Planetary Science Letters*, 19(2), 290-300. doi:https://doi.org/10.1016/0012-821X(73)90129-5

- Pedro G. (1982).** The conditions of formation of secondary constituents. Pp. 63-81 in: Constituents' and Properties' of Soils (M. Bonneau & B. Souchier, editors) Academic Press, London.
- Perri, F., Critelli, S., Martín-Algarra, A., Martín-Martín, M., Perrone, V., Mongelli, G., & Zattin, M. (2013).** Triassic redbeds in the Malaguide Complex (Betic Cordillera — Spain): Petrography, geochemistry and geodynamic implications. *Earth-Science Reviews*, 117(0), 1-28. doi:http://dx.doi.org/10.1016/j.earscirev.2012.11.002
- Perri, F., & Ohta, T. (2014).** Paleoclimatic conditions and paleoweathering processes on Mesozoic continental redbeds from Western-Central Mediterranean Alpine Chains. *Palaeogeography, Palaeoclimatology, Palaeoecology*, 395, 144-157. doi:http://dx.doi.org/10.1016/j.palaeo.2013.12.029
- Pettijohn, F. J. (1975).** *Sedimentary Rocks* (3rd ed.). New York : Harper & Row.
- Pettijohn, F. J., Potter, P. E., & Siever, R. (1973).** *Sand and Sandstone*. New York: Springer-Verlag
- Pittman, E. D. (1963).** Use of zoned plagioclase as an indicator of provenance. *Journal of Sedimentary Research*, 33(2), 380-386. doi:10.1306/74d70e61-2b21-11d7-8648000102c1865d
- Pittman, E. D. (1970).** Plagioclase feldspar as an indicator of provenance in sedimentary rocks. *Journal of Sedimentary Research*, 40(2), 591-598. doi:10.1306/74d71fdc-2b21-11d7-8648000102c1865d
- Pober, E. F., P. (1988).** The chemistry of detrital chromian spinels and its implications for the geodynamic evolution of the Eastern Alps. *Geologische Rundschau*, 77(3), 641-670.
- Potter, P. E. (2003).** Mudrocks. In *Sedimentology*. Dordrecht, Netherlands: Springer. doi: https://doi-org.dbgw.lis.curtin.edu.au/10.1007/978-1-4020-3609-5
- Potter, P.E., Maynard, J.B., Depetris, P.J. (2005).** *Mud and Mudstones*. doi:10.1007/b138571
- Powers, M. C. (1953).** A new roundness scale for sedimentary particles. *Journal of Sedimentary Research*, 23(2), 117-119. doi: https://doi.org/10.1306/D4269567-2B26-11D7-8648000102C1865D

- Proenza, J. A., Zaccarini, F., Escayola, M., Cábana, C., Schalamuk, A., & Garuti, G. (2008).** Composition and textures of chromite and platinum-group minerals in chromitites of the western ophiolitic belt from Pampean Ranges of Córdoba, Argentina. *Ore Geology Reviews*, 33, 32-48. doi:10.1016/j.oregeorev.2006.05.009
- Prothero, D. R., & Schwab, F. (2013).** *Sedimentary Geology*: W. H. Freeman.
- Rahl, J. M., Reiners, P. W., Campbell, I. H., Nicolescu, S., & Allen, C. M. (2003).** Combined single-grain (U-Th)/He and U/Pb dating of detrital zircons from the Navajo Sandstone, Utah. *Geology*, 31(9), 761-764. doi:10.1130/G19653.1
- Rahman M. J. J. and Suzuki. S. (2007).** Geochemistry of sandstones from the Miocene Surma Group, Bengal Basin, Bangladesh: implications for provenance, tectonic setting and weathering. *Geochemical Journal*, 41 (6), 415-428 doi: <https://doi.org/10.2343/geochemj.41.415>
- Ramachandran, A., Madhavaraju, J., Ramasamy, S., Lee, Y. I., Rao, S., Chawngthu, D. L., & Velmurugan, K. (2016).** Geochemistry of Proterozoic clastic rocks of the Kerur Formation of Kaladgi-Badami Basin, North Karnataka, South India: implications for paleoweathering and provenance. *Turkish Journal of Earth Sciences*, 25(2), 126-144. doi:10.3906/yer-1503-4
- Ramkumar, M., Santosh, M., Nagarajan, R., Li, S.S., Mathew, M., Menier, D., Siddiqui, N., Rai J., Sharma, A., Farroqui, S., Poppelreiter, M.C., Lai, J., Prasad, V. (2018)** Late Middle Miocene volcanism in the Northern Borneo, Southeast Asia: Implications for Tectonics, Paleoclimate and stratigraphic marker. *Palaeogeography, Palaeoclimatology, Palaeoecology*, 490:141-162. <https://doi.org/10.1016/j.palaeo.2017.10.022>
- Ratcliffe, K.T., Morton, A., Ritcey, D., & Evenchick, C. E. (2007).** Whole rock geochemistry and heavy mineral analysis as exploration tools in the Bowser and Sustut Basins, British Columbia, Canada. *Journal of Canadian Petroleum Geology*, 55, 320-337. doi: <http://dx.doi.org/10.2113/gscpgbull.55.4.320>
- Reiche, P. (1950).** A Survey of Weathering Processes and Products. *University of New Mexico Publications in Geology*, 3, 95.

- Reimann Zumsprekel, C. R., Bahlburg, H., Carlotto, V., Boekhout, F., Berndt, J., & Lopez, S. (2015).** Multi-method provenance model for early Paleozoic sedimentary basins of southern Peru and northern Bolivia (13°–18°S). *Journal of South American Earth Sciences*, 64, Part 1, 94-115. doi:<http://dx.doi.org/10.1016/j.jsames.2015.08.013>
- Ristau, J. (2013).** Plate Tectonics. In P. Bobrowsky (Ed.), *Encyclopedia of Natural Hazards* (pp. 769-772): Springer Netherlands.
- Roddaz, M., Viers, J., Brusset, S., Baby, P., Boucayrand, C., & Hérail, G. (2006).** Controls on weathering and provenance in the Amazonian foreland basin: Insights from major and trace element geochemistry of Neogene Amazonian sediments. *Chemical Geology*, 226(1–2), 31-65. doi:<http://dx.doi.org/10.1016/j.chemgeo.2005.08.010>
- Rodrigues, A.G., Goldberg, K., (2014).** Primary composition and diagenetic patterns of sandstones from Barra de Itiúba Formation in Atalaia High, Sergipe Sub-Basin Brazilian Journal of Geology, 44(4): 545-56. doi: 10.5327/Z23174889201400040003
- Rollinson, H. R. (1993).** Using geochemical data: evaluation, presentation, interpretation. *Harlow, Essex, England: New York: Longman Scientific & Technical.*
- Roser, B. P., & Korsch, R. J. (1986).** Determination of Tectonic Setting of Sandstone-Mudstone Suites SiO₂ Content and K₂O/Na₂O Ratio. *The Journal of Geology*, 94(5), 635-650. doi:10.2307/30078330
- Roser, B. P., & Korsch, R. J. (1988).** Provenance signatures of sandstone-mudstone suites determined using discriminant function analysis of major-element data. *Chemical Geology*, 67(1–2), 119-139. doi:[http://dx.doi.org/10.1016/0009-2541\(88\)90010-1](http://dx.doi.org/10.1016/0009-2541(88)90010-1)
- Ryan, K. M., & Williams, D. M. (2007).** Testing the reliability of discrimination diagrams for determining the tectonic depositional environment of ancient sedimentary basins. *Chemical Geology*, 242(1), 103-125. doi: <https://doi.org/10.1016/j.chemgeo.2007.03.013>
- Sáez, A., Inglès, M., Cabrera, L., & De las Heras, A. (2003).** Tectonic–palaeoenvironmental forcing of clay-mineral assemblages in nonmarine settings: the Oligocene–Miocene As Pontes Basin (Spain). *Sedimentary Geology*, 159(3-4), 305-324. doi:10.1016/s0037-0738(02)00333-0

- Saigal G.C., Morad S., Bjørlykke K., Egeberg P.K., Aagaard P. (1988).** Diagenetic albitization of detrital K-feldspars in Jurassic, Lower Cretaceous, and Tertiary clastic reservoirs from offshore Norway; I, Textures and origin. *Journal of Sedimentary Petrology*, 58(6), 1003-1013. doi: <https://doi.org/10.1306/212F8EE5-2B24-11D7-8648000102C1865D>
- Salama, W., Anand, R. R., & Verrall, M. (2016).** Mineral exploration and basement mapping in areas of deep transported cover using indicator heavy minerals and paleoredox fronts, Yilgarn Craton, Western Australia. *Ore Geology Reviews*, 72, Part 1, 485-509. doi:<http://dx.doi.org/10.1016/j.oregeorev.2015.07.014>
- Saminpanya, S., Duangkrayom, J., Jintasakul, P., & Hanta, R. (2014).** Petrography, mineralogy and geochemistry of Cretaceous sediment samples from western Khorat Plateau, Thailand, and considerations on their provenance. *Journal of Asian Earth Sciences*, 83(0), 13-34. doi:<http://dx.doi.org/10.1016/j.jseaes.2014.01.007>
- Satyana, A. H., Nugroho, D., & Surantoko, I. (1999).** Tectonic controls on the hydrocarbon habitats of the Barito, Kutei, and Tarakan Basins, Eastern Kalimantan, Indonesia: major dissimilarities in adjoining basins. *Journal of Asian Earth Sciences*, 17(1), 99-122. doi:[https://doi.org/10.1016/S0743-9547\(98\)00059-2](https://doi.org/10.1016/S0743-9547(98)00059-2)
- Schwab, F. L. (1975).** Framework mineralogy and chemical composition of continental margin-type sandstone. *Geology* 3, 487-490.
- Schieber, J. (1992).** A combined petrographical—geochemical provenance study of the Newland Formation, Mid-Proterozoic of Montana. *Geological Magazine*, 129, (2) 223-237 <https://doi.org/10.1017/S0016756800008293>
- Sevastjanova, I., Hall, R., & Alderton, D. (2012).** A detrital heavy mineral viewpoint on sediment provenance and tropical weathering in SE Asia. *Sedimentary Geology*, 280, 179-194. doi:<http://dx.doi.org/10.1016/j.sedgeo.2012.03.007>
- Shi, G., Wang, H., Huang, C., Yang, S., & Song, G. (2016).** Provenance and tectonic setting of middle-upper Devonian sandstones in the Qinling Orogen (Shanyang area): New insights from geochemistry, heavy minerals and tourmaline chemistry. *Tectonophysics*, 688, 11-25. doi:<http://dx.doi.org/10.1016/j.tecto.2016.09.023>

- Siddiqui, N.A., Abd Rahman, A.H., Sum, C.W., & Murtaza, M. (2017).** Sandstone Facies Reservoir Properties and 2D-Connectivity of Siliciclastic Miri Formation, Borneo. *Proceedings of the International Conference on Integrated Petroleum Engineering and Geosciences (ICIPEG2016)*, 581-595. Singapore-Springer
- Simonen, A. & Kouvo, O. (1955).** Sandstones in Finland. *Bulletin de la Commission Géologique de Finlande*, 168, 57-87. Retrieved from http://tupa.gtk.fi/julkaisu/bulletin/bt_168_pages_057_087.pdf
- Singh, Y., Amin, K. A., Alvarez, E., Hernandez, J., Liniawati, A., & Fauzi, M. (2009).** Reservoir properties prediction in the West Baram Delta through data integration constrained by rock physics. *The Leading Edge*, 28(12), 1486-1491. doi:10.1190/1.3272704
- Smyth, H. R., Hall, R., & Nichols, G. J. (2008).** Significant Volcanic Contribution to Some Quartz-Rich Sandstones, East Java, Indonesia. *Journal of Sedimentary Research*, 78, 335-356. doi: 10.2110/jsr.2008.039
- Song, Y.-H., & Choi, M. S. (2009).** REE geochemistry of fine-grained sediments from major rivers around the Yellow Sea. *Chemical Geology*, 266(3), 328-342. doi:<http://dx.doi.org/10.1016/j.chemgeo.2009.06.019>
- Sorby, H. C. (1880).** On the structure and origin of non-calcareous stratified rocks. *Geological Society of London Proc*, 36, 46-92.
- Suttner, L. J. (1974).** Sedimentary petrographic provinces: an evaluation. In C.A Ross (Eds.), *Paleogeographic provinces and provinciality*, Society of Economic Paleontologists and Mineralogists Special Publications, 21, p. 75-84.
- Suttner, L. J., Basu, A., & Mack, G. H. (1981).** Climate and the origin of quartz arenites. *Journal of Sedimentary Research*, 51(4), 1235-1246. doi:10.1306/212f7e73-2b24-11d7-8648000102c1865d
- Suzuki, S., Shizuo, T., Graciano, P.Y., Sevillo, D.D., Daniel, K.A., (2000).** Composition and provenance of the upper cretaceous to Eocene sandstones in central Palawan, Philippines: constraints on the tectonic development of Palawan. *Island Arc*, 9, 611–626. doi: <https://doi.org/10.1111/j.1440-1738.2000.00306.x>

- Tankard, A. J. (2002).** Sedimentary Petrology. In Maurice E. Tucker (3rd ed.), Blackwell, Oxford, 2001, 262 pp. *Sedimentary Geology*, 152(1–2), 159-160. doi: [http://dx.doi.org/10.1016/S0037-0738\(01\)00254-8](http://dx.doi.org/10.1016/S0037-0738(01)00254-8)
- Tawfik, H. A., M.Ghandour, I., Maejima, W., Armstrong-Altrin, J. S., & Abdeel-Hamed, A.-M. T. (2015).** Petrography and geochemistry of the siliciclastic Araba Formation (Cambrian), east Sinai, Egypt: implications for provenance, tectonic setting and source weathering. *Geological Magazine*, 154(1), 1-23. doi:10.1017/S0016756815000771
- Taylor, S. R. & McLennan., S.M. (1985).** The continental crust: its composition and evolution. *Blackwell Scientific Publication, Carlton*, 312 pages
- Thiel, G. A. (1940).** The relative resistance to abrasion of mineral grains of sand size. *Journal of Sedimentary Petrology*, 10, 103-124. doi:<https://doi.org/10.1306/D42690A3-2B26-11D7-8648000102C1865D>
- Tijani, M. N., Nton, M. E., & Kitagawa, R. (2010).** Textural and geochemical characteristics of the Ajali Sandstone, Anambra Basin, SE Nigeria: Implication for its provenance. *Comptes Rendus Geoscience*, 342(2), 136-150. doi: <https://doi.org/10.1016/j.crte.2009.09.009>
- Tiju I.V., Prakash, T. N., Nagendra, R., Nagarajan, R. (2018)** Sediment geochemistry of coastal environments, southern Kerala, India: implication for provenance. *Arabian Journal of Geosciences*. 11, 61. doi:10.1007/s12517-018-3406-9.
- Todd, T. W., Folk, R.L. (1957).** Basal Claiborne of Texas, record of Appalachian tectonism during Eocene. *American Association Petroleum Geologists Bulletin*, 41(11), 2545-2566.
- Togunwa, O. S., Abdullah, W. H., Hakimi, M. H., & Barbeito, P. J. (2015).** Organic geochemical and petrographic characteristics of Neogene organic-rich sediments from the onshore West Baram Delta Province, Sarawak Basin: Implications for source rocks and hydrocarbon generation potential. *Marine and Petroleum Geology*, 63, 115-126. doi:<http://dx.doi.org/10.1016/j.marpetgeo.2015.02.032>
- Tortosa, A., Palomares, M., & Arribas, J. (1991).** Quartz grain types in Holocene deposits from the Spanish Central System: some problems in provenance analysis. *Geological Society, London, Special Publications*, 57(1), 47-54. doi:10.1144/gsl.sp.1991.057.01.05

- Totten, M. W., Hanan, M. A., & Weaver, B. L. (2000).** Beyond whole-rock geochemistry of shales: The importance of assessing mineralogic controls for revealing tectonic discriminants of multiple sediment sources for the Ouachita Mountain flysch deposits. *Geological Society of America Bulletin*, 112(7), 1012-1022. doi:10.1130/0016-7606(2000)112<1012:bwgost>2.0.co;2
- Trevena, A. S. & Nash, W.P. (1981).** An electron microprobe study of detrital feldspar. *Journal of Sedimentary Research*, 51(1), 137-150.
- Tucker, E. (2001).** *Sedimentary Petrology: An Introduction to the Origin of Sedimentary Rocks*: Wiley.
- Ulfa, Y., Sapari, N., & Harith, Z. (2011).** Combined Tide and Storm Influence on Facies Sedimentation of Miocene Miri Formation, Sarawak. *Eksplorium*, 32(2), 77-90
- Ulery, A.L., & Drees, L.R. (2008).** Methods of Soil Analysis: Part 5-Mineralogical Methods. *American Society of Agronomy*, 544 pages.
- Um, I. K., Choi, M. S., Bahk, J. J., & Song, Y. H. (2013).** Discrimination of sediment provenance using rare earth elements in the Ulleung Basin, East/Japan Sea. *Marine Geology*, 346, 208-219. doi:http://dx.doi.org/10.1016/j.margeo.2013.09.007
- Van de Kamp, P. C., & Leake, B. E. (1985).** Petrography and geochemistry of feldspathic and mafic sediments of the northeastern Pacific margin. *Transactions of the Royal Society of Edinburgh: Earth Sciences*, 76(04), 411-449.
- van der Zee, W., & Urai, J. L. (2005).** Processes of normal fault evolution in a siliciclastic sequence: a case study from Miri, Sarawak, Malaysia. *Journal of Structural Geology*, 27(12), 2281-2300. doi:http://dx.doi.org/10.1016/j.jsg.2005.07.006
- van Hattum, M. W. A., Hall, R., Pickard, A. L., & Nichols, G. J. (2006).** Southeast Asian sediments not from Asia: Provenance and geochronology of north Borneo sandstones. *Geology*, 34(7), 589-592. doi: https://doi.org/10.1130/G21939.1
- van Hattum, M. W. A, Hall, R., Pickard, A. L, & Nichols, G. J. (2013).** Provenance and geochronology of Cenozoic sandstones of northern Borneo. *Journal of Asian Earth Sciences*, 76, 266-282. doi:10.1016/j.jseaes.2013.02.033
- Velde, B., & Meunier, A. (2008).** *The origin of clay minerals in soils and weathered rocks*. Berlin: Springer.

- Wang, P. C., Li, S. Z., Guo, L. L., Jiang, S. H., Somerville, I. D., Zhao, S. J., Zhu, B. D., Chen, J., Dai, L. M., Suo, Y. H., and Han, B. (2016).** Mesozoic and Cenozoic accretionary orogenic processes in Borneo and their mechanisms. *Geological Journal*, *51*, 464–489. doi: 10.1002/gj.2835.
- Weaver, C. E. (1956).** A discussion on the origin of Clay Minerals in Sedimentary Rocks. *Clays and Clay Minerals*, *5*(1), 159-173. doi:10.1346/CCMN.1956.0050113
- Wilson, M. J. (1999).** The origin and formation of clay minerals in soils: past, present and future perspectives. *Clay Minerals*, *34*(01), 7-25. doi:10.1180/000985599545957
- Xie, Q., Qiu, G., Chen, T., Xu, X., Wang, X., Lu, H., & Ji, J. (2015).** Palygorskite in the Late Miocene Red Clay Sediment from the Chinese Loess Plateau and Its Paleoclimatic Implications. *Springer Geochemistry/Mineralogy*, 425-440. doi:10.1007/978-3-319-13948-7_42
- Zhao, Y., Zou, X., Liu, Q., Wang, C., Ge, C., & Xu, M. (2018).** Clay mineralogy indicates the muddy sediment provenance in the estuarine-inner shelf of the East China Sea. *Journal Of Asian Earth Sciences*, *152*, 69-79. doi: 10.1016/j.jseas.2017.11.036

Every reasonable effort has been made to acknowledge the owners of copyright material. I would be pleased to hear from any copyright woner who has been omitted or incorrectly acknowledged.

APPENDIX 1.0

Raw observations on the thin section:

Sample Number	Observations Details
Sample S2B4	This is a sandstone sample. Most abundant grain in the sample is quartz, followed by lithic fragments and feldspar. The grains are medium to coarse grained and ranging from moderate to poorly-sorted. Quartz was easily identified by its' undulose extinction. The observation on feldspar was slightly confusing whether the grain is belong to perthite or albite. Lithic fragments were identified to be sedimentary rocks; chert. Fine grained material made of shale or slate was identified. A small elongated muscovite grain was found inside the shale/slate.
Sample S3B4	This sample is a sandstone sample. The most abundant mineral observed in this sample is quartz which can be identified easily based on the undulose extinction, followed by rock fragments and feldspar. Quartz minerals present in sub-rounded to angular form with sphericity ranging from low to high. Mica (muscovite) also observed in the sample (~1%). The existence of mica although very few indicated that there is influences of granitic or schistose as source rock. Cement presents in the sample which indicated by brownish to yellowish colour and could be iron oxide. Meanwhile, the matrix consists of clay that is slightly darker brown in colour. Feldspar presents in the sample (~10%) and can be identified based on the Carlsbad twinning and multiple twinning. Carlsbad twinning is more common in this sample; could be because of their highly resistant characteristics towards weathering compared to plagioclase series. Presence of alkali feldspars dominated the sample indicate that the sources probably originated from quartz a granite or gneiss. Multiple twinning only observed in one or two isolated grains; could be belongs to plagioclase series. Another isolated feldspar grains seemed to show perthitic intergrowth. However, the present of this grain is very uncommon in sedimentary rocks and it can be regarded as isolated cases of existence. Rock fragments observed in this sample is mostly identified as chert.
Sample B5A	This sample also a sandstone sample. Grains were identified as medium-grained, sub-angular to sub-rounded with sphericity varies across the sample. Among observable grains are quartz of both monocrystalline and polycrystalline. Lithics fragments served as the second abundance grains found in the thin section. Most common fragments found were belong to chert fragments. Presence of feldspar identified from the Carlsbad twinning.
Sample 19A	This is a sandstone sample. The grains are sub-rounded to sub-angular in term of roundness and having medium to high sphericity. The grains are categorized as fine-grained (X10 magnification). Quartz appeared as the most abundance mineral followed by lithic fragments. The sample also considered as well-sorted with all grains almost in similar sizes. The smaller sizes limiting the observation view as the grains appeared blur under high magnification.

Sample 56	Angular to sub-rounded grains, most of the grains showing low sphericity, grain sizes varied across the samples (ranging from coarse sand to fine-sand), observable grains are quartz and feldspar (minor quantity).
Sample 54	This is a sandstone sample. This is a fine-grained and well-sorted sample. The grains are rounded to sub-angular. Sphericity ranging from low to high. Most observable grains are quartz and lithic fragments. Feldspar is absence or probably very limited in number.
Sample 54 (b)	This is a sandstone sample. It is the similar rock as observed in 5.1.2.4 but in different cutting view. The sample is medium to coarse grained. Grains are sub-rounded to angular. It is moderately sorted. Most abundance grain is quartz; both monocrystalline and polycrystalline. Lithic fragments are the second most abundance grain and feldspar exists in one or two grains, minority. This sample contains the most abundance polycrystalline quartz in compared with other samples. Lithic fragments are consists of sedimentary rocks and chert. Chert presence in large grains. There a several grains with “veins”. Biotite also observed in this sample but in a very minor amount.
Sample 7A	This is a sandstone sample. The grains were subrounded to angular, slightly low sphericity. Most abundance grains type is quartz with majority are monocrystalline followed by lithics fragmensts as the second abundance. Feldspar is minor in presence or almost non-observable. The lithics fragments are majority from sandstone fragments.
Sample 42	This is a sandstone sample. The grains are angular to sub-rounded. Majority observed grains are consists of quartz (both monocrystalline and polycrystalline), lithics fragments and minority amount of feldspar. Feldspar are identified through the observation of Carlsbad twinning.
Sample 1	This is a sandstone sample. The grains are coars-grained and well-sorted. Grains are rounded to sub-angular with medium sphericity. Most abundance grain is quartz followed by lithic fragments. Quartz grains are consists of both monocrystalline and polycrystalline. Lithic fragments majority are chert.
Sample B4B	This sample is a sandstone sample. The grains were medium to coarse grained and showing angular to sub-rounded grains. The sample is moderately sorted. Observable grains were quartz as the most abundance grains, lithic fragments and with rare feldspar occurrence. Lithic fragments in the sample are dominated by volcanic fragments. In the observation, a grain had been identified having probability as fragment of schistose quartz.
Sample 14D	This is a sandstone sample. Sample is identified to be rounded to subrounded, medium to high sphericity. This sample is a semi-consolidated sample. Minerals observed in the sample are quartz, lithic fragments and minor presence of feldspar.
Sample B2C	Angular to sub-rounded grains (mostly showing high angularity), medium to low sphericity, observable grain consist of quartz
Sample 30A	Sub-angular to sub-rounded, medium sphericity, medium to fine-grained, observable grains are quartz (majority)
Sample 4B	Medium to Fine-grained, angular to sub-rounded, low to medium sphericity, majority observed grains are made of quartz followed by minor amount of lithic fragments.




Sample B7A	Angular to sub-rounded, observable grains consist of quartz and feldspar grains are spotted showing Karlsbad twinning.
Sample B7C	This sample is a sandstone sample. Grains observed were showing sub-angular to sub-rounded grains with majority of the grains have higher sphericity. The sample is moderately sorted. Quartz presents as the dominant minerals with more monocrystalline than polycrystalline quartz. The second abundance species is lithic fragments. Lithic fragments were dominated by sedimentary fragments followed by volcanic fragments. Feldspar grains identified by the multiple twinning. However, only one or two feldspar grains were found in the thin section slide.
Sample 9	Sub-angular to rounded grains, medium-grained, Observable grains are quartz and lithic fragments.
Sample S3B4	This sample is a sandstone sample. The most abundant mineral observed in this sample is quartz which can be identified easily based on the undulose extinction, followed by rock fragments and feldspar. Quartz minerals present in sub-rounded to angular form with sphericity ranging from low to high. Mica (muscovite) also observed in the sample (~1%). The existence of mica although very few indicated that there is influences of granitic or schistose as source rock. Cement presents in the sample which indicated by brownish to yellowish colour and could be iron oxide. Meanwhile, the matrix consists of clay that is slightly darker brown in colour. Feldspar presents in the sample (~10%) and can be identified based on the Karlsbad twinning and multiple twinning. Karlsbad twinning is more common in this sample; could be because of their highly resistant characteristics towards weathering compared to plagioclase series. Presence of alkali feldspars dominated the sample indicate that the sources probably originated from granite or gneiss. Multiple twinning only observed in one or two isolated grains; could be belongs to plagioclase series. Another isolated feldspar grains seemed to show perthitic intergrowth. However, the present of this grain is very uncommon in sedimentary rocks and it can be regarded as isolated cases of existence. Rock fragments observed in this sample is mostly identified as chert.
Sample O6B4	This sample is a sandstone sample. The most abundant mineral observed in this sample is quartz with monocrystalline quartz dominates against polycrystalline quartz. Polycrystalline quartz observed in this sample showed sutured boundaries. Sutured boundary is a characteristics of quartz originated from metamorphic sources. The sutured boundaries can be seen clearly under XPL view. The quartz grains also showing subrounded to angular grains. Meanwhile, the sphericity varies from low to high. Rock fragments also observed in the sample such as chert and volcanic rock fragments. Observed volcanic rock fragments have fine-grained which could be belongs to basic rock. Chert is quite common across the sample as it is highly resistant to weathering. Similarly, the inner grains were too fine to be identified.
Sample S3B2	This is a sandstone sample. The grains are medium-grained showing rounded to sub-angular. Most abundant grain in the sample is quartz. Monocrystalline quartz dominates over polycrystalline type. Lithic fragments are consists of chert with an area showing presence of




	shale/slate fragments. As for feldspar, Carlsbad and multiple twinning can be found in one or two grains. There are also minor presence of mica.
Sample S2B9	This is a sandstone sample. Grains are showing subangular to angular texture. This thin section is not fully observed due to the poor quality of the thin section. The most abundance mineral is quartz. Lithic fragments is the second most observable component in the sample. The rock fragments are identified as chert.
Sample S2B11	This sample is a sandstone sample. Majority of the grains are sub-rounded to sub-angular and generally well-sorted. Most abundance grain is quartz, lithic fragments, mica and feldspar. The feldspar found in this sample is most probably plagioclase based on the Carlsbad twinning. Mica group are consists of both muscovite and biotite. Cement identified as iron oxide. Point contacts and long contacts are the common contacts observed between grains.
Sample S2B7	This is a sandstone sample. The sample is medium-grained with quartz dominates the composition followed by lithic fragementts. Grains are showing subrounded to angular roundness.
Sample S2B4	This is a sandstone sample. Most abundant grain in the sample is quartz, followed by lithic fragments and feldspar. The grains are medium to coarse grained and ranging from moderate to poorly-sorted. Quartz was easily identified by its' undulose extinction. The observation on feldspar was slightly confusing whether the grain is belong to perthite or albite. Lithic fragments were identified to be sedimentary rocks; chert. Fine grained material made of schist fragment was identified. A small elongated muscovite grain was found next to the schist fragment.
Sample O5B1	This is a sandstone sample. Most abundant grain in the sample is quartz followed by lithic fragments and feldspar. Feldspar was identified from the observation of Carlsbad twinning. Lithic fragments were majority consists of chert. The grains are medium to coarse grained. All grains showed rounded to angular with high sphericity.
Sample O5B2	This is a sandstone sample. Most abundant grain in this sample is quartz followed by lithic fragments, feldspar and minor mica constituents. The sample observed is considered as moderately sorted based on the variation of isolated larger grains in smaller grains. Quartz grains in this sample are rounded to subangular with most grains showing high sphericity. In this sample, again several quartz grains observed showed undulose extinction. Feldspar identified by the presence of Carlsbad twinning with one or two grains showing multiple twinning. Rock fragments consist of chert, sedimentary and volcanic fragments. Volcanic fragments in this sample was identified based on the appearance where the tiny blades of feldspar presence within the fine groundmass. Sedimentary rocks meanwhile presence as a large sandstone fragments. Presence of mica in this sample showed that the source for the sediment is most probably granitic and schistose rock. However, in the section where mica is presence, no alignment or bedding was observed.
Sample O5B6	This is a sandstone sample. The grain sized of this sample can be classified under fine to medium grained. Smaller grains caused the difficulty in identifying the mineral types. Abundant mineral in this sample is quartz. Quartz observed in this sample are mostly rounded to subangular with majority showing high sphericity. Under cross polars

	<p>(XPL), some of the quartz grains showed undulose extinction. Generally, undulose extinction is common in quartz grains that originated from igneous or metamorphic sources. Apart from that, some monocrystalline quartz grains also showed sutured boundaries when seen under cross polars. This is another indicator that the source rock is from metamorphic sources. Feldspars are low in composition for this sample. Among the observed ones showed Carlsbad twinning which is representing the alkali feldspar series. Meanwhile for the rock fragments, chert is among the most encountered in the sample.</p>
Sample O1B1	<p>This is a sandstone sample. Most abundant mineral in this sample is quartz. Quartz observed in this sample are majority sub rounded to angular with sphericity varies from low to high sphericity. Again in this sample, we can find quartz showing undulose extinction which indicate metamorphic sources. Feldspars are found in the sample isolated all across the sample with alkali feldspars are easily identified from the Carlsbad twinning. There are one to three grains of plagioclase observed in the sample; identified from the multiple twinning. The feldspars are seemed to be undergone alteration based on the cloudy feature its' display under plane polars (PPL). Rock fragments also observed in the sample could be chert and volcanic fragments. Volcanic fragments in this sample could suggest that the source is originated from basic rocks. The minerals contained inside the rock fragments fine grained and thus making the identification impossible. Cement present in brownish colour which is most probably iron oxide. Matrix also present and consists of clay.</p>
Sample 36C	<p>This is a sandstone sample. The sample is moderately sorted, medium to coarse grained showing sub-rounded to angular grains. Most abundant mineral is quartz followed by lithic fragments. Meanwhile, feldspar presence as minor occurrence and identified from Carlsbad and multiple twinning. Quartz presence in the form of monocrystalline and polycrystalline. Lithic fragments consists of chert and one quartz-rich rock fragments was observed.</p>

APPENDIX 2.0

Process of thin sections preparation:

Step Number	Pictures	Details
1		<p>Drying out the samples using laboratory oven. Samples were left to dry in an oven set at a temperature of 40°C or less for roughly 8 hours to eliminate the moisture contents.</p>
2		<p>The samples later impregnated by using 50ml of part A (Resin), 50ml of part B (Hardener) and 25ml of acetone.</p>
3		<p>The samples were left to harden for roughly 3 hours (on heating plate) with temperature < 80°C.</p>

4		<p>Hardened samples were cut using the thin section machines into a slab roughly 2 cm x 3 cm for each of the sample.</p>
5		<p>One side of the slab was labeled while the other side of the slab was flattened and lightly polished on a glass plate with 400-600 grit carborundum powder.</p>
6		<p>The glass slide is glued to the lapped surface using the epoxy glue (Loctite Hysol 0151). The sample was left for at least overnight to ensure the glue is sticking to the slide. Later, using the thin section saw, the slab was cut-off close to the slide. The thickness of the slab should be close enough to 3mm.</p>



Contents lists available at ScienceDirect

Journal of Asian Earth Sciences

journal homepage: www.elsevier.com/locate/jseas



Full length Article

An integrated study of geochemistry and mineralogy of the Upper Tukai Formation, Borneo Island (East Malaysia): Sediment provenance, depositional setting and tectonic implications



Ramasamy Nagarajan^{a,*}, Priyadarsi D. Roy^b, Franz L. Kessler^c, John Jong^d, Vivian Dayong^e, M.P. Jonathan^e

^a Department of Applied Geology, Curtin University Malaysia Miri, 98009 Sarawak, Malaysia

^b Instituto de Geología, Universidad Nacional Autónoma de México, Ciudad Universitaria, CP 04510 Ciudad de México, Mexico

^c Goldbach Geoconsultants O & G, Glanbach, Aschaffenburg, Germany

^d JX Nippon Oil and Gas Exploration (Deepwater Sabah) Limited, Level 15, Menara Prestige, No. 1, Jalan Pinnang, 50450 Kuala Lumpur, Malaysia

^e Centro Interdisciplinario de Investigaciones y Estudios sobre Medio Ambiente y Desarrollo, Instituto Politécnico Nacional, Calle 30 de Junio de 1520, Barrio la Laguna Ticomán, Del Gustavo A. Madero, CP 07340 Ciudad de México, Mexico

ARTICLE INFO

Keywords

Geochemistry
Mineralogy
Mineral chemistry
Zircon geochronology
Provenance
Borneo

ABSTRACT

An integrated study using bulk chemical composition, mineralogy and mineral chemistry of sedimentary rocks from the Tukai Formation of Borneo Island (Sarawak, Malaysia) is presented in order to understand the depositional and tectonic settings during the Neogene. Sedimentary rocks are chemically classified as shale, wacke, arkose, litharenite and quartz arenite and consist of quartz, illite, feldspar, rutile and anatase, zircon, tourmaline, chromite and monazite. All of them are highly matured and were derived from a moderate to intensively weathered source. Bulk and mineral chemistries suggest that these rocks were recycled from sedimentary to metasedimentary source regions with some input from granitoids and mafic-ultramafic rocks. The chondrite normalized REE signature indicates the presence of felsic rocks in the source region. Zircon geochronology shows that the samples were of Cretaceous and Triassic age. Comparable ages of zircon from the Tukai Formation sedimentary rocks, granitoids of the Schwaner Mountains (southern Borneo) and Tin Belt of the Malaysia Peninsular suggest that the principal provenance for the Rajang Group were further uplifted and eroded during the Neogene. Additionally, presence of chromian spinels and their chemistry indicate a minor influence of mafic and ultramafic rocks present in the Rajang Group. From a tectonic standpoint, the Tukai Formation sedimentary rocks were deposited in a passive margin with passive collisional and rift settings. Our key geochemical observation on tectonic setting is comparable to the regional geological setting of northwestern Borneo as described in the literature.

1. Introduction

Chemistry of fine-grained clastic sediments provides useful information about provenance, depositional environments (climate and tectonic setting), and post depositional processes (McLennan et al., 1993; Rahman and Suzuki, 2007; Ohta, 2008; Lee, 2009; Nagarajan et al., 2014; Armstrong-Altrin et al., 2015; Sahoo et al., 2015; Zak, 2015; Paclé et al., 2016; Zhang et al., 2016). However, heavy mineral assemblages are better indicators of provenance compared to the whole rock chemistry as the major and trace element distributions are controlled by multiple and complex mineralogical associations (Mange and Maurer, 1992; Ratcliffe et al., 2007; Sevastjanova et al.,

2012). Similarly, chemistry of different heavy mineral grains has also been used to infer provenance of different sedimentary basins (Henry and Guidotti, 1985; Morton, 1991; Asiedu et al., 2000; Weltje and Von Eynatten, 2004; Mange and Morton, 2007; Meinhold et al., 2009; Stern and Wagnreich, 2013; Baxter et al., 2016; White et al., 2016). For example, presence of tourmaline indicates granite, granite pegmatite, contact and regionally metamorphosed rocks as the possible provenance. It also relates the provenance to recrystallized schist and gneiss (Mange and Maurer, 1992). Occurrence of chromian spinel suggests mafic and ultramafic provenance (i.e., peridotite, serpentinite and ophiolite) (Irvine, 1965; Dick and Bullen, 1984; Mange and Morton, 2007; Al-Juboury et al., 2009; Meinhold et al., 2009). Thus, an

* Corresponding author.

Email address: nagamjan@curtin.edu.my, nagageochem@yahoo.com (R. Nagarajan).

<http://dx.doi.org/10.1016/j.jseas.2017.04.002>

Received 25 August 2016; Received in revised form 31 March 2017; Accepted 4 April 2017

Available online 05 April 2017

1367-9120/ © 2017 Elsevier Ltd. All rights reserved.